









































- 27 Cendron, L., Ramazzina, I., Puggioni, V., Maccacaro, E., Liuzzi, A., & Secchi, A. et al. (2016). The Structure and Function of a Microbial Allantoin Racemase Reveal the Origin and Conservation of a Catalytic Mechanism. *Biochemistry*, 55(46), 6421–6432. doi:10.1021/acs.biochem.6b00881
- 28 Bovigny, C., Degiacomi, M.T., Lemmin, T., Dal Peraro, M., & Stenta, M. (2014). Reaction Mechanism and Catalytic Fingerprint of Allantoin Racemase. *Journal of Physical Chemistry B*, 118(27), 7457–7466. doi:10.1021/jp411786z
- 29 Kahn, K., & Tipton, P.A. (2000). Kinetics and Mechanism of Allantoin Racemization. *Bioorganic Chemistry*, 28(2), 62–72. doi:10.1006/bioo.2000.1162
- 30 Zhu, J., Fleming, A.M., Orendt, A.M., & Burrows, C.J. (2015). pH-Dependent Equilibrium between 5-Guanidinohydantoin and Iminoallantoin Affects Nucleotide Insertion Opposite the DNA Lesion. *Journal of Organic Chemistry*, 81(2), 351–359. doi:10.1021/acs.joc.5b02180
- 31 Lubowe, I.I. (1966). *U.S. Patent No. 3275643*. Washington, DC: U.S. Patent and Trademark Office.
- 32 Mecca, S.B. (1971). *U.S. Patent No. 3578656*. Washington, DC: U.S. Patent and Trademark Office.
- 33 Mecca, S.B. (1975). *U.S. Patent No. 3898243*. Washington, DC: U.S. Patent and Trademark Office.
- 34 Mecca, S.B. (1980). *U.S. Patent No. 4181804*. Washington, DC: U.S. Patent and Trademark Office.
- 35 Mecca, S.B. (1975). *U.S. Patent No. 3927021*. Washington, DC: U.S. Patent and Trademark Office.
- 36 Mecca, S.B. (1972). *U.S. Patent No. 3632596*. Washington, DC: U.S. Patent and Trademark Office.
- 37 Mecca, S.B. (1956). *U.S. Patent No. 2761867*. Washington, DC: U.S. Patent and Trademark Office.
- 38 Lubowe, I.I. (1963). *U.S. Patent No. 3107252*. Washington, DC: U.S. Patent and Trademark Office.
- 39 Margraf, H.W. (1974). *U.S. Patent No. 3856805*. Washington, DC: U.S. Patent and Trademark Office.
- 40 Puszyńska-Tuszkano, M., Grabowski, T., Daszkiewicz, M., Wietrzyk, J., Filip, B., & Maciejewska, G. et al. (2011). Silver(I) complexes with hydantoins and allantoin: Synthesis, crystal and molecular structure, cytotoxicity and pharmacokinetics. *Journal of Inorganic Biochemistry*, 105(1), 17–22. doi:10.1016/j.jinorgbio.2010.09.013
- 41 Margraf, H.W. (1976). *U.S. Patent No. 3932627*. Washington, DC: U.S. Patent and Trademark Office.
- 42 Sumrada, R., & Cooper, T.G. (1974) Oxaluric Acid: A Non-Metabolizable Inducer of the Allantoin Degradative Enzymes in *Saccharomyces cerevisiae*. *Journal of Bacteriology*, 117(3), 1240–1247.
- 43 Vogels, G.D., de Windt, F.E., & Bassie, W. (2010). Hydrolysis and racemization of allantoin. *Recueil Des Travaux Chimiques Des Pays-Bas*, 88(8), 940–950. doi:10.1002/recl.19690880807
- 44 Saqib, M., Lou, B., Halawa, M.I., Kitte, S.A., Liu, Z., & Xu, G. (2017). Chemiluminescence of Lucigenin-Allantoin and Its Application for the Detection of Allantoin. *Analytical Chemistry*, 89(3), 1863–1869. doi: 10.1021/acs.analchem.6b04271
- 45 Chen, X., Tao, Y., Zhao, L., Xie, Z., & Chen, G. (2005). Preliminary electrochemiluminescence study of allantoin in the presence of tris(2,2'-bipyridine)ruthenium (II). *Luminescence*, 20(3), 109–116. doi:10.1002/bio.828
- 46 Biltz, H. (1910). Methylierung und Konstitution von Allantoin. *Berichte Der Deutschen Chemischen Gesellschaft*, 43(2), 1999–2003. doi:10.1002/cber.191004302139
- 47 Goyal, R.N., & Rastogi, A. (1997). Electrochemical and peroxidase catalysed oxidation of 9-β-D-ribofuranosyluric acid 5'-monophosphate. *Journal of the Chemical Society, Perkin Transactions*, 2(11), 2423–2430. doi:10.1039/a701601h
- 48 Berke, P.A., & Rosen, W.E. (1984). *U.S. Patent No. 4459303*. Washington, DC: U.S. Patent and Trademark Office.
- 49 Berke, P.A., & Rosen, W.E. (1984). *U.S. Patent No. 4487939*. Washington, DC: U.S. Patent and Trademark Office.
- 50 Lehmann, S., Hoeck, U., Breinholdt, J., Olsen, C.E., & Kreilgaard, B. (2006). Characterization and chemistry of imidazolidiny urea and diazolidiny urea. *Contact Dermatitis*, 54(1), 50–58. doi: 10.1111/j.0105–1873.2006.00735.x
- 51 Liebert, M. (1990). Final Report on the Safety Assessment of Diazolidiny Urea. *International Journal of Toxicology*, 9(2), 229–245. doi: 10.3109/10915819009078735
- 52 Chemical Selection Working Group NCI Imidazolididiny urea. *ntp.niehs.nih.gov* Retrieved from [https://ntp.niehs.nih.gov/ntp/htdocs/chem\\_background/exsumpdf/imidazolidinyurea\\_508.pdf](https://ntp.niehs.nih.gov/ntp/htdocs/chem_background/exsumpdf/imidazolidinyurea_508.pdf)
- 53 De Groot, A., & Veenstra, M. (2010). Formaldehyde-releasers in cosmetics in the USA and in Europe. *Contact Dermatitis*, 62, 221–224. doi: 10.1111/j.1600–0536.2009.01623.x
- 54 De Groot, A., White, I., Flyvholm, M., Lensen, G., & Coenraads, P. (2010). Formaldehyde-releasers in cosmetics: relationship to formaldehyde contact allergy. Part I. Characterization, frequency and relevance of sensitization, and frequency of use in cosmetics. *Contact Dermatitis*, 62, 2–17. doi: 10.1111/j.1600–0536.2009.01615.x
- 55 De Groot, A., White, I., Flyvholm, M., Lensen, G., Coenraads, P., & Menne, T. (2009). Formaldehyde-releasers: relationship to formaldehyde contact allergy. Contact allergy to formaldehyde and inventory of formaldehyde-releasers. *Contact Dermatitis*, 61, 63–85. doi: 10.1111/j.1600–0536.2009.01582.x
- 56 Rosen, M., & McFarland, A. (1984). Free formaldehyde in anionic shampoo. *Journal of Society Cosmetics Chemistry*, 35, 157–169.
- 57 Doi, T., Kajimura, K., & Taguchi, S. (2010). Survey of formaldehyde (FA) concentration in cosmetics containing FA-donor preservatives. *Journal of Health Science*, 56, 116–122. doi: 10.1248/jhs.56.116
- 58 Doi, T., Kajimura, K., Takatori, S., Fukui, N., Taguchi, S., & Iwagami, S. (2009). Simultaneous measurement of diazolidiny urea, urea, and allantoin in cosmetic samples by hydrophilic interaction chromatography. *Journal of chromatography B: Analytical technologies in the biomedical and life sciences*, 877(10), 1005–1010. doi: 10.1016/j.jchromb.2009.02.032
- 59 Doi, T., Kajimura, K., & Taguchi, S. (2010). The different decomposition properties of diazolidiny urea in cosmetics and patch test materials. *Contact Dermatitis*, 65, 81–91. doi: 10.1111/j.1600–0536.2010.01862.x
- 60 Palu, A.K., West, B.J., & Jensen, C.J. (2012). Noni Seed Oil Topical Safety, Efficacy, and Potential Mechanisms of Action. *Journal of Cosmetics, Dermatological Sciences and Applications*, 2(2), 74–78. doi: 10.4236/jcda.2012.22017
- 61 Rietschel, R.L., Fowler, J.F., & Fisher, A.A. (1995). *Fisher's Contact Dermatitis*. Baltimore: Williams & Wilkins.



















parameters [9]. Although the mechanism of the effect of microwave irradiation on the behavior of the chemical processes is still poorly understood, many studies have been published confirming the advantages of using of microwave activation to prepare various organic compounds [10–13].

At the moment, the use of the microwave activation in the vanillin (3) synthesis is described only for its production by curcumin oxidation [14], and the use of such an approach to the guaiacol (1) condensation with glyoxalic acid has not been found in the available literature.

## 2 Experimental

### 2.1 Materials and methods

Commercially available guaiacol (99 %, Aldrich Organics) and an aqueous solution of glyoxalic acid (50 %, Aldrich) were used as reagents. A solution of sodium hydroxide (30 %) was obtained by dissolving a portion of sodium hydroxide (chemically pure, Vecton).

The experiments using microwave irradiation were carried out using the «Speedwave four» microwave sample preparation system (Berghof Products + Instruments GmbH) with a maximum power of 1450 W and a magnetron frequency of 2450 MHz that allowed varying the temperature in the range of 50–230°C.

To control the progress of the reactions, a reverse phase HPLC method was used on a Shimadzu LC-20 Prominence liquid chromatograph equipped with a PDA-20A UV detector.

### 2.2 Synthesis using microwave irradiation

A portion of 0.94 g (0.0075 mol) of guaiacol was mixed with 11.5 ml of water and 1.1 g of a 30 % sodium hydroxide solution with vigorous stirring. 0.7 g (0.0047 mol) of a 50 % glyoxalic acid solution and 5.0 ml of water were mixed separately. The resulting solutions were combined, placed in a fluoroplastic autoclave of the microwave system and kept for 10, 20 and 30 minutes at different temperatures and irradiation powers.

### 2.3 Synthesis by the conventional procedure

9.3 g of guaiacol and 115.0 ml of water were placed in a round bottom flask. 10.6 g of a 30 % sodium hydroxide solution were added to the reaction mixture with a vigorous stirring. Then a mixture of 7.4 g of a 50 % solution of glyoxalic acid and 50.0 g of water was added to the resulting sodium guaiacolate solution. The reaction mixture was kept at a temperature of 30 °C from 5 to 25 hours.

### 2.4 Synthesis by the conventional procedure

To isolate the desired product (2), the reaction mixture was acidified up to a pH level of 4–5 by the addition of hydrochloric acid and the excess of guaiacol was separated by extraction with benzene. The aqueous phase was acidified up to pH = 1 and the desired product was extracted with the ethyl acetate. The extract was evaporated to dryness and the bottom residue was recrystallized from a minimum amount of ethyl acetate. The product (2) was obtained with the MP = 131–133 °C (132–133 °C in Ref. [3]). The IR spectrum:  $\nu$ ,  $\text{cm}^{-1}$ : 3336 (OH), 2971 ( $\text{CH}_3$ ), 2932 ( $\text{CH}_3$ ), 1744 (C=O), 1713 (C=O).  $^1\text{H}$  NMR spectrum:  $\delta$ , ppm (DMSO- $d_6$ ): s.w. 12.47, s. 8.96, d. 6.96, d. 6.78, d. 6.72, s.w. 5.68, s. 4.89, s. 3.75.

## 3 Results and discussion

In the present work we studied the opportunity to synthesize vanillylmandelic acid (2) by the guaiacol (1) condensation with glyoxalic acid under the effect of the microwave irradiation as compared with the traditional synthesis method. With that, we conducted a series of experiments to determine the optimal synthesis conditions. The reaction mixture was subjected to the microwave irradiation with a power of 290, 580, 870, and 1160 W.

While conducting the experiments with varying the irradiation power without the additional heating (Table 1), no increase in the reaction rate is observed compared to the conventional synthesis procedure. The maximum yield achieved in 1 hour of the experiment for the product (2) (34 %) is comparable with the one obtained without the irradiation for the same synthesis time.

An increase in the heating of the reaction mixture contributed to an increase in the VMA yield. The best results were obtained when carrying out the reaction at a temperature of 70 °C (Table 1). The maximum VMA yield was achieved by irradiating the reaction mixture at a power of 870 W for 30 minutes. Further exposure of the reaction mixture is not feasible, since the yield of the desired product is gradually reduced that is probably due to the progressing side processes.



















































## References

- 1 Wiseman B. Isonicotinic acid hydrazide conversion to Isonicotinyl-NAD by catalase-peroxidases / B. Wiseman, X. Carpena, M. Feliz, L.J Donald, M. Pons, I. Fita, P.C. Loewen // *J. Biol. Chem.* — 2010. — Vol. 285, No. 34. — P. 26662–26673. DOI: 10.1074/jbc.M110.139428.
- 2 Judge V. Isonicotinic acid hydrazide derivatives: Synthesis, antimicrobial activity, and QSAR studies / V. Judge, B. Narasimhan, M. Ahuja, D. Sriram, P. Yogeewari, E.D. Clereq, C. Pannecouque, J. Balzarini // *Med. Chem. Res.* — 2012. — Vol. 21. — P. 1451–1470. DOI 10.1007/s00044-011-9662-9.
- 3 Zimmer S. Cyclodextrin promotes atherosclerosis regression via macrophage reprogramming / S. Zimmer, A. Grebe, S. Bakke, N. Bode, B. Halvorsen, T. Ulas, M. Skjelland et al. // *Science Translational Medicine.* — 2016. — Vol. 8, Iss. 333. — P. 333–350. DOI: 10.1126/scitranslmed.aad6100.
- 4 Szejtli J. Past, present and future of cyclodextrin research / J. Szejtli // *Pure and Applied Chemistry.* — 2004. — Vol. 76, No. 10. — P. 1825–1845.
- 5 Sabadini E. Solubility of cyclomaltooligosaccharides (cyclodextrins) in H<sub>2</sub>O and D<sub>2</sub>O: a comparative study / E. Sabadini // *Carbohydrate Research.* — 2006. — Vol. 341, No. 2. — P. 270–274.
- 6 Das S.K. Cyclodextrins — the molecular container / S.K. Das // *Research Journal of Pharmaceutical, Biological and Chemical Sciences.* — 2013. — Vol. 4, No. 2. — P. 1694–1720.
- 7 Szejtli J. *Cyclodextrin Technology* / J. Szejtli // Dordrecht, Netherlands: Kluwer Academic Publishers, 1988. — 441 p.
- 8 Dodziuk H. *Cyclodextrins and Their Complexes. Chemistry, Analytical Methods, Applications* / H. Dodziuk — Warsaw: Wiley-VCH, Weinheim, 2006. — 504 p.
- 9 Maazaoui R. Applications of cyclodextrins: formation of inclusion complexes and their characterization / R. Maazaoui // *International Journal of Advanced Research.* — 2015. — Vol. 3, No. 2. — P. 757–781.
- 10 Нуркенов О.А. Синтез, строение и антирадикальная активность новых гидразонов изоникотиновой кислоты / О.А. Нуркенов, Г.Ж. Карипова // *Материалы XX Международ. науч.-практ. конф. студ. и молодых ученых (20 мая 2019 г.)*. — Томск, 2019. — С. 169, 170.
- 11 Nurkenov O.A. Synthesis and anti-microbial activity of N'-(2-hydroxy-5-nitrobenzylidene)-isonicotinohydrazide / O.A. Nurkenov, G.Zh. Karipova, T.S. Zhivotova, S.B. Akhmetova, T.M. Seilkhanov, S.D. Fazylov // *News of NAS RK. Chemistry and Technology Series.* — 2019. — No. 2(434). — P. 26–30.
- 12 Нуркенов О.А. Гидразид изоникотиновой кислоты и его производные / О.А. Нуркенов, С.Д. Фазылов, Г.Ж. Карипова. — Караганда: Гласир, 2019. — 156 с.
- 13 Miller L.A. Practical considerations in development of solid dosage forms that contain cyclodextrin / L.A. Miller // *Journal of Pharmaceutical Sciences.* — 2007. — Vol. 96, No. 7. — P. 1691–1707.
- 14 Singh R. Characterization of cyclodextrin inclusion complexes — a review / R. Singh // *Journal of Pharmaceutical Science and Technology.* — 2010. — Vol. 2, No. 3. — P. 171–183.
- 15 Javery S. Preparation and characterization of Cyclodextrin inclusion complexes: a review / S. Javery, A. Dosh // *International journal of Universal Pharmacy and Bio Sciences.* — 2014. — Vol. 3, No. 3. — P. 674–691.
- 16 Loftsson T. Cyclodextrins in drug delivery / T. Loftsson // *Expert opinion on drug delivery.* — 2005. — Vol. 2, No. 2. — P. 335–351.
- 17 Wang Q.F. Preparation of inclusion complex of paeonol and  $\beta$ -cyclodextrin by sealed control temperature method / Q.F. Wang // *China Journal of Chinese Materia Medica.* — 2007. — Vol. 32, No. 3. — P. 218–221.
- 18 Marques C.H.M. Studies of cyclodextrin inclusion complexes. I. The salbutamolcyclodextrin complex as studied by phase solubility and DSC / C.H.M. Marques // *International Journal of Pharmaceutics.* — 1990. — Vol. 63, No. 3. — P. 259–266.
- 19 Xiang T.X. Inclusion complexes of purine nucleosides with cyclodextrins: II. Investigation of inclusion complex geometry and cavity microenvironment / T.X. Xiang // *International Journal of Pharmaceutics.* — 1990. — Vol. 59, No. 1. — P. 45–55.
- 20 Beni S. Cyclodextrin/imatinib complexation: binding mode and charge dependent stabilities / S. Beni // *European Journal of Pharmaceutical Sciences.* — 2007. — Vol. 30, No. 2. — P. 167–174.
- 21 Nurkenov O.A. Complexes of inclusion of functionally-substituted hydrazons of isonicotinic acid with cyclodextrines and their antiradical activity / O.A. Nurkenov, S.D. Fazylov, A.Zh. Issayeva, T.M. Seilkhanov, T.S. Zhivotova, Z.T. Shulgau, Zh.M. Kozhina // *News of NAS RK. Chemistry and Technology Series.* — 2018. — No.6 (432). — P.57–66.

О.А. Нуркенов, С.Д. Фазылов, Т.М. Сейлханов, А.Ж. Мұқашева,  
Г.Ж. Кәріпова, А.Т. Тәкібаева, А.Ф. Томабаева

### **N'-(5-нитрофуран-2-ил)метиленизоникотиногидразид негізінде циклодекстриндік нанокешендерді алу және олардың құрылымын физикалық-химиялық әдістермен зерттеу**

Мақалада N'-(5-нитрофуран-2-ил)метиленизоникотиногидразидтің  $\beta$ -циклодекстринмен ( $\beta$ -ЦД) және 2-гидроксипропил- $\beta$ -циклодекстринмен (2-ГП- $\beta$ -ЦД) супрамолекулярлық кешендер алынып, зерттелген. Бір өлшемді <sup>1</sup>H, <sup>13</sup>C спектроскопия ЯМР әдістерімен алынған қосу кешендерінің құрылысы расталды. Гомо-және гетероядер табиғатының спин-спинді өзара әрекеттесуін орнатуға мүмкіндік беретін ЯМР COSY (<sup>1</sup>H-<sup>1</sup>H) және НМҚС (<sup>1</sup>H-<sup>13</sup>C) екі өлшемді спектроскопия әдістерімен анықталған.

Супрамолекулярлы кешендерде  $^1\text{H}$  ЯМР сигналдарының интегралдык қарқындылығын  $\beta$ - және 2-ГП- $\beta$ -ЦД-мен салыстыру екі жағдайда да рецепторлардың бір молекуласына субстраттың бір молекуласының құрам кешені түзілетіндігін көрсетті.  $\text{N}'$ -((5-нитрофуран-2-ил)метилен)изоникотиногидразидтің зерттелетін  $\beta$ -циклодекстриндермен өзара әрекеттесуі кезінде субстрат молекуласының рецептордың қуысына пиридин фрагменімен кіруімен  $\beta$ -ЦД қолданғанда және фураноздық циклмен кіруімен 2-ГП- $\beta$ -ЦД қолданғанда қосу кешендері пайда болатыны байқалды. Алынған супрамолекулярлық кешендер суда еруі немесе тұрақты су дисперсияларын құруы мүмкін.

*Кілт сөздер:* гидразидтер,  $\text{N}'$ -((5-нитрофуран-2-ил)метилен)изоникотиногидразид,  $\beta$ -циклодекстрин, 2-гидроксипропил- $\beta$ -циклодекстрин, қосу кешендері, ЯМР спектроскопиясы, супрамолекулярлы кешендер, COSY ( $^1\text{H}$ - $^1\text{H}$ ), HMQC ( $^1\text{H}$ - $^{13}\text{C}$ ).

О.А. Нуркенов, С.Д. Фазылов, Т.М. Сейлханов, А.Ж. Мукашева,  
Г.Ж. Карипова, А.Т. Такибаева, А.Г. Томабаева

### Получение циклодекстриновых наноккомплексов на основе $\text{N}'$ -((5-нитрофуран-2-ил)метилен)изоникотиногидразида и исследование их структуры физико-химическими методами

В статье впервые были получены и изучены супрамолекулярные комплексы  $\text{N}'$ -((5-нитрофуран-2-ил)метилен)изоникотиногидразида с  $\beta$ -циклодекстрином ( $\beta$ -ЦД) и 2-гидроксипропил- $\beta$ -циклодекстрином (2-ГП- $\beta$ -ЦД). Методами  $^1\text{H}$ ,  $^{13}\text{C}$  ЯМР спектроскопии было подтверждено строение полученных комплексов включения. Строение соединений было изучено также методами двумерной спектроскопии ЯМР COSY ( $^1\text{H}$ - $^1\text{H}$ ) и HMQC ( $^1\text{H}$ - $^{13}\text{C}$ ), позволяющей установить спин-спиновые взаимодействия гомо- и гетероядерной природы. Сопоставление интегральных интенсивностей сигналов  $^1\text{H}$  ЯМР исходного субстрата с  $\beta$ - и 2-ГП- $\beta$ -ЦД-нами в супрамолекулярных комплексах показало, что обоих случаях образуются комплексы состава: одна молекула субстрата на одну молекулу рецептора. Установлено, что при взаимодействии  $\text{N}'$ -((5-нитрофуран-2-ил)метилен)изоникотиногидразида с изучаемыми  $\beta$ -циклодекстринами образуются комплексы включения с вхождением молекулы субстрата во внутреннюю полость рецептора пиридиновым фрагментом в случае использования  $\beta$ -ЦД и фуранозным циклом — в случае 2-ГП- $\beta$ -ЦД. Полученные супрамолекулярные комплексы способны растворяться в воде или образовывать устойчивые водные дисперсии.

*Ключевые слова:* гидразиды,  $\text{N}'$ -((5-нитрофуран-2-ил)метилен)изоникотиногидразид,  $\beta$ -циклодекстрин, 2-гидроксипропил- $\beta$ -циклодекстрин, комплексы включения, спектроскопия ЯМР, супрамолекулярные комплексы, COSY ( $^1\text{H}$ - $^1\text{H}$ ), HMQC ( $^1\text{H}$ - $^{13}\text{C}$ ).

### References

- 1 Wiseman, B., Carpena, X., Feliz M., Donald, L.J., Pons, M., Fita, I., & Loewen, P.C. (2010). Isonicotinic acid hydrazide conversion to Isonicotinyl-NAD by catalase-peroxidases. *J. Biol. Chem.*, 285, 34, 26662–26673. DOI: 10.1074/jbc.M110.139428.
- 2 Judge, V., Narasimhan, B., Ahuja, M., Sriram, D., Yogeewari, P., & Clereq E.D., et al. (2012). Isonicotinic acid hydrazide derivatives: Synthesis, antimicrobial activity, and QSAR studies. *Med. Chem. Res.*, 21, 1451–1470. DOI 10.1007/s00044-011-9662-9.
- 3 Zimmer, S., Grebe, A., Bakke, S., Bode, N., Halvorsen, B., Ulas T. et al. (2016). Cyclodextrin promotes atherosclerosis regression via macrophage reprogramming. *Science Translational Medicine*, 8, 333, 333–350. DOI: 10.1126/scitranslmed.aad6100.
- 4 Szejtli, J. (2004). Past, present and future of cyclodextrin research. *Pure and Applied Chemistry*. 76, 10, 1825–1845.
- 5 Sabadini, E. (2006). Solubility of cyclomaltoo-ligosaccharides (cyclodextrins) in  $\text{H}_2\text{O}$  and  $\text{D}_2\text{O}$ : a comparative study. *Carbohydrate Research*, 341, 2, 270–274.
- 6 Das, S.K. (2013). Cyclodextrins — the molecular container. *Research Journal of Pharmaceutical, Biological and Chemical Sciences*, 4, 2, 1694–1720.
- 7 Szejtli, J. (1988). *Cyclodextrin Technology*. Dordrecht, Netherlands: Kluwer Academic Publishers.
- 8 Dodziuk, H. (2006). *Cyclodextrins and Their Complexes. Chemistry, Analytical Methods, Applications*. Warsaw: Willey-VCH, Weinheim.
- 9 Maazaoui, R. (2015). Applications of cyclodextrins: formation of inclusion complexes and their characterization. *International Journal of Advanced Research*, 3, 2, 757–781.
- 10 Nurkenov, O.A., & Karipova, G.Zh. (2019). Sintez, stroenie i antiradikalnaia aktivnost novykh hidrazonov izonikotinovoi kisloty [Synthesis, structure and antiradical activity of new isonicotinic acid hydrazones]. Proceedings from *The XX International Scientific and Practical Conference of students and young scientists* (May, 20, 2019). (pp. 169–170). Tomsk [in Russian].
- 11 Nurkenov, O.A., Karipova, G.Zh., Zhivotova, T.S., Akhmetova, S.B., Seilkhanov, T.M., & Fazylov, S.D. (2019). Synthesis and anti-microbial activity of  $\text{N}'$ -(2-hydroxy-5-nitrobenzylidene)-isonicotinohydrazide. *News of NAS RK. Chemistry and Technology Series*. 2, 434, 26–30.



**В. Totkhuskyzy<sup>1</sup>, L.K. Yskak<sup>1</sup>, I.S. Saparbekova<sup>1</sup>, N.O. Myrzakhmetova<sup>1</sup>,  
T.K. Jumadilov<sup>2</sup>, J.V. Gražulevicius<sup>3</sup>**

<sup>1</sup>*Kazakh National Women's Teacher Training University, Almaty, Kazakhstan;*

<sup>2</sup>*A.B. Bekturov Institute of chemical sciences, Almaty, Kazakhstan;*

<sup>3</sup>*Kaunas University of Technology, Kaunas, Lithuania  
(E-mail: leilakinyazovna@gmail.com)*

### **Features of the extraction of yttrium and lanthanum with an intergel system based on hydrogels of polyacrylic acid and poly-4-vinylpyridine**

To predict the sorption activity and selectivity of hydrogels, the effect of mutual activation of polymer networks in the intergel system was studied. The intergel system of the hydrogel of polyacrylic acid (hPAA) and the hydrogel of poly-4-vinylpyridine (hP4VP), which was studied at a distance through the volume of the solvent in the absence of direct contact between the polymer networks, were chosen as the object of study. Intergel systems have been investigated using methods for measuring electrical conductivity, pH, and gravimetry. The mutual activation of La<sup>3+</sup> and Y<sup>3+</sup> ions with the intergel system in an aqueous medium was also studied. It has been established that as a result of the remote interaction of the studied hydrogels, their mutual activation occurs, leading to a significant change in their electrochemical and conformational properties. At certain ratios of acidic and basic hydrogels, a significant increase in the sorption of lanthanum and yttrium ions is observed in comparison with the initial hydrogels. These results indicate the appearance of ionized structures with optimal conformation, providing an optimal ligand environment around lanthanum and yttrium ions.

*Keywords:* intergel systems, polyacrylic acid, poly-4-vinylpyridine, hydrogels, remote interaction, La<sup>3+</sup> ions, Y<sup>3+</sup> ions, sorption, desorption.

#### *Introduction*

It is known that polymer hydrogels having functional groups capable of binding metal ions are classified as highly selective polymer structures. This contributes to the fact that such polymers have a sorption ability with respect to metal ions, including ions of rare earth elements.

According to the phenomenon of the remote interaction of polymer hydrogels in an aqueous medium, nonionic macromolecules that are unable to undergo ionization and subsequent dissociation cannot participate in the process of remote interaction. Therefore, the remote interaction of polymers of various structures leads to their functionalization.

Previous studies showed that the remote interaction of polymer hydrogels leads to a significant change in their electrochemical and conformational properties. As a result of remote interaction, functional groups are formed without counter ions, stabilized by intramolecular interactions; electrochemical and conformational changes in macromolecules lead to a significant increase in the sorption ability of the intergel system, consisting of two hydrogels; the «long-range effect» under certain conditions leads to high selectivity with respect to metal ions [1–4].







The dependence of the concentration of yttrium ions on the molar ratio of hydrogels in time in the hPAA:hP4VP intergel system in a medium of 6-<sup>90</sup>yttrium nitrate is shown in Figure 4. The results obtained indicate that mutual activation leads to a significant increase in the sorption properties of polymer hydrogels in the intergel system.

The starting hydrogel of polyacrylic acid has a higher degree of extraction of yttrium ions. As can be seen from Figure 4, the highest activation of yttrium ions occurs at a ratio of 2:4 hPAA:hP4VP. In the figure, one can observe the general regularity of the degree of activation of yttrium ions in the intergel system. The lowest activation point corresponds to a 4:2 ratio after 4.5 hours of interaction. And in a 2:4 ratio of the intergel system, a decrease in the concentration of yttrium ions is observed. The main reason for such a high degree of extraction is the high ionization of polymer structures as a result of their mutual activation. Further, the extraction of yttrium ions by the intergel system decreases and the polybase present in the solution shows the lowest activation with yttrium ions. These results indicate the appearance of ionized structures with optimal conformation, providing an optimal ligand environment around lanthanum and yttrium ions.

Table 1 presents the values of the degree of extraction of lanthanum ions by the hPAA:hP4VP intergel system. It can be seen that in the hPAA:hP4VP intergel pairs, the degree of sorption is much higher compared to individual hydrogels. This is due to the high degree of ionization of the starting polymers in the intergel system during their remote interaction as a result of mutual activation. The highest ionization of hPAA:hP4VP occurs at a ratio of 50 % hPAA – 50 % hP4VP, as a result of which the degree of extraction of lanthanum ions reaches maximum values (97.6 %).

Table 1

**Degree of extraction of lanthanum ions with hydrogels PAA, P4VP**

$\tau$ , h	$\eta(\text{La})$ , %						
	hPAA:hP4VP, %						
	100	83:17	67:33	50:50	33:67	17:83	100
0	0	10.2	10.2	9.4	9.4	0	3.7
0.5	10.2	19	25.4	21.4	13.4	12.6	13.4
1.5	25.4	22.2	13.4	26.2	18.2	9.4	19
2.5	30.2	22.2	28.6	26.2	21.4	18.2	7
4.5	39.9	30.2	28.6	49.5	27.8	14.2	8.6
24	59.8	67.1	67.1	97.6	56.7	37.5	27.8

Table 2 shows the values of the degree of extraction of lanthanum ions by the hPAA: hP4VP intergel system. The highest ionization of hPAA:hP4VP occurs at a ratio of 33 % hPAA – 67 % hP4VP, as a result of which the degree of extraction of yttrium ions reaches maximum values (26.9 %).

Table 2

**Degree of extraction of yttrium ions with hydrogels PAA, P4VP**

$\tau$ , h	$\eta(\text{Y})$ , %						
	hPAA:hP4VP, %						
	100	83:17	67:33	50:50	33:67	17:83	100
0	37	22	10.2	9.4	9.4	0	3.7
0.5	6.4	13.3	14.5	3.2	26.9	4.9	2.6
1.5	24.3	10.3	17.3	13.1	17.3	13.1	9.2
2.5	24.3	10.3	11.7	13.1	17.3	13.1	9.2
4.5	13.6	9.9	2.1	3	4.6	4.5	3.6
24	18.1	15.1	13.6	1.6	21.1	13.6	13.6

*Conclusions*

Based on the obtained data on the electrical conductivity, pH, and swelling coefficient, we can conclude that sorption of lanthanum ions by polymer hydrogels occurs. When the molar ratio of hPAA: hP4VP hydrogels is equivalent, the intergel system has the highest sorption ability with respect to lanthanum ions in

comparison with the initial hydrogels. The maximum degree of binding of the polymer chain to yttrium ions is manifested when the ratio of hPAA:hP4VP = 33 %:67 %. The mutual activation of hPAA and hP4VP hydrogels in the intergel system allows one to achieve a significantly higher degree of sorption for the intergel pair than for individual hydrogels. As can be seen from the data obtained, most of the lanthanum is recovered within 24 hours. In this case, the highest sorption occurs at the ratios of 67 % hPAA – 33 % hP4VP and 33 % hPAA – 67 % hP4VP, 67.1 and 56.7 % of lanthanum are recovered, respectively. The largest amount (97.6 %) of lanthanum is recovered at a ratio of 50 % hPAA – 50 % hP4VP at 24 h [10–13].

## References

- 1 Jumadilov T.K. Phenomenon of remote interaction and sorption ability of rare cross-linked hydrogels of polymethacrylic acid and poly-4-vinylpyridine in relation to erbium ions / T.K. Jumadilov, R. Kondaurov, A. Imangazy, N. Myrzakhmetova, I. Saparbekova // *Chem. Chem. Technol.* — 2019. — Vol. 13, No. 4. — P. 451–458.
- 2 Saparbekova I.S. Some features of the remote interaction of KU 2–8 cation exchanger with AB-17 anion exchanger / I.S. Saparbekova, O.V. Suberlyak, L.K. Yskak, Z.O. Malimbayeva, N.O. Myrzakhmetova, T.K. Dzhumadilov // *International Scientific And Technical Conference «Modern Technologies Of Production And Processing Of Polymeric Materials» Collection of Abstracts.* — 2019. — P. 87.
- 3 Yskak L.K. Features of distance interaction and mutual activation of hydrogel polymethacrylic acid and anionite AV-17 / L.K. Yskak T.K. Dzhumadilov, N.O. Myrzakhmetova, O.V. Suberlyak // *Ye.A. Buketov Karaganda State University Institute of polymer materials and technology international science and technology center. Proceedings of the international symposium on specialty polymers.* — Karaganda, 2019. — P. 106.
- 4 Totkhuskyzy B. Some peculiarities of the interaction of scandium and yttrium ions with activated hydrogels / B. Totkhuskyzy T.K. Dzhumadilov, J.V. Gražulevicius // *Ye.A. Buketov Karaganda State University Institute of polymer materials and technology international science and technology center. Proceedings of the international symposium on specialty polymers.* — 2019. — P. 104.
- 5 Donia A.M. Selective Separation of Uranium (VI), Thorium (IV), and Lanthanum (III) from their aqueous solutions using a chelating resin containing amine functionality / A.M. Donia, A.A. Atia, T.E. Amer, M.N. El-Hazek, M.H. Ismael // *Journal of dispersion science and technology.* — 2011. — Vol. 32. — P. 1673–1681.
- 6 Benaissa E. Comparative study on lanthanum (III) sorption onto Lewatit TP 207 and Lewatit TP 260 / E. Benaissa, O. Abderahim, M.A. Didi // *Journal of radioanalytical and nuclear chemistry.* — 2014. — Vol. 299. — P. 439–446.
- 7 Кондрашова Ю.Г. Перманентное набухание гидрогелей полиакриловой и полиметакриловой кислот / Ю.Г. Кондрашова, А.П. Сафронов // *Тез. докл. 16 Рос. молод. науч. конф., посвящ. 85-летию со дня рожд. проф. В.П. Кочергина.* — 2006. — С. 232, 233.
- 8 Kim S.J. Effect of the water state on the electrical bending behavior of chitosan/poly(diallyldimethylammonium chloride) hydrogels in NaCl solutions / S.J. Kim, S.G. Yoon, S.I. Kim // *J. Polym. Sci.* — 2004. — Vol. 42, No. 5. — P. 914–921.
- 9 Sitnikova N.L. Role of the nature of counterions on the swelling behavior and dielectric properties of poly(methacrylic acid) gels in methanol / N.L. Sitnikova, I.A. Malyshkina, N.D. Gavrilova, O.E. Philippova // *Proceedings of 4 International Symposium Molecular Order and Mobility in Polymer Systems.* — 2002. — P. 229.
- 10 Jumadilov T.K. Influence of initial state of hydrogels on self-organization of polymer networks of polymethacrylic acid and poly-4-vinylpyridine at their remote interaction in an aqueous medium / T.K. Jumadilov, R.G. Kondaurov, S.A. Khakimzhanov, H. Himersen, G.K. Yeskaliyeva // *Chemical Journal of Kazakhstan.* — 2018. — No. 1. — P. 42–48.
- 11 Jumadilov T.K. Influence of polyacrylic acid and poly-4-vinylpyridine hydrogels mutual activation in intergel system on their sorption properties in relation to lanthanum (III) ions / T.K. Jumadilov, R.G. Kondaurov, Zh.A. Abilov, J.V. Gražulevicius, A.A. Akimov // *Polymer Bulletin.* — 2017. — Vol. 74. — P. 116–122.
- 12 Jumadilov T.K. Ionic equilibrium and conformational state in intergel system based on polyacrylic acid and poly-4-vinylpyridine hydrogels / T.K. Jumadilov, Zh.A. Abilov, S.S. Kaldayeva, H. Himersen, R.G. Kondaurov // *Journal of Chemical Engineering and Chemistry Research.* — 2014. — Vol. 1. — P. 253–261.
- 13 Chen L. Reswelling behavior of polycation hydrogels carrying charges on the chain backbone by two-step surfactant bindings / L. Chen, Y. Xiao, L. Qingya // *J. Appl. Polym. Sci.* — 2006. — Vol. 102, No. 4. — P. 3791–3794.

Б. Тотхусқызы, Л.К. Ысқак, И.С. Сапарбекова, Н.О. Мырзахметова,  
Т.К. Джумадиллов, Ю.В. Гражулявичюс

## Полиакрил қышқылы мен поли-4-винилпирдин гидрогельдері негізіндегі интергельді жүйеден иттрий мен лантанды алу ерекшеліктері

Гидрогельдердің сорбциялық белсенділігі мен селективтілігін болжау үшін интергельді жүйедегі полимерлік торларды өзара активтендірудің әсері зерттелген. Зерттеу объектісі ретінде полиакрил қышқылының гидрогелі (гПАК) және поли-4-винилпирдиннің (гП4ВП) гидрогелі таңдалды. Интергельді жүйенің рН, электр өткізгіштігі гравиметриялық өлшеу әдістерімен анықталды. Сондай-ақ сулы ортада интергельді жүйемен  $\text{La}^{3+}$  және  $\text{Y}^{3+}$  иондарының өзара активациясы зерттелді. Ең жоғары электр өткізгіштік 24 сағаттан кейін орын алды. Электр өткізгіштігінің ең төменгі мәндері гПАК:гП4ВП = 0:6 интергельді жүйесінде

байқалған. Ол интергельді жүйенің әлсіз диссоциациясымен байланысты. гПАК:гП4ВП интергельді жүйесінде сутегі иондарының концентрациясының ұлғаюы гПАК:гП4ВП = 5:1 арақатынасында көрінген. Зерттелген гидрогельдердің қашықтықтан өзара әрекеттесуі нәтижесінде олардың электрохимиялық және конформациялық қасиеттерінің айтарлықтай өзгеруіне әкеліп соқтыратыны және өзара активтендіру жүргізілгені анықталды. Егер біз осы деректерді электр өткізгіштігі туралы деректер бойынша салыстырсақ, бұл ретте карбоксильді топтардың диссоциациясы процесі протондардың винил пиридинге қосылу процесінен басым болады деген қорытынды жасауға болады. Қышқылдық және негіздік гидрогельдердің белгілі бір арақатынасында бастапқы гидрогельдермен салыстырғанда лантан және иттрий иондарының сорбциясының айтарлықтай өсуі байқалған. Бұл нәтижелер лантан және иттрий иондарының айналасында оңтайлы лигандты ортаны қамтамасыз ететін оңтайлы конформациясы бар иондалған құрылымдардың пайда болуын көрсетеді.

*Кілт сөздер:* интергельді жүйе, полиакрил қышқылы, поли-4-винилпиридин,  $\text{La}^{3+}$  ионы,  $\text{Y}^{3+}$  ионы, сорбция, десорбция.

Б. Тотхускызы, Л.К. Ыскак, И.С. Сапарбекова, Н.О. Мырзахметова,  
Т.К. Джумадилов, Ю.В. Гражулявичюс

## Особенности извлечения иттрия и лантана интергелевой системой на основе гидрогелей полиакриловой кислоты и поли-4-винилпиридина

Для прогнозирования сорбционной активности и селективности гидрогелей было исследовано влияние взаимной активации полимерных сеток в интергелевой системе. В качестве объекта исследования была выбрана интергелевая система «гидрогель полиакриловой кислоты (гПАК) – гидрогель поли-4-винилпиридина (гП4ВП)», которая изучалась на расстоянии через объем растворителя при отсутствии непосредственного контакта между полимерными сетками. Интергелевые системы были изучены методами измерения электропроводности, pH и гравиметрии. Также рассмотрена взаимная активация ионов  $\text{La}^{3+}$  и  $\text{Y}^{3+}$  с интергелевой системой в водной среде. Зависимость удельной электропроводности от молярного соотношения гидрогелей во времени, увеличение электропроводности происходит при соотношении гПАК:гП4ВП = 5:1 на протяжении всего времени удаленного взаимодействия. Максимальная электропроводность была достигнута через 24 ч. Минимальные значения электропроводности отмечены в области интергелевой системой гПАК:гП4ВП = 0:6, что связано с его слабой диссоциацией. Зависимость концентрации ионов водорода гПАК:гП4ВП, увеличение концентрации ионов водорода происходит при соотношении гПАК:гП4ВП = 5:1. Установлено, что в результате дистанционного взаимодействия изучаемых гидрогелей происходит их взаимная активация, приводящая к значительному изменению их электрохимических и конформационных свойств. Эти результаты указывают на возникновение ионизованных структур с оптимальной конформацией, обеспечивающих оптимальное лигандное окружение вокруг ионов лантана и иттрия.

*Ключевые слова:* интергелевая система, полиакриловая кислота, поли-4-винилпиридин, сорбция, десорбция, ионы  $\text{La}^{3+}$ , ионы  $\text{Y}^{3+}$ .

## References

- 1 Jumadilov, T.K., Kondaurov, R.G., Imangazy, A.M., Myrzakhmetova, N.O., & Saparbekova, I.S. (2019). Phenomenon of remote interaction and sorption ability of rare cross-linked hydrogels of polymethacrylic acid and poly-4-vinylpyridine in relation to erbium ions. *Chem.-Chem. Technol*, 13, 4, 451–458.
- 2 Saparbekova, I.S. (2019). Some features of the remote interaction of KU 2–8 cation exchanger with AB-17 anion exchanger '19: Proceedings from Modern technologies of production and processing of polymeric materials: *International scientific and technical conference* (p. 87). Lviv.
- 3 Yskak, L.K., Dzhumadilov, T.K., Myrzahmetova, N.O., & Suberlyak, O.V. (2019). Features of distance interaction and mutual activation of hydrogel polymethacrylic acid and anionite AV-17. Proceedings from *the International symposium on specialty polymers*. (Ye.A. Buketov Karaganda State University Institute of polymer materials and technology international science and technology center). (p. 106). Karaganda.
- 4 Totkhuskyzy, B., Dzhumadilov, T.K., & Gražulevicius, J.V. (2019). Some peculiarities of the interaction of scandium and yttrium ions with activated hydrogels. Proceedings from *the International symposium on specialty polymers*. (Ye.A. Buketov Karaganda State University Institute of polymer materials and technology international science and technology center). (p. 104). Karaganda.
- 5 Donia, A.M., Atia, A.A., Amer, T.E., El-Hazek, M.N., & Ismael, M.H. (2011). Selective Separation of Uranium (VI), Thorium (IV), and Lanthanum (III) from their aqueous solutions using a chelating resin containing amine. *Journal of dispersion science and technolog*, 32, 1673–1681.
- 6 Benaissa, E., Abderrahim, O., & Didi, M.A. (2014). Comparative study on lanthanum (III) sorption onto Lewatit TP 207 and Lewatit TP 260. *Journal of radioanalytical and nuclear chemistry*, 32, 439–446.
- 7 Kondrashova, Yu.G., & Safronov, A.P. (2006). Permanentnoe nabukhanie hidrohelei poliakrilovoi i polimetakrilovoi kislot [Permanent swelling of hydrogels of polyacrylic and polymethacrylic acids]. *Tezisy dokladov 16 Rossiiskoi molodezhnoi nauchnoi*

*konferentsii, posvyashchenoi 85-letiiu so dnia rozhdeniia professora V.P. Kocherhina — Abstracts of the 16th Russian Youth Scientific Conference dedicated to the 85th birthday of Professor V.P. Kochergin.* (Vol. 2, p. 232, 233) [in Russian].

8 Kim, S.J., Seung, Y.G., & Kim, S.I. (2004). Effect of the water state on the electrical bending behavior of chitosan / poly(diallyldimethylammonium chloride) hydrogels in NaCl solutions. *J. Polym. Sci. B.*, 42, 5, 914–921.

9 Sitnikova, N.L. (2002). Role of the nature of counterions on the swelling behavior and dielectric properties of poly(methacrylic acid) gels in methanol. Proceedings from 4 *International Symposium Molecular Order and Mobility in Polymer Systems.* (p. 229).

10 Jumadilov, T.K., Kondaurov, R.G., Khakimzhanov, S.A., Himersen, H., & Yeskaliyeva, G.K. (2018). Influence of initial state of hydrogels on self-organization of polymer networks of polymethacrylic acid and poly-4-vinylpyridine at their remote interaction in an aqueous medium. *Chemical Journal of Kazakhstan*, 1, 42–48.

11 Jumadilov, T.K., Kondaurov, R.G., Abilov, Zh.A., Grazulevicius, J.V., & Akimov, A.A. (2017). Influence of polyacrylic acid and poly-4-vinylpyridine hydrogels mutual activation in intergel system on their sorption properties in relation to lanthanum (III) ions, *Polymer Bulletin*, 74, 116–122.

12 Jumadilov, T.K., Abilov, Zh.A., Kaldayeva, S.S., Himersen, H., & Kondaurov, R.G. (2014). Ionic equilibrium and conformational state in intergel system based on polyacrylic acid and poly-4-vinylpyridine hydrogels. *Journal of Chemical Engineering and Chemistry Research*, 1, 253–261.

13 Chen, Li, Yu, Xiao, & Li, Qingya (2006). Reswelling behavior of polycation hydrogels carrying charges on the chain backbone by two-step surfactant bindings. *J. Appl. Polym. Sci.*, 102, 4, 3791–3794.

M.Zh. Burkeev, G.M. Zhumanazarova, E.M. Tazhbayev,  
G.K. Kudaibergen, S.B. Aukadieva, E.Zh. Zhakupbekova

*Ye.A. Buketov Karaganda State University, Kazakhstan  
(E-mail: gaziza.zhumanazarova@mail.ru)*

## **Poly(propylene fumarate phthalate) and acrylic acid radical copolymerization constants and parameters**

Poly(propylene fumarate phthalate) and acrylic acid radical copolymerization in dioxane solution at various molecular ratios of original monomeric mixture was studied in this work for the first time. An unsaturated polyester resin was obtained using the polycondensation reaction. The composition of the obtained poly(propylene fumarate phthalate) was determined according to elemental analysis. The studied copolymers are promising for further study due to their swelling ability, antioxidant activity, and biodegradable ability. Copolymerization reaction kinetics has been studied. The composition of the copolymers was determined using chromatemass spectrometry. Radical copolymerization constants and parameters have been calculated by Mayo-Lewis integral method. Based on the copolymerization constants the Q-e parameters was calculated according to the Alfrey-Price equation. It was proved that non-solvable polymers of a net-shaped structure are formed in the whole range of the researched comonomer ratios during the radical copolymerization of p-PFF with AA. Based on the results presented in the article, we can say that all copolymer compounds based on poly(propylene fumarate phthalate) and acrylic acid demonstrate the ability to control physical and chemical properties. This in turn will allow to create new materials with a pre-defined behavior program. It was found that the unsaturated polyester resin is characterized by a lower reactivity in case of acrylic acid and poly(propylene fumarate phthalate) copolymerization.

*Keywords:* poly(propylene fumarate phthalate), acrylic acid, biodegradable, polycondensation, radical copolymerization, kinetics, copolymerization.

### *Introduction*

Over the past few decades fumaric acid-based polyesters comprising Krebs cycle [1, 2] are of much interest in biomedicine due to great biocompatibility and biodegradability [3, 4]. Moreover, polyester resins are relatively cheap products, which in some cases makes materials based on them competitive comparing to other sorts of plastics [5–8].

Poly(propylene fumarate phthalate) is the most researched material among the. It is a perfect option for cross-linking with various monomers, such as acrylic and methacrylic acid.

Cross-linked poly(propylene fumarate phthalate) can satisfy a number of medical requirements, such as biocompatibility, osteoconductivity, sterilisability and manageability [9–14]. It can be polymerized in situ [15] forming solid composite with mechanical properties identical to those of spongy bone.

In this regard, the poly(propylene fumarate phthalate) (p-PFF) and acrylic acid (AA) copolymerization constants and parameters determination, as well as the development of new methods for vinyl monomers radical polymerization control and polymer characteristics improvement are one of research priorities for high-molecular compounds chemistry development.

External factors sensitive copolymers were previously synthesized by reaction of polyglycolefumarates radical copolymerization with various unsaturated carboxylic acids and dimethylaminoethyl metacrylate [16–21]. Due to this fact, further research in this area appeared to be advantageous.

Reactions of poly(propylene fumarate phthalate)(p-PFF) and acrylic acid (AA) radical copolymerization were studied in this work for the first time.

### *Experimental*

Initial p-PFF was received by fumaric acid, phthalic anhydride and propylene glycol polycondensation at temperatures 423–453 K [22, 23]. The reaction was monitored by determining the acid number and the amount of water emission. The synthesized polyester is a light yellow fusible resinous substance that can dissolve in chloroform and dioxane. Received resin was obtained from original monomers by multiple acetone washing. Received substance content was defined by elemental analysis data.

P-PFP molecular weight was determined by light scattering method at NACH 2100 AN nephelometer and by gel-permeation chromatography, which is 2272 and 2394 atomic mass units.

P-PFP and AA radical copolymerization was performed in solution of dioxane at different original copolymer molecular ratios with benzoyl peroxide (BP) as initiating agent at 333 K. Synthesized polymers were washed by dioxane and dried in vacuum multiple times in order to refine them from remaining unreacted monomers until reaching constant weight.

Contents of received copolymers were defined with potentiometric titration and by a highly efficient chromatograph LC-20 Prominence, Shimadzu (Japan) [24, 25]. In order to find amount of copolymers unreacted double bonds (degree of unsaturation) bromide-bromate method was used [26].

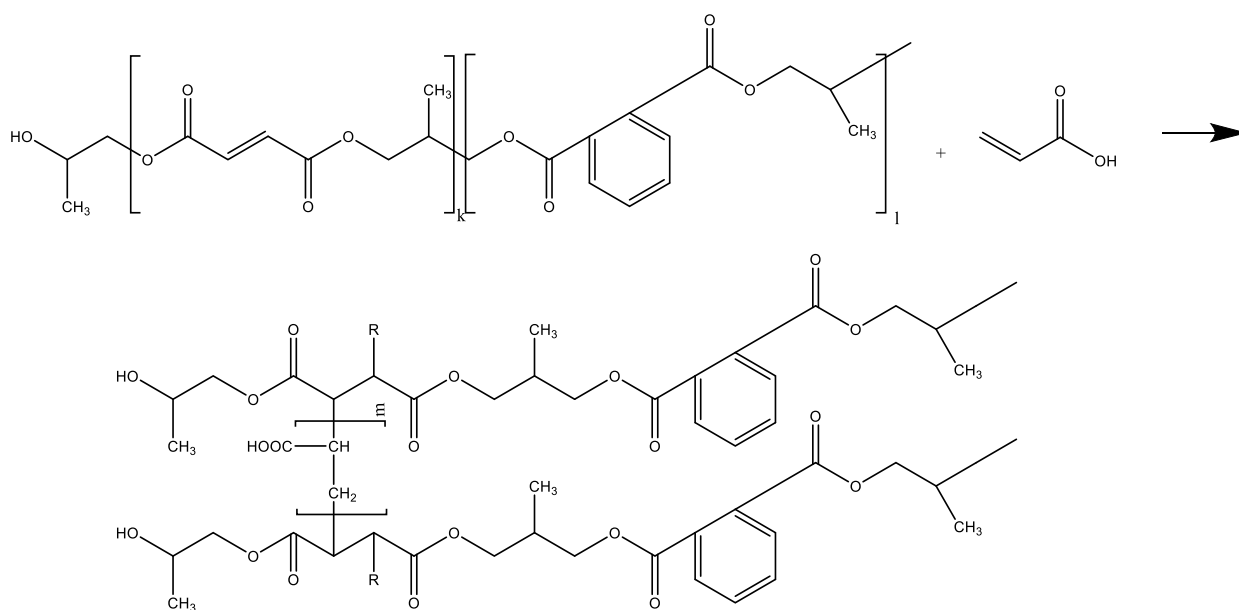
P-PFP and AA radical copolymerization kinetics was investigated by dilatometric method in dioxane. Constants of copolymerization  $r_1$  and  $r_2$  were defined based on contents of copolymers received at deep conversion using Mayo-Lewis integral equation [27].

### Results and Discussion

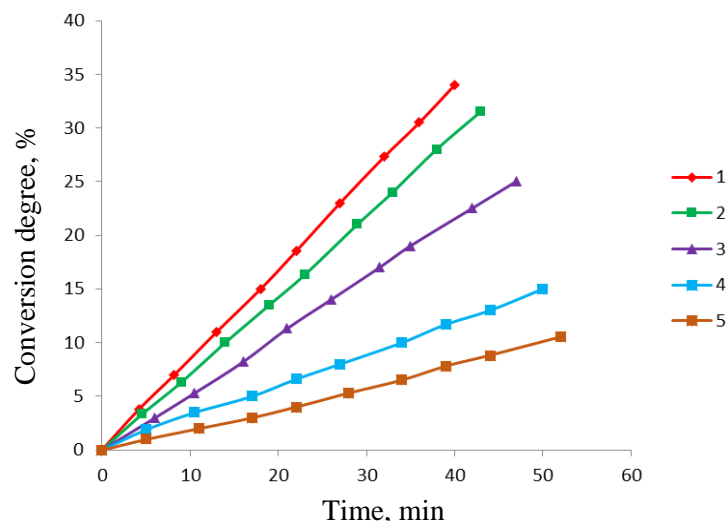
Elaborate development of thorough research in the area of radical copolymerization allows controlling properties of polymers, their structure and molecular mass, and also suggests more methods for producing polymers with the desired properties. As mentioned above, unsaturated polyesters-based products cured with vinyl monomers and having specific physico-chemical and mechanical properties are most desirable. Unsaturated double bonds in p-PFP molecules allow using it as polymeric matrix to receive cross-linked polymers in case of copolymerization with acrylic acid.

P-PFP was received by fumaric acid, phthalic anhydride and propylene glycol polycondensation [22, 23].

Cross-linked copolymer formation as result of p-PFP oligomeric molecule and AA radical copolymerization in presence of BP as initiating agent can be shown by the following diagram:



Copolymerization constant and parameters values are important characteristics when considering monomers relative reaction ability depending on their structure. However, more comprehensive information on monomers relative reaction ability at copolymerization can be obtained from kinetic data (Fig. 1).



1 — 6.77:93.23; 2 — 20.34:79.66; 3 — 44.17:55.17; 4 — 68.42:31.58; 5 — 86.67:13.33 mol.%

Figure 1. p-PFP:AA copolymerization kinetic graph

P-PFP and AA radical copolymerization kinetics at various initial molecular ratios was studied deeply in order to estimate monomers relative activity (Fig. 1). It was found that the reaction rate and copolymer yield increase with increasing AA content in the initial monomer mixture. However, these parameters decrease with increasing p-PFP in the reaction mixture. This seems to be determined by presence of  $-\text{COO}$  carboxyl functional group in acrylic acid chain, which can participate in reactions of polymer transfer followed by molecular mass growth due to branching processes. As can be seen in Figure 1, the radical copolymerization kinetics data indicate a constant process acceleration in the case of AA molecular mass increase in initial monomeric mixture.

As mentioned above, cross-linked insoluble polymers are formed throughout the range of studied copolymer ratios in process of p-PFP and AA radical copolymerization.

Experimental data received after studying radical copolymerization processes in p-PFP – AA systems are shown in Table 1. Copolymer yield ranges from 83 % to 62 %.

Table 1

**Copolymer content dependence on initial mixture composition in process of p-PFP ( $M_1$ ) and AA ( $M_2$ ) [BP] =  $8 \cdot 10^{-3}$  mole/ $m^3$ , T = 333 K**

Initial monomer ratio, % by mass		Copolymer content, % by mass		Yield, %
$M_1$	$M_2$	$m_1$	$m_2$	
10.22	89.78	6.77	93.23	83.70
25.00	75.00	20.34	79.66	78.73
50.00	50.00	44.17	55.17	79.33
73.91	26.09	68.42	31.58	71.93
90.00	10.00	86.67	13.33	62.09

As can be seen in Table 1, p-PFP-AA copolymers are enriched with AA components throughout the range of initial mixtures. At that, the proportion of AA components in the copolymer composition increases symbolically with respect to their content in initial monomeric mixture.

Copolymer yield and swelling rating increase as share in original AA mixture rises; this seems to be determined by high degree of branching and cross-linking.

The branching and cross-linking reactions decrease correspondingly with AA molecular concentration reducing since benzene rings cannot participate in homopolymerization reactions. While the copolymer unsaturation degree increases. Besides, the abovementioned reactions are more complicated when p-PFP concentration rises in initial monomeric mixture, which leads to higher viscosity.

Copolymer content dependence on initial mixture composition can be shown more conveniently on content diagram (Fig. 2).

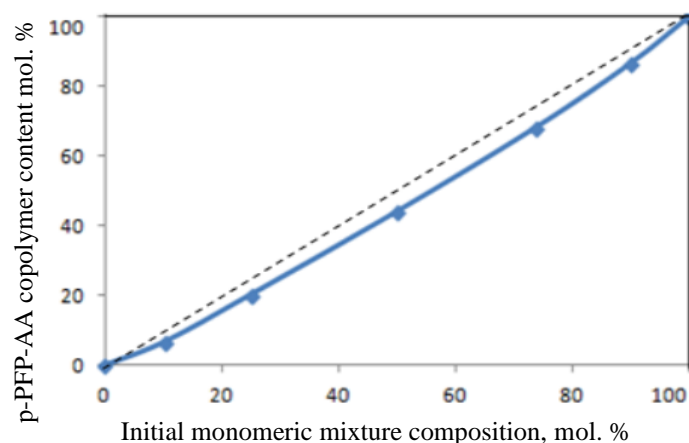


Figure 2. Composition diagram showing p-PFP – AA copolymer content dependence on initial monomeric mixture composition

Copolymer relative activity based on copolymer content and initial monomeric mixture composition has been calculated using Mayo-Lewis integral equation [9], Fineman-Ross and Kelen-Tudos standard methods. Table 2 shows the calculated data that illustrate the higher AA activity in the process of radical copolymerization.

Table 2

**p-PFP – AA binary systems radical copolymerization constants and parameters**

$M_1$	$M_2$	$r_1$	$r_2$	$r_1 \cdot r_2$	$1/r_1$	$1/r_2$	$Q_1$	$e_1$	$Q_2$	$e_2$
p-PFP	AA	0,76	1,21	0,92	1,32	0,83	1,19	1,06	1,15	0,77

As can be seen in Table 2, the relative activity value  $r_1$  in p-PFP-AA system is below one ( $r_1 < 1$ ). This suggests a higher activity of macroradical ending with p-PFP component towards «outer» monomer or radicals, but macroradical ending with AA second co-monomer tends to react with «inner» monomer. Copolymerization stabilizer derivatives are close to each other, i.e. copolymer macroradicals can be created by static structures.

### Conclusions

Therefore, a brief summary of the studies described in this article shows that new crosslinked polymers can be obtained by poly(propylene fumarate phthalate) and acrylic acid radical copolymerization.

The obtained result demonstrates the ability to control the physicochemical properties of a poly(propylene fumarate phthalate) and acrylic acid based copolymer by changing the content of the polymer composition, which allows you to create new materials with preset properties.

### References

- 1 Diez-Pascual A.M. Antibacterial SnO<sub>2</sub> nanorods as efficient fillers of propylene fumarate-co-ethylene glycol) biomaterials / A.M. Diez-Pascual, A.L. Diez-Vicente // Mater. Sci. Eng. C Mater. Biol. Appl. — 2017. — No. 78. — P. 806–816.
- 2 Kasper F.K. Synthesis of poly(propylene fumarate) / F.K. Kasper, K. Tanahashi, J.P. Fisher, A.G. Mikos // Nat Protoc. — 2009. — Vol. 4, No. 4. — 518 p.
- 3 Boddle E.W. Degradable hydrogel scaffolds for in vivo delivery of single and dual growth factors in cartilage repair / E.W. Boddle, T.A. Holland, L.S. Baggett, A.G. Mikos, V.M. Cuijpers, Y. Tabata, J.A. Jansen // Osteoarthritis Cartilage. — 2007. — No. 15. — P. 187–197.
- 4 Yasko A.W. Injectable biodegradable polymer composites based on poly(propylene fumarate) with poly(ethylene glycol)-dimethacrylate / A.W. Yasko, S. He, P.S. Engel, J.M. Yaszemski, A.G. Mikos // Biomaterials. — 2000. — No. 21. — P. 2389–2394.
- 5 Brydson J.A. Polyesters / J.A. Brydson // Plastics Materials. 7<sup>th</sup> ed. — 1999. — P. 694–743.
- 6 Kandelbauer A. Handbook of Thermoset Plastics / A. Kandelbauer, G. Tondi, O.C. Zaske, S.H. Goodman. — San Diego: William Andrew, 2014. — 111 p.
- 7 Kandelbauer A. Unsaturated Polyesters and Vinyl esters / A. Kandelbauer, G. Tondi, S.H. Goodman // Handbook of Thermoset Plastics, 3<sup>rd</sup> ed. — H. Dodiuk, S.H. Goodman (Eds.). — San Diego: William Andrew Publications, 2014. — P. 111–172.

- 8 Козик В.В. Композиционные материалы на основе природных силикатов и ненасыщенной полиэфирной смолы / В.В. Козик, Л.П. Борило // Наука и образование: материалы VIII Всерос. науч. конф. — Томск: Изд-во ТГПУ, 2004. — С. 43, 44.
- 9 Park H. In vitro generation of an osteochondral construct using injectable hydrogel composites encapsulating rabbit marrow mesenchymal stem cells / H. Park, X. Guo, W. Lui, G. Liu, Y. Tabata, F.K. Kasper, Y. Cao, A.G. Mikos // *Biomaterials*. — 2009. — P. 2741–2752.
- 10 Guo X. Repair of osteochondral defects with biodegradable hydrogel composites encapsulating marrow mesenchymal stem cells in a rabbit model / X. Guo, H. Park, S. Young, J.D. Kretlow, J.J. van den Beucken, L.S. Baggett, Y. Tabata, F.K. Kasper, A.G. Mikos, J.A. Jansen // *Acta Biomater.* — 2010. — No. 6. — P. 39–47.
- 11 Holland T.A. Osteochondral repair in the rabbit model utilizing bilayered, degradable oligo(poly(ethylene glycol)fumarate) hydrogel scaffolds / T.A. Holland, E.W. Bodde, L.S. Baggett, Y. Tabata, A.G. Mikos, J.A. Jansen // *J. Biomed. Mater. Res. A*. — 2005. — No. 75. — P. 156–167.
- 12 Bodde E.W. Degradable hydrogel scaffolds for in vivo delivery of single and dual growth factors in cartilage repair / E.W. Bodde, T.A. Holland, A.G. Mikos, L.S. Baggett, V.M. Cuijpers, Y. Tabata, J.A. Jansen // *Osteoarthritis Cartilage*. — 2007. — No. 15. — P. 187–197.
- 13 Holland T.A. In vitro release of transforming growth factor-beta 1 from gelatin microparticles encapsulated in biodegradable oligo(poly(ethylene glycol)fumarate) hydrogels / T.A. Holland, Y. Tabata, A.G. Mikos // *J. Control Release*. — 2003. — No. 91. — P. 299–313.
- 14 Park H. Delivery of TGF-beta1 and chondrocytes via injectable, biodegradable hydrogels for cartilage tissue engineering applications / H. Park, J.S. Temenoff, T.A. Holland, Y. Tabata, A.G. Mikos // *Biomaterials*. — 2005. — No. 25. — P. 7095–7103.
- 15 Park H. Injectable biodegradable hydrogel composites for rabbit marrow mesenchymal stem cell and growth factor delivery for cartilage tissue engineering / H. Park, J.S. Temenoff, Y. Tabata, A.I. Caplan, A.G. Mikos // *Biomaterials*. — 2007. — No. 28. — P. 3217–3227.
- 16 Анисимов Ю.Н. Привитая сополимеризация винилацетата с ненасыщенной олигоэфирной смолой и характеристики отвержденных композиций / Ю.Н. Анисимов, Н.А. Вонсович, О.Б. Грехова // *ЖПХ*. — 1996. — Т. 69, № 2. — С. 312–316.
- 17 Burkeev M.Zh. Thermal destruction of copolymers of polypropylene glycol maleate with acrylic acid / M.Zh. Burkeev, A.Zh. Sarsenbekova, E.M. Tazhbaev // *Russian Journal of Physical Chemistry A*. — 2015. — Vol. 89, No. 12. — P. 2183–2189.
- 18 Tazhbaev E.M. Nanocatalytic Systems Based on Poly(ethylene glycol maleate) – Acrylamide Copolymers / E.M. Tazhbaev, G.K. Burkeeva, A.K. Kovaleva // *Russian Journal of Applied Chemistry*. — 2015. — No. 2(88). — P. 314–319.
- 19 Burkeev M.Zh. Constants and parameters of radical copolymerization of poly(ethylene glycol fumarate) with acrylic acid / M.Zh. Burkeev, G.K. Kudaibergen, E.M. Tazhbaev et al. // *Хим. журн. Казахстана*. — 2018. — № 1(61). — С. 215–222.
- 20 Burkeev M.Zh. Constants and parameters of radical copolymerization of poly(propylene glycol fumarate) with acrylic acid / M.Zh. Burkeev, Ye.M. Tazhbaev et al. // *Bulletin of the Karaganda University. Ser. Chemistry*. — 2019. — No. 1(93). — P. 32–37.
- 21 Burkeev M.Zh. Synthesis and investigation of copolymer properties on the basis of poly(ethylene glycol fumarate) and methacrylic acid / M.Zh. Burkeev, Ye.M. Tazhbaev et al. // *Bulletin of the Karaganda University. Ser. Chemistry*. — 2019. — No. 1(93). — P. 25–31.
- 22 Пат. № 31052. Способ получения ненасыщенных полиэфирных смол на основе пропиленгликоля, фталевого ангидрида и фумаровой кислоты / М.Ж. Буркеев, Е.М. Тажбаев и др.; опубл. 16.03.2016. — 8 с.
- 23 Burkeev M.Zh. The number average and mass average molar masses of poly(ethylene(propylene)glycol fumarates / M.Zh. Burkeev, G.K. Kudaibergen, G.K. Burkeeva et al. // *Bulletin of the Karaganda University. Ser. Chemistry*. — 2018. — No. 2(90). — P. 17–22.
- 24 Гольберт К.А. Введение в газовую хроматографию / К.А. Гольберт, М.С. Виндергауз. — М.: Химия, 1990. — 352 с.
- 25 Золотов Ю.А. Физико-химические методы анализа / Ю.А. Золотов, Е.Н. Дорохова, В.И. Фадеева; под ред. Ю.А. Золотова. — М.: Высш. шк., 2000. — 356 с.
- 26 Артеменко А.И. Справочное руководство по химии / А.И. Артеменко, В.А. Малеванный, И.В. Тикунова. — М.: Высш. шк., 1990. — 303 с.
- 27 Гладышев Г.П. Радикальная полимеризация при глубоких степенях превращения / Г.П. Гладышев, В.А. Попов. — М.: Наука, 1974. — 340 с.

М.Ж. Буркеев, Г.М. Жуманазарова, Е.М. Тажбаев,  
Г.К. Құдайбергел, С.Б. Аукадиева, Э.Ж. Жакупбекова

## Полипропиленфумаратфталатты акрил қышқылымен радикалды сополимерлеудің константалары мен параметрлері

Мақалада алғаш рет полипропиленфумаратфталаттың бастапқы мономерлік қоспаның түрлі мольдық қатынасында диоксан ортасында акрил қышқылымен бинарлы радикалды сополимерленуі зерттелген. Поликонденсация реакциясымен қанықпаған полиэфирлі шайыр алынды. Сополимерлену үрдісінің кинетикасы зерттелді. Хромато-масс спектроскопия әдісін қолдану арқылы синтезделген сополимерлердің құрамы нақтыланған. Майо-Льюистің интегралдық әдісімен радикалды сополимерлену константалары мен параметрлері анықталған. Алфрей-Прайс теңдеуі бойынша сополимерлену константасының негізінде Q-е параметрлері есептелген. п-ПФФ пен АҚ радикалды сополимерлеу кезінде сомономерлердің зерттелген ара қатынасының барлық интервалында торлы құрылымның ерімейтін полимерлері

түзілетіндігі дәлелденді. Мақалада келтірілген нәтижелер бойынша полипропиленфумарат пен акрил қышқылы негізіндегі сополимерлердің барлық қосылыстары физика-химиялық қасиеттерді басқару мүмкіндігін көрсетеді деп айтуға болады. Бұл өз кезегінде алдын ала берілген бағдарлама тәртібі бойынша жана материалдарды жасауға мүмкіндік береді. Акрил қышқылын полипропиленфумаратфталатпен сополимерлеу кезінде қанықпаған полиэфир шайыры аз реакциялық қабілеттілікпен сипатталған.

*Кілт сөздер:* полипропиленфумаратфталат, акрил қышқылы, биоыдырағыштық, поликонденсация, радикалды сополимерлену, кинетика, сополимерлену.

М.Ж. Буркеев, Г.М. Жуманазарова, Е.М. Тажбаев,  
Г.К. Кудайберген, С.Б. Аукадиева, Э.Ж. Жакупбекова

### Константы и параметры радикальной сополимеризации полипропиленфумаратфталата с акриловой кислотой

В статье впервые исследована бинарная радикальная сополимеризация полипропиленфумаратфталата с акриловой кислотой в растворе диоксана при различных мольных соотношениях исходной мономерной смеси. Реакцией поликонденсации получена ненасыщенная полиэфирная смола. Состав полученного полипропиленфумаратфталата устанавливали по данным элементного анализа. Исследованные сополимеры перспективны для дальнейшего изучения их набухающей способности, антиоксидантной активности, биодegradуемой способности. Исследована кинетика реакции сополимеризации. Состав сополимеров определен с помощью хромато-масс-спектрокопии. Параметры радикальной сополимеризации и константы рассчитаны интегральным методом Майо-Льюиса. Параметры Q-е рассчитаны на основании констант сополимеризации по уравнению Алфрея-Прайса. Было доказано, что нерастворимые полимеры сетчатой структуры во всем интервале исследованных соотношений сомономеров образуются при радикальной сополимеризации п-ПФФ с АК. По приведенным в статье результатам можно заключить, что все соединения сополимеров на основе полипропиленфумаратфталата и акриловой кислоты демонстрируют возможности управления физико-химическими свойствами. Это, в свою очередь, позволит создать новые материалы с заранее заданной программой поведения. Установлено, что при сополимеризации полипропиленфумаратфталата с акриловой кислотой ненасыщенная полиэфирная смола характеризуется меньшей реакционной способностью.

*Ключевые слова:* полипропиленфумаратфталат, биодegradуемость, акриловая кислота, поликонденсация, радикальная сополимеризация, кинетика, сополимеризация.

### References

- 1 Diez-Pascual, A.M., & Diez-Vicente, A.L. (2017). Antibacterial SnO<sub>2</sub> nanorods as efficient fillers of propylene fumarate-co-ethylene glycol biomaterials. *Mater. Sci. Eng. C Mater. Biol. Appl.*, 78, 806–816.
- 2 Kasper, F.K., Tanahashi, K., Fisher, J.P., & Mikos, A.G. (2009). Synthesis of poly(propylene fumarate). *Nat Protoc.*, 4, 4, 518.
- 3 Boddle, E.W., Holland, T.A., Baggett, L.S., Mikos, A.G., Cuijpers, V.M., & Tabata, Y., et al. (2007). Degradable hydrogel scaffolds for in vivo delivery of single and dual growth factors in cartilage repair. *Osteoarthritis Cartilage*, 15, 187–197.
- 4 Yasko, A.W., He, S., Engel, P.S., Yaszemski, J.M., & Mikos, A.G. (2000). Injectable biodegradable polymer composites based on poly(propylene fumarate) with poly(ethylene glycol)-dimethacrylate. *Biomaterials*, 21, 2389–2394.
- 5 Brydson, J.A. (1999). Polyesters. *Plastics Materials* (7th ed.).
- 6 Kandelbauer, A., Tondi, G., Zaska, O.C., & Goodman, S.H. (2014). *Handbook of Thermoset Plastics*. San Diego: William Andrew, 111.
- 7 Kandelbauer A., Tondi G., & Goodman S.H. (2014). Unsaturated Polyesters and Vinyl esters. *Handbook of Thermoset Plastics* (3<sup>rd</sup> ed.). H. Dodiuk, S.H. Goodman (eds.). San Diego: William Andrew Publications, 111–172.
- 8 Kozik, V.V. & Borilo, L.P. (2004). Kompozitsionnye materialy na osnove prirodnykh silikatov i nenasyshchennoi poliefirnoi smoly [Composites based on natural silicates and unsaturated polyester resin]. Proceedings from Science and education: *VIII Vserossiyskaya nauchnaya konferentsiya — VIII All-Russian Scientific Conference*. (p. 43, 44). Tomsk: Izdatelstvo THPU [in Russian].
- 9 Park, H., Guo, X., Lui, W., Liu, G., Tabata, Y., & Kasper, F.K., et al. (2009). In vitro degradation of an osteochondral construct using injectable hydrogel composites encapsulating rabbit marrow mesenchymal stem cells. *Biomaterials*, 2741–2752.
- 10 Guo, X., Park, H., Young, S., Kretlow, J.D., van den Beucken, J.J., & Baggett, L.S., et al. (2010). Repair of osteochondral defects with biodegradable hydrogel composites encapsulating marrow mesenchymal stem cells in a rabbit model. *Acta Biomater.*, 6, 39–47.
- 11 Holland, T.A., Bodde, E.W., Tabata, Y., Holland, T.A., Mikos, A.G., & Baggett, L.S. et al. (2005). Osteochondral repair in the model utilizing bilayered, degradable oligo(poly(ethylene glycol)fumarate) hydrogel scaffolds, *J. Biomed. Mater. Res. A.*, 75, 156–167.
- 12 Bodde, E.W., Holland, T.A., Mikos, A.G., Baggett, L.S., Cuijpers, V.M., & Tabata, Y., et al. (2007). Degradable hydrogel scaffolds for in vivo delivery of single and dual growth factors in cartilage repair. *Osteoarthritis Cartilage*, 15, 187–197.

- 13 Holland, T.A., Tabata, Y., & Mikos, A.G. (2003). In vitro release of transforming growth factor-beta 1 from gelatin microparticles encapsulated in biodegradable, injectable oligo(poly(ethylene glycol)fumarate) hydrogels. *J. Control. Release*, 91, 299–313.
- 14 Park, H., Temenoff, J.S., Holland, T.A., Tabata, Y., & Mikos, A.G. (2005). Delivery of TGF-beta1 and chondrocytes via injectable, biodegradable hydrogels for cartilage tissue engineering applications. *Biomaterials*, 25, 7095–7103.
- 15 Park, H., Temenoff, J.S., Tabata, Y., Caplan, A.I., & Mikos, A.G. (2007). Injectable biodegradable hydrogel composites for rabbit marrow mesenchymal stem cell and growth factor delivery for cartilage tissue engineering. *Biomaterials*, 28, 3217–3227.
- 16 Anisimov, Yu.N., Vonsovich, N.A., & Grekhova, O.B. (1996). Privitaia sopolimerizatsiia vinilatsetata s nenasyshchennoi olihoefirnoi smoloi i kharakteristiki otverzhdennykh kompozitsii [Graft copolymerization of vinyl acetate with an unsaturated polyether resin and characteristics of cured compositions]. *Zhurnal prikladnoi khimii — Journal of Applied Chemistry*, 69, 2, 312–316 [in Russian].
- 17 Burkeev, M. Zh., Sarsenbekova, A. Zh., & Tazhbaev, E.M. (2015). Thermal destruction of copolymers of polypropylene glycol maleate with acrylic acid. *Russian Journal of Physical Chemistry A*, 12, 89, 2183–2189.
- 18 Tazhbaev, E.M., Burkeeva, G.K., & Kovaleva, A.K. (2015). Nanocatalytic Systems Based on Poly(ethylene glycol maleate) — Acrylamide Copolymers. *Russian Journal of Applied Chemistry*, 2, 88, 314–319.
- 19 Burkeyev, M.Zh., Kudaibergen, G.K., & Tazhbayev, E.M. et al. (2018). Constants and parameters of radical copolymerization of poly(ethylene glycol fumarate) with acrylic acid. *Khimicheskii zhurnal Kazakhstana — Chemical journal of Kazakhstan*, 1, 61, 215–222.
- 20 Burkeyev, M.Zh., & Tazhbayev, Ye.M. et al. (2019). Constants and parameters of radical copolymerization of poly(propylene glycol fumarate) with acrylic acid. *Bulletin of the Karaganda University. Ser. Chemistry*, 1(93), 32–37.
- 21 Burkeev, M.Zh., Kudaibergen, G.K., & Tazhbayev, Ye.M. et al. (2019). Synthesis and investigation of copolymer properties on the basis of poly(ethylene glycol fumarate) and methacrylic acid. *Bulletin of the Karaganda University. Ser. Chemistry*, 1(93), 25–31.
- 22 Burkeyev, M.Zh., & Tazhbayev, Ye.M., et al. (2016). Sposob poluchenii nenasyshchennykh poliefirnykh smol na osnove propilenhlikolia, ftalevoho anhidrida i fumarovoi kisloty [Method for the preparation of unsaturated polyester resins based on propylene glycol, phthalic anhydride and fumaric acid]. *Patent No. 31052 Kazakhstan*. Publ. 16.03.2016 [in Russian].
- 23 Burkeev, M.Zh., Kudaibergen, G.K., & Burkeeva, G.K. et al. (2018). The number average and mass average molar masses of polyethylene (propylene)glycol fumarates. *Bulletin of the Karaganda University. Ser. Chemistry*, 2(90), 17–22.
- 24 Golbert, K.A., & Vindergauz, M.S. (1990). *Vvedenie v hazovuiu khromatografiiu [Introduction to Gas Chromatography]*. Moscow: Khimiia [in Russian].
- 25 Zolotov, Yu.A., Dorokhova, E.N., & Fadeeva, V.I. (2000). *Fiziko-khimicheskie metody analiza [Physico-chemical methods of analysis]*. Moscow: Vysshiaia shkola [in Russian].
- 26 Artemenko, A.I., Malevanny, V.A., & Tikunova, I.V. (1990). *Spravochnoe rukovodstvo po khimii [Chemistry reference guide]*. Moscow: Vysshiaia shkola [in Russian].
- 27 Gladyshev, G.P., & Popov, V.A. (1974). *Radikalnaia polimerizatsiia pri hlubokikh stepeniakh prevrashcheniia [Radical polymerization with deep degrees of conversion]*. Moscow: Nauka [in Russian].

A.Zh. Sarsenbekova<sup>1</sup>, A.I. Khalitova<sup>1</sup>, T.E. Klimova<sup>2</sup>, T.O. Khamitova<sup>1</sup>,  
G.K. Kudaibergen<sup>1</sup>, I.V. Figurinene<sup>3</sup>, A.T. Medeshova<sup>3</sup>, R.K. Sotchenko<sup>3</sup>

<sup>1</sup>E.A. Buketov Karaganda State University, Kazakhstan;

<sup>2</sup>National Autonomous University of Mexico, Mexico;

<sup>3</sup>Karaganda Medical University, Kazakhstan

(E-mail: chem\_akmaral@mail.ru)

## Study of acid properties of new polymeric complexes of maleic acid polymethylvinyl ether cross-linked by polypropylene glycol

Dissociation course of polymethylvinyl ether of maleic acid cross-linked by polypropylene glycol (PMVE-MA with PPG) was investigated using classical potentiometric titration and colloid titration. It is assumed, that in the course of colloid titration monovalent counter-ions are replaced by the oppositely charged polycation, therefore it was determined the general concentration of anionic groups of hydrogel of polymethylvinyl ether of maleic acid cross-linked by polypropylene glycol. The apparent constant of dissociation (pseudo constant of dissociation) depends on the forming of the polyelectric complex but does not depend on the degree of dissociation. While it is known that potentiometric titration are determined by the apparent constant of dissociation that decreased simultaneously with the increase of the dissociation degree. Protons releasing from acid groups of hydrogel of polymethylvinyl ether of maleic acid cross-linked by polypropylene glycol leads to the formation of the complex with stronger cationic polyelectrolyte. Therefore, comparison of the results of potentiometric and colloid titration makes it possible to take in the information about the interrelation of acid characteristics of the surface of PMVE-MA with PPG and its functional properties. As a result we can define its application area for creation of new high-efficient composite material.

*Keywords:* polyelectrolyte, colloid titration, potentiometric titration, dissociation, hydrogel.

### Introduction

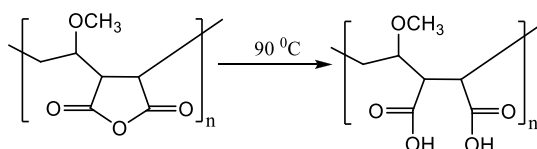
In recent decades hydrogels are widely used for producing the composite materials, filtering elements for liquid and gaseous mediums, adsorbents used for cleaning the water from heavy and toxic metals and gathering the oil and oil-product, carriers of nanoparticles of different nature [1]. Their application area depends on physical and chemical compositions of polymers, and structural and acid-base surface characteristics of polymers [2]. It is necessary know the protolytic properties of polymer surfaces, the origin and the number of active sites for the determination the degree of adsorption activity and selectiveness of polymer materials. Inhomogeneity and high degree of dispersion of these materials make it more difficult to control the surface adsorptive and acid-base properties of polymer with the use of the method of surface analysis (the study of moistening (wetting) phenomenon by the use of test liquids).

At the present day adsorptive-chemical method mainly used for the defining surface acidity of finely dispersed materials [3]. This method is practically not used for the study of polymer materials surface. Considering that active sites of hydrogel surfaces are characterized with weak protolytic properties, it will be reasonable to use methods of potentiometric and colloid titration in non-aqueous or mixed solvents in order to estimate their quantity and values of pK (these methods are capable to strengthen donor-acceptor properties).

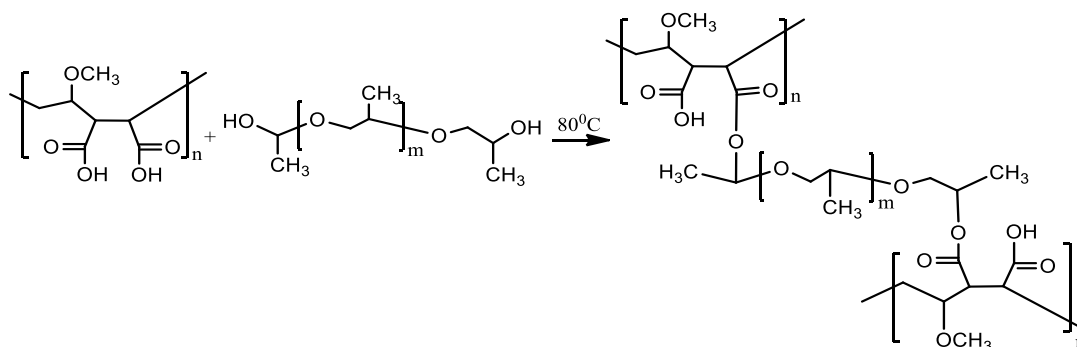
The article is devoted to the experimental evaluation of apparent constant of dissociation (pseudo constant of dissociation) (pK) of hydrogel of PMVE-MA with PPG in water and aqueous organic media by the use of potentiometric and colloid titration.

### Experimental

Hydrogel of polymethylvinyl ether of maleic acid, cross-linked by polypropylene glycol (PMVE-MA with PPG) was used as the object of the research:



Poly(methyl-vinyl-co-maleic acid) or polymethylvinyl ether of maleic acid (PMVE-MA) were obtained by the hydrolysis of polymethylvinyl ether of maleic anhydride (PMVE-MAH). Process was performed on the unit composed of round-bottomed flask (volume 100 ml) and backflow condenser. Initial mixture was prepared from 0.65 g PMVE-MAH and 20 ml distilled water. Hydrolysis was carried out during 2 hours at 90 °C. Aqueous solution of polypropylene glycol (PPG) was gradually added into obtained solution of polymethylvinyl ether of maleic acid (PMVE-MA) up to obtaining the homogeneous mixture. Excess water was removed by the use of rotary evaporator. Reaction mixture was solidified 24 hours at 80 °C. The gel of PMVE-MA with PPG [4] was obtained as a result of the esterification reaction among polymethylvinyl ether of maleic acid and polypropylene glycol:



Potentiometric titration of hydrogel of PMVE-MA with PPG was performed in water and aqueous organic media 0.05 M using the NaOH solution in the presence of 0.1 M NaCl accurate within 0.001 units of pH. The titration was carried out using «I-160MI» ionomer with the function of push-button controlled mixing. The temperature was kept constant at 22 °C. Ethyl alcohol and acetone were chosen as organic solvents for the purpose of intensification of acidic sites. These solvents are characterized by the more distinctive basic properties than water and their acidity scale span is longer (ethanol 19.5; acetone 32.5) and consequently the discriminating fineness (differentiating ability) is greater. Mixed solvent «water – ethyl alcohol» (70 % by ethanol weight), «water – acetone» (70 % by acetone weight) is the most perspective solvent for the study the slightly acidic properties of carbonaceous resin (carboxylic cation exchange resin).

Colloid titration of hydrogel of PMVE-MA with PPG 0.05 M was performed by the use of NaOH solution in the 0.1 M NaCl presence.

The curves of potentiometric and colloid titration and the dependency of  $pK_a$  on the degree of dissociation  $\alpha_D$  for hydrogel of PMVE-MA with PPG were obtained.

### Results and Discussion

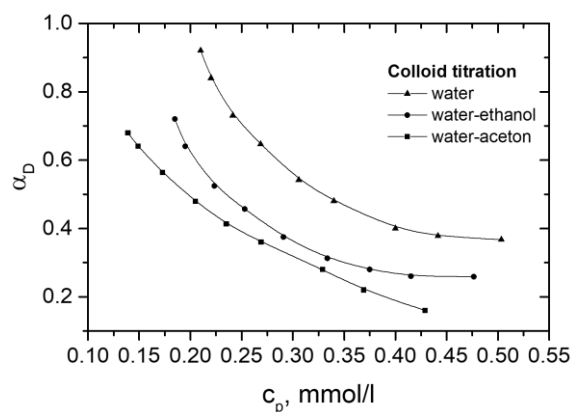
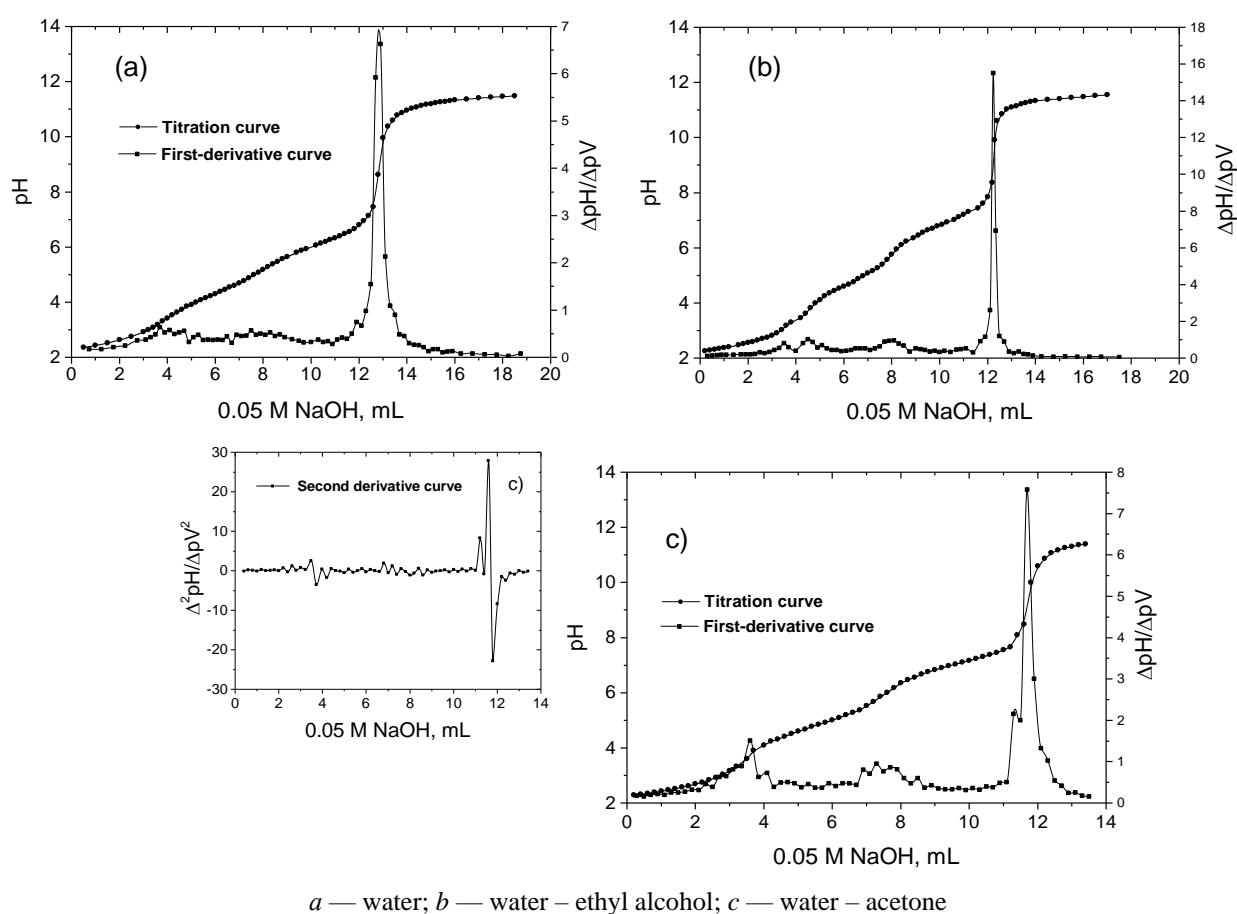
With the aim to study the process of dissociation of polymethylvinyl ester of maleic acid, linked with polypropyleneglycole, we obtained the curves of potentiometric and colloid titration and dependence of  $pK_a$  on the degree of dissociation  $\alpha_D$  for hydrogel.

The dependency of the dissociation degree  $\alpha_D$  of hydrogel of PMVE-MA with PPG in neutral medium ( $\alpha_N = 0.96$ ) on the polymer concentration  $c_p$  are presented in Figure 1. The degree of weak acid dissociation  $\alpha_D$  was defined according to the equation 1:

$$\alpha_D = \frac{c_{A^-}}{c_{A^-} + c_{HA}} \quad (1)$$

As can be seen in Figure 1, the dissociation level of the acid is decreased in presence of organic solvents, which is confirmed with constant values of autoprotolysis of these solvents (ethanol, acetone), as well as with values of dipole moment and dielectric capacity.

Dissociation of hydrogel of polymethylvinyl ester of maleic acid, linked with polypropyleneglycole, was studied by method of potentiometric titration as well (Fig. 2, a, b and c).

Figure 1. Dependence of dissociation level  $\alpha_D$  on polymer concentration  $c_p$ 

*a* — water; *b* — water – ethyl alcohol; *c* — water – acetone

Figure 2. Integral and differential curves of titration of hydrogel of PMVE-MA with PPG in the presence of NaCl electrolyte, across different environments

According to the literature data water, acetone and ethanol have the following values of dipole moment ( $\mu$ , D) and dielectric permeability ( $\epsilon$ ) [5] (at 20 °C) (Table 1):

Table 1

## Dipole moment and dielectric permeability

Solvent	$\mu$ , D	$\epsilon$
Water	1.8	78.5
Ethanol	1.7	24.3
Acetone	2.7	20.7

Figure 2a presents the titration curve of hydrogel of PMVE-MA with PPG, which functional groups are entirely protonated by the solvent of sodium hydroxide in aqueous media. As can be seen in Figure 2a, the differential curve has poorly resolved jumps of titration. The same dependency was obtained for the titration curves of hydrogel in water-ethanol mixtures (Fig. 2b). Replacing ethanol in the water-organic mixture to acetone being the less polar solvent we obtain the titration curves (Fig. 2c) that significantly differ, in the case of using the most polar solvent jump of titration will be sharper.

Addition of organic solvents decreases the level of dissociation, and thus charge quantity of macromolecule is decreased as well, and its shape is changed to nodular one. Here is cumulative effect in increase of availability of ionogenic groups and decrease of steric factor.

Observed indexes pH are graphically determined depending on neutralization degree  $\alpha_N$ , which has been calculated according to the equation 2:

$$\alpha_N = \frac{c_{NaOH}}{c_p}, \quad (2)$$

where  $c_{NaOH}$  is the concentration of added titrating solution, and  $c_p$  is the concentration of polymer in functional groups equivalent.

Both types of concentration are adjusted taking into dilution procedure. Taking into the consideration the simultaneous change of the titration curves and the decrease of ionic strength, it was assumed that there is the influence of electrostatic interaction (Coulomb interaction) as it was noted by authors of the work [6].

The degree of dissociation  $\alpha_D$  was estimated according to the equation 3:

$$\alpha_D = \alpha_N + \frac{c_{H_3O^+} - c_{OH^-}}{c_p}, \quad (3)$$

where  $\alpha_N$  is the neutralization degree and  $c_p$  is the total concentration of hydrogel of PMVE-MA with PPG in functional groups equivalent.

Concentration of hydroxonium  $c_{H_3O^+}$  was obtained from measured pH. Concentration of hydroxide  $c_{OH^-}$  was estimated using this value from ionic product of water  $K_w$  ( $K_w = 1.01 \times 10^{-14} \text{ mol}^2/\text{L}^2$  at 22 °C).

On the titration curves (Fig. 3) we can see the jumps corresponding to double-stage dissociation of hydrogel of PMVE-MA with PPG. The degree of dissociation  $\alpha_D$  increases along with growth of pH.

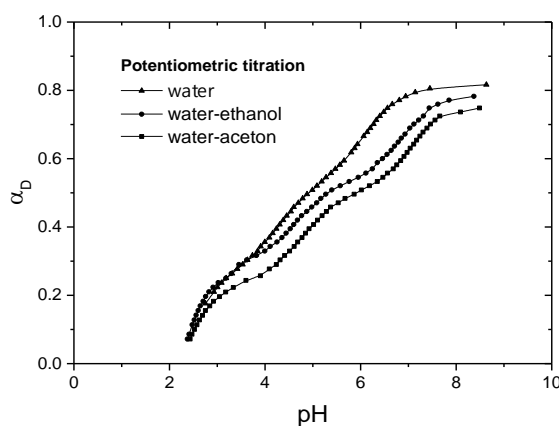


Figure 3. Dependence pH on the neutralization degree  $\alpha_N$  of hydrogel of PMVE-MA with PPG in the presence of 0.1 M NaCl determined by the potentiometric titration

In Figures 4 and 5 experimental data of potentiometric titration of hydrogel of PMVE-MA with PPG were presented as the functions of apparent constant of dissociation (pseudo constant of dissociation) pK on the degree of dissociation  $\alpha_D$ . They were calculated according to Henderson-Hasselbach equation (equation 4) at the values of dissociation degree  $\alpha_D$  ( $0 \leq \alpha_D \leq 1$ ) and according to Lifson-Katchalsky theory (equation 5).

$$pK = pH - \log \frac{\alpha_D}{1 - \alpha_D}; \quad (4)$$

$$pK = pK_0 + \Delta pK(\alpha_D), \quad (5)$$

where  $K_0$  — ionization constant of functional groups of the polymer, and  $\Delta pK(\alpha_D)$  represents the contribution of electrostatic interaction (Coulomb interaction) of functional groups. It can be determined using the integration of the area under the curve  $pK - f(\alpha)$ .

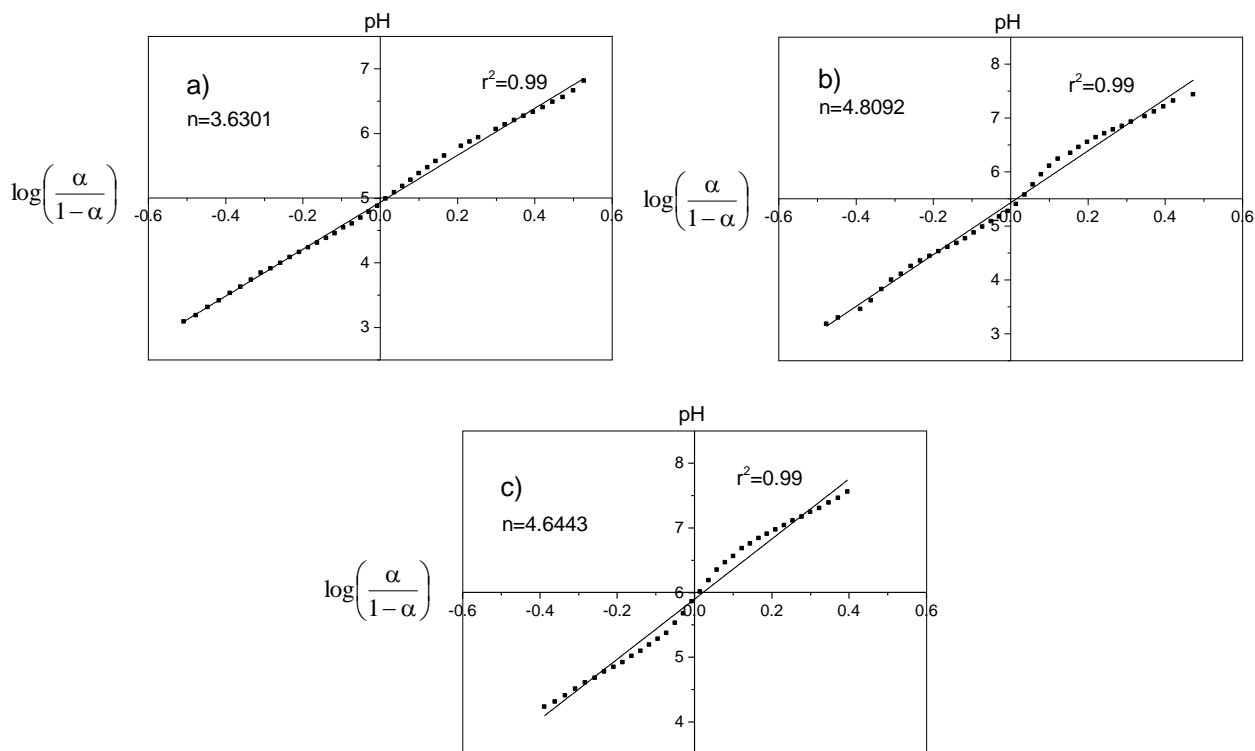


Figure 4. Curves of Henderson-Hasselbalch for potentiometric titration of hydrogel PMVE-MA with PPG in presence of electrolyte NaCl, in different media: a) water; b) water-ethyl alcohol; c) water-acetone

The apparent constant of dissociation (pseudo constant of dissociation)  $pK$  for hydrogel of PMVE-MA with PPG depends on the degree of dissociation  $\alpha_D$  evaluated according to the data of potentiometric and colloid titration (Fig. 5).

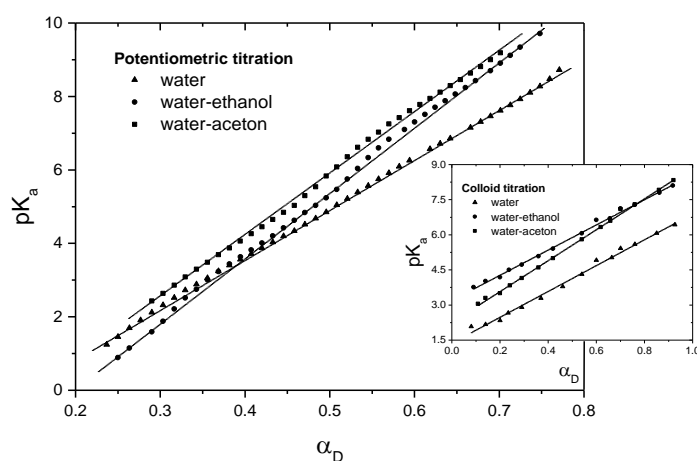


Figure 5. Dependency  $pK$  on the degree of dissociation  $\alpha_D$  for hydrogel of PMVE-MA with PPG in the presence of NaCl obtained by the potentiometric and colloid titration

Consequently, surface acid sites of hydrogel of PMVE-MA with PPG can be identified as carboxylic groups. This is confirmed by the results of IR-spectroscopy of hydrogel of PMVE-MA with PPG. In the infrared spectrum

absorption bands have been found in the areas of 1712 cm<sup>-1</sup> and 1640 cm<sup>-1</sup>. They are corresponding to valent asymmetrical and symmetrical oscillations (vibrations) of carboxylic group C=O [7].

The aim of the research was the definition of apparent constant of dissociation (pseudo constant of dissociation)  $K^{\#}$  of hydrogel of PMVE-MA with PPG according to the experimental data of colloid titration. For this purpose it was performed the computation according to equation system used for mathematical processing of the titration curves of the monobasic weak acid (HA) by (NaOH) strong base. Using these equations we determined the dissociation constant of weak acid according to mass action law (Guldberg and Waage's Law of Mass Action) (equation 6), ionic product of water (equation 7), condition of electrical neutrality (equation 8) and the expression for the mass balance (equation 9) [8, 9].

$$K_a = \frac{c_{H_3O^+} \cdot c_{A^-}}{c_{HA}}; \tag{6}$$

$$K_w = c_{H_3O^+} \cdot c_{OH^-}; \tag{7}$$

$$c_{H_3O^+} + c_{Na^+} = c_{OH^-} + c_{A^-}; \tag{8}$$

$$c_{A^-} + c_{HA} = c_p. \tag{9}$$

After the transformation we obtain the cubic equation:

$$c_{H_3O^+}^3 + c_{H_3O^+}^2(c_{Na^+} + K_a) + c_{H_3O^+}(c_{Na^+}K_a - c_pK_a - K_w) - K_aK_w = 0. \tag{10}$$

As  $c_{H_3O^+}^3 \gg K_aK_w$  then the equation takes the following form:

$$c_{H_3O^+} = -\frac{c_{Na^+} + K_a}{2} + \sqrt{\left(\frac{c_{Na^+} + K_a}{2}\right)^2 - K_a(c_{Na^+} + c_p) + K_w}. \tag{11}$$

Replacing  $c_{Na^+} = \alpha_N \cdot c_p$  we obtain the dependence:

$$c_{H_3O^+} = -\frac{\alpha_N c_p + K_a}{2} + \sqrt{\left(\frac{\alpha_N c_p + K_a}{2}\right)^2 - K_a c_p (1 - \alpha_N) + K_w}. \tag{12}$$

The degree of dissociation  $\alpha_D$  for hydrogel of PMVE-MA with PPG and the apparent constant of dissociation (pseudo constant of dissociation)  $K_a$  depending on  $c_p$  and  $\alpha_N$  were estimated according to the equations 12 and 3 (Table 2).

Table 2

**Value of pK<sub>a</sub> and n for hydrogel PMVE-MA with PPG at t = 25 °C in different media**

Solvent	pK <sub>a</sub> <sup>#</sup>	n (equat. 4)	pK <sub>a</sub>
Water	1.4±0.1	3.6301	1.8±0.1
Water – Ethyl alcohol	3.2±0.2	4.8092	3.4±0.1
Water – Acetone	2.3±0.1	4.6443	2.5±0.2

Calculated values pK<sub>a</sub><sup>#</sup>, pK<sub>a</sub> and n are represented in the Table 2. As can be seen, obtained results comply with each other well.

### Conclusions

Dissociation indexes of the hydrogel of PMVE-MA with PPG were determined by the potentiometric titration in water and water-organic medium. Index of apparent constant of dissociation (pseudo constant of dissociation) pK depends on the change of dissociation degree  $\alpha_D$  for the studied polymer. It was necessary to extrapolate pK and  $\alpha_D = 0$  for the purpose of determination of pK<sub>0</sub>.

Contrary to data of potentiometric titration, the apparent constant of dissociation (pseudo constant of dissociation) pK<sup>#</sup> was determined by the use of colloid titration with the oppositely charged polycation is essentially independent of the degree of dissociation  $\alpha_D$ . In the case of the hydrogel of PMVE-MA with PPG

the results of colloid titration do not point on the presence of two different ionized groups. This is explained by the fact that in the process of titration the monovalent counter-ion entirely replaced into polycation. Therefore we can measure the general concentration of polyacids anionic groups in hydrogel. Using the dissociation constants determined by the colloid titration, it becomes possible to determine the degree of dissociation and properly the charge of hydrogel of PMVE-MA with PPG for the wide spectrum of concentrations and neutralization degree in the case if there will be the oppositely charged macromolecules or surfaces in them. This has importance for the practical use of hydrogels if there is the replacement of counter-ions (for example, in adsorption process).

### References

- 1 Филиппова О.Е. «Восприимчивые» полимерные гели / О.Е. Филиппова // Высокомолекулярные соединения. — 2000. — Т. 42, № 12. — С. 2328.
- 2 Буркеев М.Ж. Полигликольмалеинаты в реакциях радикальной сополимеризации: моногр. / М.Ж. Буркеев, Е.М. Тажбаев, А.Ж. Сарсенбекова. — Beau Bassin: LAP LAMBERT Academic Publishing, 2017. — 192 с.
- 3 Галаев И.Ю. «Умные» полимеры в биотехнологии и медицине / И.Ю. Галаев // Успехи химии. — 1995. — Т. 65, № 5. — С. 505–524.
- 4 Burkeev M.Zh. Synthesis and investigation of copolymer properties on the basis of poly(ethylene glycol)fumarate and methacrylic acid / M.Zh. Burkeev, G.K. Kudaibergen, Ye.M. Tazhbayev et al. // Bulletin of the Karaganda University. Ser. Chemistry. — 2019. — No. 1(93). — P. 32–38.
- 5 Торопцева А.М. Лабораторный практикум по химии и технологии высокомолекулярных соединений / А.М. Торопцева, К.В. Белгородская, В.М. Бондаренко. — М.: Химия, 1972. — 223 с.
- 6 Быкова Л.Н. Кислотно-основные равновесия в среде амфипротонных растворителей и потенциометрическое титрование / Л.Н. Быкова, С.И. Петров // Успехи химии. — 1972. — Т. 42. — С. 2065–2093.
- 7 Nagasawa M. Potentiometric titration of stereoregular polyelectrolytes / M. Nagasawa, T. Murase, K. Kondo // J. Phys. Chem. — 1965. — Vol. 69. — P. 4005–4012.
- 8 Казицына Л.А. Применение ИК-, УФ-, ЯМР-спектроскопии в органической химии: учеб. пос. для вузов / Л.А. Казицына, Н.Б. Куплетская. — М.: Высш. шк., 1971. — 48 с.
- 9 Ebel S. Calculation of titration curves of weak acids and bases. Calculation of titration curves / S. Ebel // Arch Pharm. — 1969. — Vol. 302. — P. 856–862.
- 10 Lappan U. Apparent dissociation constants of polycarboxylic acids in presence of polycations / U. Lappan, U. Geißler, M. Oelmann, S. Schwarz // Colloid Polym. Sci. — 2012. — Vol. 290. — P. 1665–1670.

А.Ж. Сарсенбекова, А.И. Халитова, Т.Е. Климова, Т.О. Хамитова,  
Г.К. Кудайберген, И.В. Фигуринене, А.Т. Медешова, Р.К. Сотченко

## Полипропиленгликольмен тігілген, малеин қышқылының полиметилвинилді эфирінің жаңа полимерлік кешендерінің қышқылдық қасиеттерін зерттеу

Полипропиленгликольмен тігілген, малеин қышқылының полиметилвинил эфирінің (ППГ-мен ПМВЭ-МҚ) диссоциациясының барысы мынадай әдістермен зерттелді: классикалық потенциометриялық титрлеу және коллоидтық титрлеу. Коллоидты титрлеу барысында бірвалентті кері иондар қарсы зарядталған поликатионмен ауыстырылды, осылайша полипропиленгликольмен тігілген малеин қышқылының полиметилвинил эфирінің негізіндегі гидрогелінің аниондық топтарының жалпы концентрациясы анықталды. Диссоциацияның көрінетін константасы бұл ретте полиэлектрлік кешеннің қалыптасуына байланысты болады, алайда диссоциация дәрежесіне байланысты емес. Бұл орайда потенциометриялық титрлеу диссоциация деңгейінің өсуімен бір мезгілде азайтылатын диссоциацияның көрінетін константасын анықтауға болатыны белгілі. Полипропиленгликольмен тігілген, малеин қышқылының полиметилвинил эфирінің қышқылы негізіндегі гидрогельдің қышқылдық топтарынан протондарды босату қатты катионды полиэлектрлікті бар кешенді қалыптастыруға алып келді. Осылайша, потенциометриялық және коллоидтық титрлеу нәтижелерін салыстыру ППП-мен тігілген ПМВЭ-МҚ беттерінің қышқылдық сипаттамаларының және оның функционалдық қасиеттерімен өзара байланысы туралы ақпарат алуға мүмкіндік береді. Осының арқасында жаңа, тиімділігі жоғары композициялық материалдарды жасау мақсатында оны қолдану аймағын анықтау мүмкіндігі ашылды.

*Кілт сөздер:* полиэлектрліт, коллоидті титрлеу, потенциометриялық титрлеу, диссоциация, гидрогель.

А.Ж. Сарсенбекова, А.И. Халитова, Т.Е. Климова, Т.О. Хамитова,  
Г.К. Кудайберген, И.В. Фигуринене, А.Т. Медешова, Р.К. Сотченко

### Исследование кислотных свойств новых полимерных комплексов полиметилвинилового эфира малеиновой кислоты, сшитого полипропиленгликолем

Ход диссоциации полиметилвинилового эфира малеиновой кислоты, сшитого полипропиленгликолем (ПМВЭ-МК с ППГ), был исследован методами классического потенциометрического титрования и коллоидного титрования. Предположено, что в ходе коллоидного титрования одновалентные противоионы заменяются противоположно заряженным поликатионом, таким образом, определяется общая концентрация анионных групп гидрогеля полиметилвинилового эфира малеиновой кислоты, сшитого полипропиленгликолем. Кажущаяся константа диссоциации при этом зависит от формирования полиэлектролитического комплекса, но не связана со степенью диссоциации. Как известно, потенциометрическим титрованием определяют кажущуюся константу диссоциации, которая уменьшается одновременно с ростом степени диссоциации. Высвобождение протонов из кислотных групп гидрогеля полиметилвинилового эфира малеиновой кислоты, сшитого полипропиленгликолем, приводит к формированию комплекса с более сильным катионным полиэлектролитом. Следовательно, сравнение результатов потенциометрического и коллоидного титрования позволяет получать информацию о взаимосвязи кислотных характеристик поверхности ПМВЭ-МК с ППГ и его функциональными свойствами. Благодаря этому открывается возможность определения области его применения для создания новых высокоэффективных композиционных материалов.

*Ключевые слова:* полиэлектролит, коллоидное титрование, потенциометрическое титрование, диссоциация, гидрогель.

#### References

- 1 Filippova, O.E. (2000). «Vospriimchivye» polimernye heli [Responsive polymer gels]. *Vysokomolekularnye soedineniia — Polymer Science*, 42, 12, 2328 [in Russian].
- 2 Burkeev, M.Zh., Tazhbaev, E.M., & Sarsenbekova, A.Zh. (2017). *Polihlikolmaleinaty v reaktziiakh radikalnoi sopolimerizatsii [Polyglycol maleate in radical polymerization reaction]*. Beau Bassin: LAP LAMBERT Academic Publishing [in Russian].
- 3 Galaev, I.U. (1995). «Umnye» polimery v biotekhnologii i meditsine [Smart Polymers in Biotechnology and Medicine] *Uspekhi khimii — Chemical Reviews*, 65, 5, 505–524 [in Russian].
- 4 Burkeev, M.Zh., Kudaibergen, G.K., Tazhbayev, Ye.M. et al. (2019). Synthesis and investigation of copolymer properties on the basis of poly(ethylene glycol)fumarate and methacrylic acid. *Bulletin of the Karaganda University. Ser. Chemistry*, 1(93), 32–38.
- 5 Toroptseva, A.M., Belogrodskaya, K.V., & Bondarenko, V.M. (1972). *Laboratornyi praktikum po khimii i tekhnologii vysokomolekuliarnykh soedinenii [Laboratory Workshop on Chemistry and Technology of High Molecular Compounds]*. Moscow: Khimiia [in Russian].
- 6 Bykova, L.N., & Petrov, S.I. (1972). Kislотно-osnovnye равновесия в среде амфипротонных растворителей и потенциометрическое титрование [Acid-basic equilibrium in amphiprotic solvent medium and potentiometric titration]. *Uspekhi khimii — Chemical Reviews*, 42, 2065–2093 [in Russian].
- 7 Nagasawa, M., Murase, T., & Kondo, K. (1965). Potentiometric titration of stereoregular polyelectrolytes. *J. Phys. Chem.*, 69, 4005–4012.
- 8 Kazitsyna, L.A., & Kupletskaya, N.B. (1971). *Primenenie IK-, UF-, YaMR-spektroskopii v orhanicheskoi khimii [Application of W-, IR-, NMR-spectroscopy in Organic Chemistry]*. Moscow: Vysshiaia shkola [in Russian].
- 9 Ebel, S. (1969). Calculation of titration curves of weak acids and bases. Calculation of titration curves. *Arch Pharm*, 302, 856–862.
- 10 Lappan, U., Geißler, U., Oelmann, M., & Schwarz, S. (2012). Apparent dissociation constants of polycarboxylic acids in presence of polycations. *Colloid Polym Sci.*, 290, 1665–1670.

B.P. Shipunov, A.V. Ryabykh

*Altai State University, Barnaul, Russia  
(E-mail: sbp@mc.asu.ru)*

## **Change in the heat of D-glucose dissolution in water exposed to electromagnetic field**

The article is devoted to the study of the influence of weak electromagnetic fields of 90, 110 and 170 MHz frequency on water properties. The calorimetric measurement of the integral heat of dissolution of non-electrolyte ( $\alpha$ -D-glucose) was chosen as an indirect method to study the change in water properties. The heat of  $\alpha$ -D-glucose dissolution was measured in relation to field frequency for the first time. The results of calorimetric measurements of the thermal effects of the carbohydrate dissolution in field-exposed water compared with unirradiated are presented. The measurements were carried out with a Beckman thermometer. The dependence of the relative heat of  $\alpha$ -D-glucose dissolution on time after field exposure was established. A cumulative character takes place for the 90 MHz and 110 MHz frequencies. That is reflected in the gradual increase of endoeffect. The dependence has a maximum on the third day in the case of 170 MHz. A sharp change in the heat of dissolution was observed within three days for the 90 MHz and 110 MHz frequencies. Further a weak time dependence is registered after twenty days. In general, there is an increase in the endothermicity of the  $\alpha$ -D-glucose dissolution process. The assumption has been made that the hydration heat of a carbohydrate molecule in field-exposed water reduces due to the increased intermolecular interactions between water particles and weakened interactions between water particles and carbohydrate molecules.

*Keywords:* electromagnetic field, glucose, heat of dissolution, calorimetry, hydration, thermodynamics, carbohydrate solutions, frequency.

### *Introduction*

Interest in the impact of weak physical fields on different objects is increasing every year. This is primarily due to the fact that the density of such fields of artificial origin grows, covering the region of ever higher frequencies for communication and navigation and increasing the density of broadcasting on the previously used ranges. In this regard, it is interesting to study the problems of efficiency and effectiveness of field impact in various processes. Water and aqueous solutions is one of the common objects of influence. It is known that fields influence the properties of water and aqueous solutions. These effects are explained by a change in the energy of water molecules interaction in a liquid state, i.e. the change in the hydrogen bond energy. Earlier a method to quantify the change in the energy of hydrogen bonds due to the influence of a magnetic field by calorimetric estimation of the heat of solids dissolution was proposed [1].

Internal energy  $dU$  and enthalpy  $dH$  are the thermodynamic functions that describe intermolecular interactions. They are related by the equation  $dH = dU + pdV$ . The volume change is minimal within solution formation process, therefore the equality of internal energy and enthalpy can be assumed. The enthalpy of dissolution (or the thermal effect of dissolution at constant pressure) can be determined experimentally by the calorimetric method.

Previously, experiments have been conducted to measure the thermal effects of salt dissolution. Starting from the fundamental works of Klassen [2] it was shown that the heat of salts dissolution in magnetized and normal water is noticeably different. In an article [3], it was found that the thermal effect of dissolution for potassium chloride during water magnetization within eight hours changes by 25 %. The results on the change in the thermodynamic properties of crystalline hydrates grown from solutions exposed to low-power high-frequency (HF) electromagnetic fields in the range of 30–200 MHz are no less interesting [4]. The presented data shows a multidirectional effect depending on the field frequency. The explanation is based on the assumption of structural reorganization of water and water clusters and changes in the degree of ion hydration, which is also confirmed by experimental data on the measurement of the electrical conductivity of salt solutions in field-affected water [5].

However, a small number of experiments with the dissolution of non-electrolytes in field-exposed water are known to date. Thermal effects of propanol-1 — water mixing are presented in [6]. When using water exposed to a high-frequency electromagnetic field, the heats of mixing noticeably change both towards the

increase of thermal effect and towards its decrease depending on the field frequency. The changes in the heat of mixing are also dependent on the exposure time and the initial temperature. The authors assume that the observed phenomena occur due to the changes in the energy of interaction of propanol molecules with a structurally reorganized solvent.

In the above studies, we measured either the heat of mixing of two liquids or the heat of dissolution (dehydration) of inorganic salts. To supplement the experimental data, it is of interest to study the dependence of the dissolution enthalpy of a non-electrolyte solid in treated water on the frequency of high-frequency (HF) field.

Natural monosaccharides such as glucose are unique on their properties. Having a chiral atom in its structure and exhibiting optical activity, these molecules are characterized by high hydration capacity due to the presence of a large number of hydroxyl groups. There are other unique properties that ensure the cycle opening in aqueous solution and the conformational transformation of molecules of these carbohydrates [7]. The interest in the thermodynamics of carbohydrates aqueous solutions has not only exhausted, but has increased even more. One of the reasons is the fact that carbohydrate aqueous solutions serve as a good model of solvation interactions [8].

Carbohydrate molecules are bifunctional in relation to their hydration capacity. Hydration includes a specific hydrophilic hydration through the formation of hydrogen bonds between hydroxyl carbohydrate groups and water particles, as well as a specific hydrophobic hydration through intermolecular interactions between CH- and CH<sub>2</sub>- carbohydrate groups and water particles [8].

Application of molecular dynamics methods to aqueous solutions of  $\beta$ -D-glucose made it possible to model the structure of hydrogen bonds. Calculations showed that the hydrogen-bond network differs little from the network in the crystal structure [9]. It is assumed that when considering the interaction of water with carbohydrate molecules, it is necessary to take into account the complementarity of the geometry of the location of hydroxyl groups and the structural matrix of the solvent [8]. Franks [10, 11] first studied the problem of stereospecific hydration of carbohydrates. The specificity of hydration is determined by the ratio of the number of axial and equatorial hydroxyl groups with a preferred hydration of the latter [12]. According to Franks, hydration is ensured by a good agreement between the geometry of the equatorial OH-groups and the water matrix. The distance between the oxygen atoms in equatorial hydroxyls is 0.485 nm, which lies in the region of the second maximum of the radial function of water distribution (0.49 nm). This fact suggests that the carbohydrate molecule is embedded in the structure of the hydrogen bonds of the solvent [8]. It follows that when glucose dissolves, the dynamic structure of hydrogen bonds is perturbed and recovered, with some water particles being replaced by glucose molecules. In [13] it was assumed that after the dissolution of the carbohydrate the hydrogen-bond network is structured.

Given the above, the research was aimed at the study of changes in the heat of glucose dissolution in water exposed to high-frequency electromagnetic field of certain frequencies.

### *Experimental*

To estimate the changes in the intermolecular interactions of glucose and field-exposed water, we used the literature data on the integral heats of dissolution. According to these data, the thermodynamic characteristics of  $\alpha$ -D-glucose dissolution in water at 298.15 K are as follows:

$\Delta H^\circ = 11.028 \pm 0.017$  kJ/mol — integral heat of dissolution at infinite dilution;

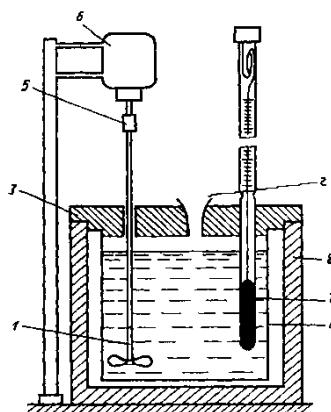
$T\Delta S^\circ = 18.1$  kJ/mol — entropy factor;

$\Delta G^\circ = 7.1 \pm 0.5$  kJ/mol — change in Gibbs dissolution energy.

The integral heat of  $\alpha$ -D-glucose monohydrate dissolution at infinite dilution is 19 kJ/mol [8].

The frequencies of the electromagnetic field of 90, 110 and 170 MHz were chosen as the most effective, based on previous studies in the field of water systems [15].

The G4-119A high-frequency generator was used to exert a field effect on water. A sample of deionized water was placed in an axial-type cell, the design of which is described in [15]. The cell was connected to a generator, which was used to set a certain frequency of HF field. The field exposure with a certain frequency lasted continuously for two hours. At the end of the field exposure, the water sample was either used immediately or placed in an airtight container and used at different time intervals after the field action. The measurements were carried out on a calorimetric setup, the scheme of which is shown in Figure 1.



1 — stirrer; 2 — hole for introducing a soluble substance; 3 — lid; 4 — inner coating;  
5 — stirrer fixing; 6 — motor; 7 — Beckman thermometer; 8 — outer coating

Figure 1. Scheme of calorimetric setup

For calorimetric measurements, we weighed 2.000 g of  $\alpha$ -D-glucose monohydrate accurate to 0.001 g and placed the sample in a control tube, afterwards the tube was weighed. A pipette was used to measure 100 ml of water, which was poured into a 400 ml porcelain beaker, which was then put into a calorimeter. Thereupon, we placed a tube with glucose and a Beckman metastatic thermometer through a hole 2. The control tube was kept in a calorimeter until a uniform variation of temperature over time was established. When the range of readings became uniform, we quickly emptied glucose out of the control tube through hole 2. After the start of the main period, the thermometer readings were recorded every 30 seconds. We completed the measurement when a uniform variation of temperature was established. The control tube was weighed, and the specified mass of dissolved glucose was calculated. The temperature drop corrected for heat exchange was found using the graphical method. A similar experiment was carried out with field-exposed water. Each experiment was repeated twice. The relative change in the dissolution enthalpy was calculated by the formula:

$$\Delta H_r = \frac{\Delta H_{ex} - \Delta H_c}{\Delta H_c} \cdot 100\%, \quad (1)$$

$\Delta H_r = \frac{\Delta H_{ex} - \Delta H_c}{\Delta H_c} \cdot 100\%$ , where  $\Delta H_r$  is the relative change in the heat of dissolution, %;  $\Delta H_{ex}$  is the heat of dissolution in field-exposed water, kJ/mol;  $\Delta H_c$  is the heat of dissolution in the control experiment (without field exposure), kJ/mol.

According to formulas 1–3, the data were reduced to the same mass of glucose sample:

$$\frac{\Delta H_{ex} \cdot m_{ex}}{M_g} = C \cdot \Delta T_{ex} \quad (2)$$

By subtracting (1) from (2), dividing the difference by (1) and performing the simplest transformations, we obtained:

$$\frac{\Delta H_{ex} - \Delta H_c}{\Delta H_c} = \frac{m_c \cdot \Delta T_{ex} - m_{ex} \cdot \Delta T_c}{m_{ex} \cdot \Delta T_c}, \quad (3)$$

where  $m_c$  is the mass of glucose in the control experiment;  $m_{ex}$  is the mass of glucose in the experiment with field exposure;  $C$  is the calorimeter constant, J/K;  $\Delta T_c$  — temperature change during dissolution in the control experiment K;  $\Delta T_{ex}$  — temperature change during dissolution in the experiment with field exposure;  $M_g$  is the molar mass of glucose monohydrate, g/mol.

Thus, there is no need to determine the calorimeter constant for each experiment, if we compare the heats of dissolution under control.

The heat of glucose dissolution was measured immediately after field action (0 days), on days 3, 11, and 21. We also used two water samples subjected to field effect 60 days ago (110 and 170 MHz) and 133 days ago (90 MHz).

### Results and Discussion

Obtained dependences of heat of glucose dissolution on time of water exposure (90, 110 and 170 MHz) are presented in Figures 2–4.

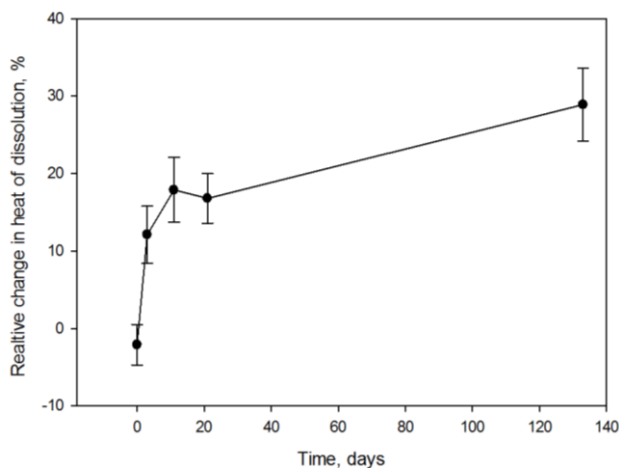


Figure 2. Dependence of heat of glucose dissolution on time of water exposure. Frequency of field exposure — 90 MHz

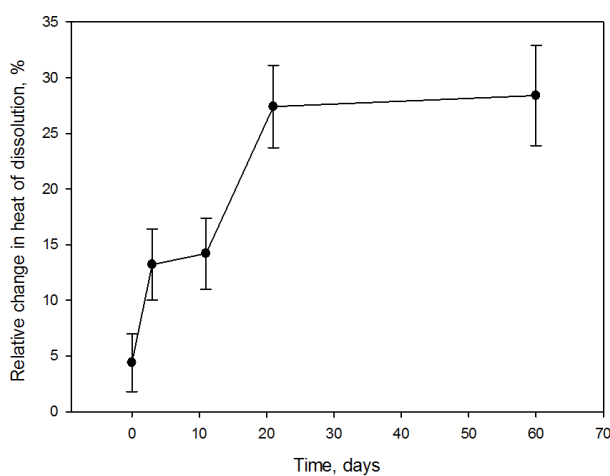


Figure 3. Dependence of heat of glucose dissolution on time of water exposure. Frequency of field exposure — 110 MHz

In all cases the dependence of the field effect on the time of water exposure is clearly observed. The heat of dissolution measured immediately after the field effect does not differ from the control one. For each of the frequencies, a sudden change in the heat of dissolution takes place on the third day after the exposure. The time dependence of the effect for the frequencies of 90 MHz and 110 MHz is similar: after the third week a «saturation» of the effect is observed, i.e. it becomes time-independent. For the 170 MHz frequency, there is an extreme dependence; the maximum is reached on the third day. Experimental data correlate with other data given in [14], which reports an increase in field effect during the week.

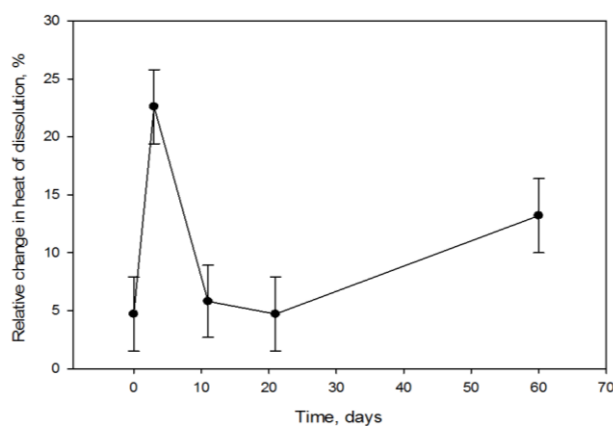


Figure 4 Dependence of heat of glucose dissolution on time of water exposure. Frequency of field exposure — 170 MHz

The solubility enthalpy can be represented as the sum of two opposite in sign components:

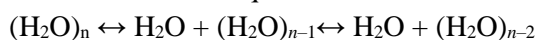
$$\Delta H_{\text{dissol}}^0 = \Delta H_{\text{cell}}^0 + \Delta H_{\text{hydrat}}^0, \quad (4)$$

where  $\Delta H_{\text{dissol}}^0$  is the dissolution enthalpy;  $\Delta H_{\text{cell}}^0$  is the enthalpy of the crystal lattice of glucose ( $> 0$ );  $\Delta H_{\text{hydrat}}^0$  is the hydration enthalpy ( $< 0$ ).

As can be seen from the literature data [8], the heat of  $\alpha$ -D-glucose dissolution is positive. It means that the energy of the crystal lattice prevails over the energy of hydration. The enthalpy of the crystal lattice can be considered constant in all calorimetric experiments, since only water was exposed to the field. Although we used the monohydrate, the heat of hydration cannot be considered equal to zero. An additional intermolecular interaction between water and glucose may occur.

In all cases (except for the first point in Figure 2), a change in the thermal effect towards endothermic values is observed. Based on Franks' assumption that a carbohydrate molecule is embedded in the solvent hydrogen bond network, we can assume an increase in the interactions of homogeneous particles: water — water and carbohydrate — carbohydrate. Additional hydration of the monohydrate occurs either to a lesser extent in the field-exposed water, or does not occur at all, or dehydration occurs. This correlates with a change in the heat value in a positive direction, i.e. the predominance of the energy of the crystal lattice over the energy of hydration.

Taking into account the existence of short-lived water molecules associates (clusters), formed by hydrogen bonds, we can assume that the HF field shifts the equilibrium:



which is characterized by the equilibrium constants  $K_1$  and  $K_2$ .

The values of the constants depend on the strength of interaction of the water molecule with the collective aggregate, which, in turn, essentially depends on the number of particles in the aggregate and the perfection of its structure. If, based on the data of some researchers [16, 17], we consider the energy of separation of water molecule from the  $n > 10$  aggregate, about 30 kJ/mol and take the size of an aggregate of hundreds or thousands of water molecules, then the values of  $K_1$  and  $K_2$  will differ slightly. Despite the fact that clusters exist for a very short time (a few picoseconds) due to heat motion, they may be formed again. Under this assumption, the time dependence can be explained by the time it takes to reach a new equilibrium between different particles in water. Based on the Figures 2–4, it is possible to conclude that the time to reach equilibrium in the case of frequencies of 90 MHz and 110 MHz is approximately three weeks. At 170 MHz frequency, an unstable equilibrium occurs on the third day, which, for reasons unknown so far, relaxes to the original.

### Conclusion

Summarizing all the above mentioned it is possible to come to the following conclusion:

1. Preliminary field effect on water with frequencies of 90, 110 and 170 MHz increases the endothermicity of  $\alpha$ -D-glucose dissolution;
2. For 90 and 110 MHz frequencies a cumulative time effect is observed, with «saturation» after 21 days. For 170 MHz frequency the maximum effect occurs on the third day;
3. It has been suggested that the interaction of water-water particles increases as a result of the field effect on the solvent that explains the decrease in the enthalpy of carbohydrate hydration;
4. For the first time, it was found that the field effect depends on water exposure time after the field action. The maximum effect for different frequencies is observed under different exposure time.

### References

- 1 Патент RU 2300757 (C2) Россия. Способ calorиметрического определения измерения энергии водородных связей после воздействия на водные системы магнитного поля / Б.П. Шипунов, К.В. Селиков. Оpub. 10.06.2007.
- 2 Классен В.И. Вода и магнит / В.И. Классен. — М.: Наука, 1973. — 111 с.
- 3 Селиков К.В. Исследование воздействия постоянного магнитного поля на некоторые свойства воды и водных растворов / К.В. Селиков, Б.П. Шипунов // Изв. вузов. Сер. Химия и хим. технол. — 2005. — Т. 28, № 9. — С. 50–54.
- 4 Чашева Ю.В. Влияние ВЧ поля на термодинамическую устойчивость кристаллогидратов хлорида кобальта / Ю.В. Чашева, Б.П. Шипунов // Изв. вузов. Сер. Физика и химия материалов. — 2014. — Т. 57, № 7/2. — С. 202–204.
- 5 Стась И.Е. Влияние высокочастотного электромагнитного поля на свойства растворов хлоридов щелочных металлов / И.Е. Стась, А.П. Гердт, Н.В. Аксенова // Изв. Алтай. гос. ун-та. — 2010. — № 3, 2. — С. 141–145.
- 6 Стась И.Е. Интегральные молярные теплоты смешения пропанола-1 и воды, подвергшейся воздействию высокочастотного электромагнитного поля / И.Е. Стась, В.Ю. Чиркова // Вестн. ВГУ. Сер. Химия. Биология. Фармация. — 2017. — № 2. — С. 36–42.

- 7 Кочетков Н.К. Химия углеводов / Н.К. Кочетков, А.Ф. Бочков, А.Б. Дмитриев и др. — М.: Химия, 1966. — 672 с.
- 8 Абросимов В.К. Биологически активные вещества в растворах. Структура. Термодинамика. Реакционная способность / В.К. Абросимов, А.В. Агафонов, Е.В. Антини. — М.: Наука, 2001. — 408 с.
- 9 Van Eijck B.P. Hydrogen-bond geometry around sugar molecules: Comparison of crystal statistics with simulated aqueous solutions / Van B.P. Eijck, L.M.J. Kroon-Batenburg, J. Kroon // J. Mol. Struct. — 1990. — Vol. 237. — P. 315.
- 10 Franks F. Water — a comprehensive treatise / F. Franks, D.S. Reid. — New York, USA: Plenum Press, 1973. — Vol. 2. — 323 p.
- 11 Franks F. Physical chemistry of small carbohydrates — equilibrium solution properties // Pure Appl. Chem. — 1982. — Vol. 59. — P. 1189.
- 12 Franks F. Water in food / F. Franks. — М.: Food industry, 1980. — 14 p.
- 13 Абросимов В.К. Достижения и проблемы теории сольватации. Структурно-термодинамические аспекты / В.К. Абросимов, А.Г. Крестов, Г.А. Альпер. — М., 1998. — 247 с.
- 14 Шипунов Б.П. Структурная организация и гомогенные равновесия в водных растворах. Влияние электромагнитного поля / Б.П. Шипунов. — Саарбрюкен (Saarbrücken): LAP LAMBERT Academic Publishing, 2014. — 104 с.
- 15 Stas' I.E. The Stripping Voltammetry // High Frequency Electromagnetic Field / I.E. Stas', B.P. Shipunov, T.S. Ivonina // Electroanalysis. — 2005. — Vol. 17, Iss. 5. — P. 794–799.
- 16 Lee H.M. Structures, energies, vibrational spectra, and electronic properties, of water monomer to decamer / H.M. Lee, S.B. Suh, J.Y. Lee, P. Tarakeshwar, K.S. Kim // J. Chem. Phys., 2000. — Vol. 112, Iss. 22. — P. 9759–9772.
- 17 Lee H.M. Structures, energies, and vibrational spectra of water undecamer and dodecamer: an ab initio study / H.M. Lee, S.B. Suh, K.S. Kim // J. Chem. Phys., 2001. — Vol. 114, Iss. 24. — P. 10749–10756.

Б.П. Шипунов, А.В. Рябых

## Электромагниттік өріс нәтижесінде суда D-глюкозаның еріген жылу әсерінің өзгеруі

Мақала судың қасиеттеріне арналған (90, 110 және 170 МГц) мегартерлердің әлсіз электромагниттік өрістерінің әсерін зерттеуге арналған. Электролит емес,  $\alpha$ -D-глюкозаны ерітудің интегралдық жылуының калориметриялық өлшемі судың қасиеттерін өзгертудің жанама әдісі ретінде таңдалған. A-D-глюкозаның ерітіндісінің жылуын өлшеу бірінші рет өріс жиілігінің функциясы ретінде өлшенді. Бекманның термометрімен салыстыруға келмеген, өрістегі суда көмірсулардың ерітіндісінің жылу әсерлерін калориметрикалық өлшеу нәтижелері келтірілген. Дала әсерінен кейінгі уақытқа  $\alpha$ -D-глюкозаны ерітудің салыстырмалы жылу тәуелділігі анықталды. 90 МГц және 110 МГц жиіліктер үшін кумулятивтік сипат бар, ал 170 МГц болған жағдайда тәуелділіктің үшінші күні ең жоғары мәнге ие. 90 МГц және 110 МГц жиіліктер үшін үш күн ішінде еріген жылудың күрт өзгеруі байқалды, содан кейін жиырмасыншы күннен кейін уақытқа тәуелділік аз болады. Жалпы,  $\alpha$ -D-глюкозаны еріту процесінің эндотермиялықтығы анықталды. Суға әсер ететін судағы көмірсулар молекуласының гидратталуының жылу су бөлшектерінің аралық молекулалық өзара әрекеттесуі және су бөлшектерімен көмірсулар молекулалары арасындағы өзара әрекеттердің әлсіреуі салдарынан азаяды деп болжануда.

*Кілт сөздер:* электромагниттік өріс, глюкоза, еріген жылу, калориметрия, ылғалдау, термодинамика, көмірсулардың ерітінділері, жиілігі.

Б.П. Шипунов, А.В. Рябых

## Изменение теплового эффекта растворения D-глюкозы в воде в результате действия электромагнитного поля

Статья посвящена исследованию влияния слабых электромагнитных полей мегагерцового диапазона (90, 110 и 170 МГц) на свойства воды. В качестве косвенного метода изучения изменения свойств воды было выбрано калориметрическое измерение интегральной теплоты растворения неэлектролита —  $\alpha$ -D-глюкозы. Впервые произведено измерение теплоты растворения  $\alpha$ -D-глюкозы в зависимости от частоты электромагнитного поля, которое воздействовало на воду. Приведены результаты калориметрических измерений тепловых эффектов растворения углевода в воде, подвергшейся полевого воздействию, по сравнению с необлученной. Измерения проводились с помощью термометра Бекмана. Установлена зависимость относительной теплоты растворения  $\alpha$ -D-глюкозы от времени после полевого воздействия. Для частот 90 и 110 МГц имеет место накопительный характер, что выражается в постепенном увеличении эндозффекта, а в случае 170 МГц зависимость возникает максимум на третьи сутки. Для частот 90 и 110 МГц наблюдается резкое изменение теплоты растворения в течение первых трех суток, затем, после двадцатых суток, прослеживается слабая зависимость от времени. В целом, наблюдается увеличение эндотермичности процесса растворения  $\alpha$ -D-глюкозы в результате полевого

воздействия на воду. Наблюдаемые эффекты объясняются на основе предположения об уменьшении теплоты гидратации молекулы углевода в воде, подвергшейся полевому воздействию, вследствие усиления межмолекулярных взаимодействий между частицами воды и ослабления взаимодействий между частицами воды и молекулами углевода.

*Ключевые слова:* электромагнитное поле, глюкоза, теплота растворения, калориметрия, гидратация, термодинамика, растворы углеводов, частота.

## References

- 1 Shipunov, B.P. & Selikov, K.V. (2007). Sposob kalorimetriceskogo opredeleniia izmereniia enerhii vodorodnykh sviazei posle vozdeistviia na vodnye sistemy mahnitnogo polia [Method for calorimetric determination of measuring hydrogen bond energy after exposure to aqueous magnetic field systems]. *Russian Patent No. RU 2300757 (C2)*. Publ. 10.06.2007 [in Russian].
- 2 Klassen, V.I. (1973). *Voda i mahnit [Water and magnet]*. Moscow: Nauka [in Russian].
- 3 Selikov, K.V. & Shipunov, B.P. (2005). Issledovanie vliianiia postoiannogo mahnitnogo polia na nekotorye svoistva vody i vodnykh rastvorov [Investigation of the effect of a constant magnetic field on some properties of water and aqueous solutions]. *Izvestiia vuzov. Seriiia Khimiia i khimicheskaiia tekhnolohiia — Russian journal of chemistry and chemical technology*, 28, 9, 50–54 [in Russian].
- 4 Chashevaya, Yu.V. & Shipunov, B.P. (2014). Vliianie vysokochastotnykh polei na termodinamicheskuiu stabilnost kristallohidratov khlorida kobalta [The effect of high-frequency fields on the thermodynamic stability of cobalt chloride crystal hydrates]. *Izvestiia vuzov. Seriiia fizika i khimiia materialov — Russian journal of physics*, 57, 7/2, 202–204 [in Russian].
- 5 Stas', I.E., Gerdt, A.P. & Aksenova, N.V. (2010). Vliianie vysokochastotnogo elektromahnitnogo polia na svoistva rastvorov khloridov shchelochnykh metallov [Effect of high-frequency electromagnetic field on the properties of alkali metal chloride solutions]. *Izvestiia Altaiskoho gosudarstvennogo universiteta — Izvestiia of Altai State University Journal*, 3–2, 141–145 [in Russian].
- 6 Stas', I.E. & Chirkova, V.U. (2017). Intehrlnaia moliarnaia teplota smesi propanola-1 i vody pod vozdeistviem vysokochastotnogo elektromahnitnogo polia [Integral molar heat of mixture of propanol-1 and water, exposed to high-frequency electromagnetic field]. *Vestnik Voronezhskoho gosudarstvennogo universiteta. Seriiia Khimiia. Biolohiia. Farmatsiia — Proceeding of Voronezh State University. Series Chemistry. Biology. Pharmacy*, 2, 36–42 [in Russian].
- 7 Kochetkov, N.K., Bochkov, A.F. & Dmitriev, A.B. (1966). *Khimiia uhlevodov [Chemistry of carbohydrates]*. Moscow: Khimiia [in Russian].
- 8 Abrosimov, V.K. (2001). *Biolohicheski aktivnye veshchestva v rastvore. Struktura. Termodinamika. Reaktivnost [Biologically active substances in solution. Structure. Thermodynamics. Reactivity]*. Moscow: Nauka [in Russian].
- 9 Van Eijck, B.P., Kroon-Batenburg, L.M.J. & Kroon, J. (1990). Hydrogen-bond geometry around sugar molecules: Comparison of crystal statistics with simulated aqueous solutions. *J. Mol. Struct.*, 237, 315.
- 10 Franks, F., Reid, D.S. (1973). *Water — a comprehensive treatise* (Vol. 2). New York: Plenum Press.
- 11 Franks, F. (1989). Physical chemistry of small carbohydrates — equilibrium solution properties. *Pure Appl. Chem.*, 59, 1189.
- 12 Franks, F. (1980). *Water in food*. Moscow: Food industry.
- 13 Abrosimov, V.K., Krestov A.G. & Alper G.A. (1998). *Dostizheniia i problemy teorii solvatatsii: strukturnyi i termodinamicheski aspekti [Achievements and problems of the theory of solvation: Structural and thermodynamic aspects]*. Moscow: Nauka [in Russian].
- 14 Shipunov, B.P. (2014). *Strukturnaia orhanizatsiia i homohennoe ravnovesie v vodnykh rastvorakh. Vliianie polevogo vozdeistviia [Structural organization and homogeneous equilibrium in aqueous solutions. The influence of the electromagnetic field]*. Saarbrücken: LAP Lambert Academic Publishing [in Russian].
- 15 Stas', I.E., Shipunov, B.P. & Ivonina, T.S. (2005). The Stripping Voltammetry in High Frequency Electromagnetic Field. *Electroanalysis*, 17, 5, 794–799.
- 16 Lee, H.M., Suh, S.B., Lee, J.Y., Tarakeshwar, P. & Kim, K.S. (2000). Structures, energies, vibrational spectra, and electronic properties, of water monomer to decamer. *Journal of Chemical Physics*, 112, 22, 9759–9772.
- 17 Lee, H.M., Suh, S.B. & Kim, K.S. (2001). Structures, energies, and vibrational spectra of water undecamer and dodecamer: an ab initio study. *Journal of Chemical Physics*, 114, 24, 10749–10756.

A.Sh. Kazhikenova<sup>1</sup>, D.B. Alibiyev<sup>1</sup>, A.B. Seitimbetova<sup>1</sup>, Zh.M. Tentekbayeva<sup>2</sup>

<sup>1</sup>Ye.A. Buketov Karaganda State University, Kazakhstan;

<sup>2</sup>Karaganda State Technical University, Kazakhstan

(E-mail: aigul-kazhikenova@mail.ru)

### Relationship of associated clusters degree with metal ionization according to the cluster-associate model

This article deals with a cluster-associate model of kinematic viscosity of liquid metals. This model was derived from the concept of chaotized particles. According to the proposed model, the authors calculated average values clusters association degree contained in liquid metal. 28 metals of the second — sixth periods of D.I. Mendeleev element table were studied for calculation. The authors compare the first potential of metal ionization with the obtained values of clusters association degree. This comparison showed a regular change in clusters association degree closely connected with the change in the first ionization potential. In combination with the Fraenkel equation, an approximate equation was obtained to calculate activation energy. The obtained equation for the cluster-associate pattern of viscosity temperature dependence is used in calculating the activation energy of viscous melt flow for twenty-eight metals. The obtained results on activation energy were compared to experimental data. This comparison showed that the activation energy data obtained from the proposed model is described better by the approximating dependence. Tables and figures are given in the work for visual confirmation of the obtained results. Thus, in the process of comparing the first potential of metal ionization for all periods of D.I. Mendeleev element system with clusters association degree, their regular connection was revealed. This connection makes it possible to assert the functional aspect of the cluster-associate pattern.

*Keywords:* viscosity, chaotized particles, degree of cluster association, cluster-associate pattern, liquid metals, activation energy, crystal mobile particles, ionization potential, modified Fraenkel equation.

#### Introduction

In 2008 in the Chemical and Metallurgical Institute named after Zh. Abishev doctors of technical sciences V.P. Malyshev and A.M. Turdukozhayeva developed a concept of chaotized particles based on Boltzmann distribution. According to the concept, three aggregate states of the substance are considered from a single point of view by its structure less component. In all cases, particles which differ only in the energy magnitude of chaotic motion are considered. According to the concept of chaotized particles in each of the three aggregate states there are *crystal mobile*, *liquid mobile* and *vapor mobile* particles. However with the temperature rise and overcoming of various chaotization energy barriers, the proportion of these particles changes.

The proportion of these particles is calculated according to the equations

$$P_{crm} = 1 - \exp(-T_m / T)$$

$$P_{vm} = \exp(-T_b / T)$$

$$P_{lqm} = 1 - P_{crm} - P_{vm} - \exp(-T_m / T) - \exp(-T_b / T).$$

Here  $P_{cm}$  is the proportion of crystal mobile particles;  $P_{vm}$  is the proportion of vapor mobile particles;  $P_{lqm}$  is the proportion of liquid mobile particles;  $T$  — temperature;  $T_m$  — melting temperature,  $T_b$  — boiling temperature.

Earlier in the work [1] three models were proposed with the consideration of different content of crystal mobile, liquid mobile and vapor mobile particles. But the need to test each of the three viscosity models and to choose the most adequate brings some elements of uncertainty in the design method of such a dependence, in addition complicating the data processing procedure. This led us to develop a single cluster-associate model

$$\nu = \nu_r (T_r / T)^a. \quad (1)$$

According to the concept of chaotized particles, a cluster is a probabilistic form of the existence of various low-energy complexes from crystal mobile particles. Calculations of clusters proportion and quantity for a mole of substance at the melting and boiling point have shown that the concept of chaotized particles allows to quantify the formation of clusters with their distribution by the number of particles in the liquid at any temperature.

In the same work [1], the model validity (1) to the calculation of liquid metals viscosity was shown. It has been shown that the model (1) for many metals most adequately describes the temperature dependence of viscosity and can be used to calculate the viscosity at high temperatures without the performance of experiment. For many metals equations for viscosity were derived.

### Experimental

In the work [2] three models (taking into account crystal mobile, liquid mobile and vapor mobile particles) of kinematic viscosity of metals were compared with their ionization potentials for all periods of D.I. Mendeleev element system, analysis of which revealed regular connection of values of this potential with model numbers ranked by increase of temperature influence on viscosity. In this work we will compare cluster-associate pattern (1) by the degree of clusters association with the first ionization potential of the considered metals for all periods of D.I. Mendeleev element system.

This comparison is shown in Table 1 and Figure 1.

Table 1

Comparison of the first ionization potentials of the metal with the degree of cluster association

Period	Me	Valence shell	$I_1$ , eV	$\bar{a}$	Period	Me	Valence shell	$I_1$ , eV	$\bar{a}$
2	Li	$2s^1$	5.390	1.01	5	Rb	$5s^1$	4.176	1.22
	Be	$2s^2$	9.320	9.51		Sr	$5s^2$	5.692	2.01
3	Na	$3s^1$	5.138	1.35		Ag	$4d^{10}5s^1$	7.574	1.82
	Mg	$3s^2$	7.644	2.57		Cd	$4d^{10}5s^2$	8.991	1.80
	Al	$3s^2p^1$	5.984	1.03		In	$4d^{10}5s^25p^1$	5.785	0.96
4	K	$4s^1$	4.339	1.22		Sn	$4d^{10}5s^25p^2$	7.342	0.97
	Ca	$4s^2$	6.111	1.68		Te	$4d^{10}5s^25p^4$	9.01	2.77
	Fe	$3d^64s^2$	7.87	3.54		6	Cs	$6s^1$	3.894
	Co	$3d^74s^2$	7.86	3.05	Ba		$6s^2$	5.211	1.56
	Ni	$3d^84s^2$	7.63	1.92	Au		$4f^{14}5d^{10}6s^1$	9.22	1.44
	Cu	$3d^{10}4s^1$	7.724	1.65	Hg		$4f^{14}5d^{10}6s^2$	10.43	0.90
	Zn	$3d^{10}4s^2$	9.391	1.90	Tl		$4f^{14}5d^{10}6s^26p^1$	6.106	1.32
	Ga	$3d^{10}4s^24p^1$	6.00	0.91	Pb		$4f^{14}5d^{10}6s^26p^2$	7.145	0.79
Ge	$3d^{10}4s^24p^2$	7.88	2.81	Bi	$4f^{14}5d^{10}6s^26p^3$		7.287	1.36	

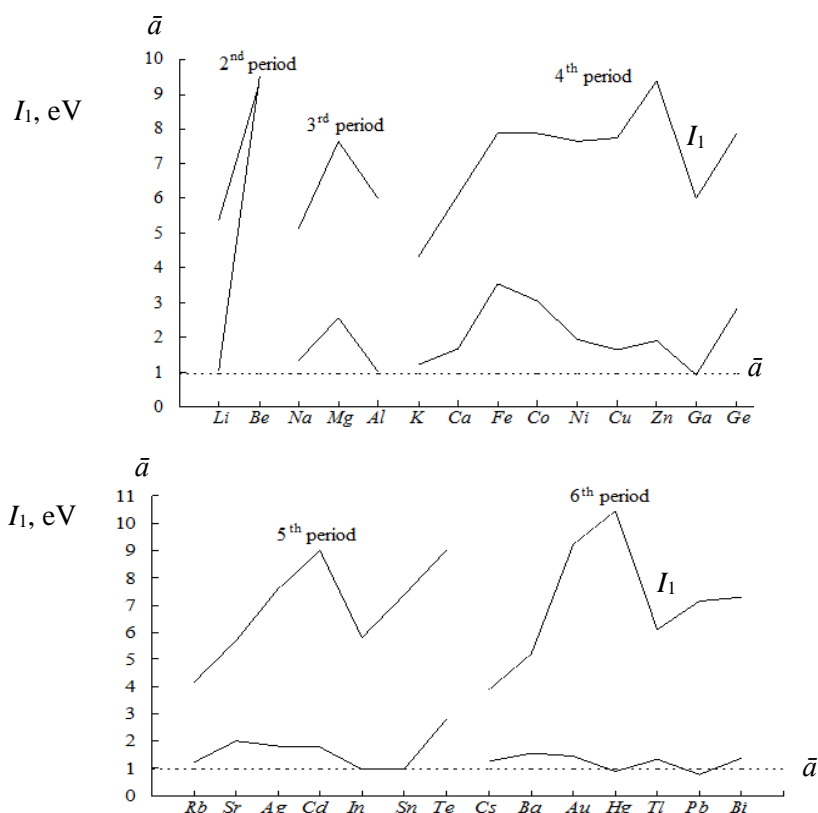
As can be seen from the table and the figure, in general there is a symbate (consistent) change in the degree of clusters association with the increase or decrease of the first potential value of metal ionization for all periods of Mendeleev element system. Some departure of this model becomes apparent for silver in the fifth period and for gold, mercury, thallium and lead in the sixth period, that is connected with big tendency to clusters association from metal atoms for beryllium, with influence of  $4d$ -subshell for silver, with completion

of 4*f*- and 5*d*-subshells development for metals of the sixth period, and mercury and lead also have 6*s*-subshell accompanied by lanthanide contraction and sharp increase in ionization potential.

The average value of cluster association for 28 metals is  $\bar{a} = 1.94$ . The obtained values of clusters association degree of the tested metals were checked for range uniformity according to equations [3]:

$$r_{\min}^{\max} = \frac{|\bar{x} - x_{\min}^{\max}|}{S(x)\sqrt{\frac{n-1}{n}}} \leq r_{cr}, \quad S(x) = \sqrt{\frac{\sum (x_i - \bar{x})^2}{n-1}},$$

where  $x_{\min}^{\max}$  is the minimax value of the range;  $\bar{x}$  is the average value;  $S(x)$  is the mean-root-square error and  $n$  is the volume of the range,  $r_{cr} = 1.483f^{0.187}$  [3; 15] where  $f = n - 2$ .



$I_1$  is the first ionization potential;  $\bar{a}$  — average degree of cluster association

Figure 1. Dependence of ionization potential and average value of clusters association degree for 28 metals in order of increasing of their atomic number

This test showed that for 28 metals, the range is not uniform: mean-root-square error  $S(x) = 1.645$ ; in equation  $r_{\min}^{\max} \leq r_{cr}$  is not observed  $r_{\min}^{\max} = 4.68 > r_{cr} = 2.73$ ;  $x_{\min}^{\max} = 9.51$  (for Be).

Therefore, it is necessary to eliminate the «jumping out» value, i.e. the beryllium data. The high value of association degree of beryllium clusters is connected with its high position in the periodic table, partial possession of covalent links, high tendency to associate clusters of metal atoms, and high ionization potential. Beryllium generally refers to semi-metals, which causes its exclusion from a variety of metals.

The elimination of beryllium and reduction of range up to 27 metals leads to validity of range uniformity:  $S(x) = 0.780$ ;  $r_{\min}^{\max} = 2.46 < r_{cr} = 2.71$ ;  $x_{\min}^{\max} = 3.54$  (for Fe).

In this case for 27 metals  $\bar{a} = 1.66 \pm 0.32$ .

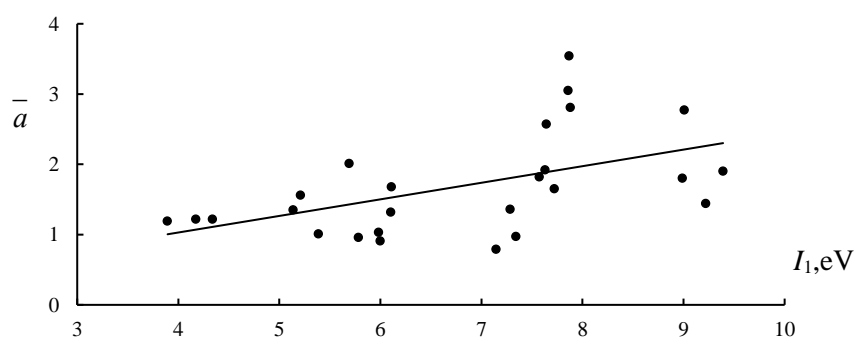
### Results and Discussion

Research for calculation of clusters association degree are conducted on the most uniform simple substances — metals, therefore this indicator has low values and changes within ~1–4 (excepting beryllium) (Table 1). Without this semimetal, and in addition lower than normal associated mercury ( $\bar{a} = 0.9$ ) at its anomalously high ionization potential (10.43 eV), generally regular and probably significant, although weakly expressed as cendant dependence of cluster association with metal ionization potentials is observed

$$\bar{a} = 0.09 + 0.24I_1, R = 0.70, t_R = 6.7 > 2. \quad (2)$$

The weakness of this connection is explained by the secondary nature of associates formation in comparison with the primary processes of elementary  $n$ -particle clusters formation from crystal mobile particles, as it was demonstrated earlier on the example of more evident interconnection of the standard three models with metal ionization potentials. The conformity consists in a great tendency to association of ionic complexes — clusters, which have stronger attraction of universal mobile electrons.

The relationship between cluster association and ionization potential for 26 metals, without mercury and beryllium, is shown in Figure 2.



$I_1$  is the first ionization potential;  $\bar{a}$  — average degree of cluster association. Points are data from Table 1, line — according to the equation (2) without data on Be and Hg

Figure 2. Relationship between cluster association and metal ionization potential

Ya.I. Fraenkel, on the basis of activation motion mechanism, obtained in 1927 the equation of dependence of dynamic viscosity on temperature

$$\eta = A \exp\left(\frac{E_a}{RT}\right), \quad (3)$$

where  $E_a$  is the activation energy;  $R$  is the gas constant;  $T$  is the temperature;  $A$  is some constant proposed by Arrhenius.

As the kinematic viscosity is connected with dynamic viscosity on a formula  $\nu = \eta/\rho$  ( $\rho$  — melt density), because of very weak dependence of density on temperature (several percent in all range of liquid state) in comparison with 3–4 multiple change of viscosity in the same range [4], it is possible to change directly in the equation (3) apparent viscosity  $\eta$  to kinematic viscosity  $\nu$ , having respectively corrected parameters  $A$  to  $A'$  and activation energy  $E_a$  to estimated value  $E'_a$

$$\nu = A' \exp\left(\frac{E'_a}{RT}\right). \quad (4)$$

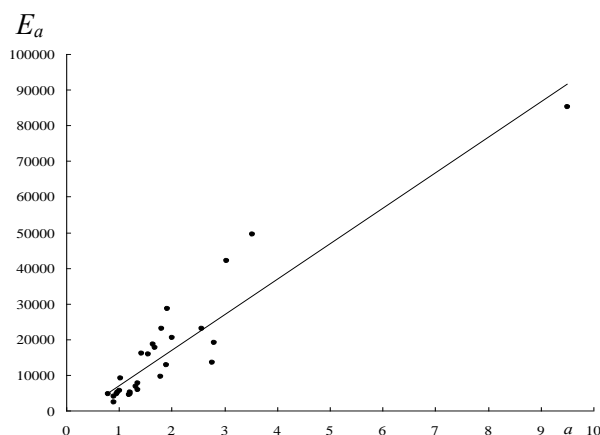
Table 2 shows the activation energy values obtained from the modified Fraenkel equation (4) based on experimental (information) and calculated on cluster-associate model (1) data for 28 metals of D.I. Mendeleev periodic system.

The activation energy values for the calculated data range from 2868 J/mole (mercury) to 128017 J/mole (beryllium). The correlation coefficient for the calculated activation energy values  $E'_a$  (calc) in comparison with experimental  $E_a$  (inf) comprised 0.8580 with its signification  $t_R = 16.6 > 2$  including beryllium. At its exception the correlation coefficient is much higher than  $-R = 0.9552$  with its signification  $t_R = 55.6 > 2$ .

Activation energy values for experimental ( $E_a$  (inf)) and calculated on cluster-associate model (1) ( $E_a'$  (calc)) data for 28 metals

Element	$E_a$ (inf), J/mole	$E_a'$ (calc), J/mole	Element	$E_a$ (inf), J/mole	$E_a'$ (calc), J/mole
Li	5463	5920	Rb	4548	5055
Be	85231	128017	Sr	20453	22723
Na	5803	6485	Ag	22981	21684
Mg	22915	22150	Cd	9487	10867
Al	9029	8871	In	4681	5629
K	5138	5812	Sn	5155	5496
Ca	17635	20171	Te	13478	21476
Fe	49404	55540	Cs	4498	5072
Co	41971	46835	Ba	15889	17543
Ni	28610	29757	Au	16038	17294
Cu	18450	22133	Hg	2262	2868
Zn	12713	14134	Tl	6652	9154
Ga	3850	4074	Pb	4714	4448
Ge	19098	31004	Bi	7649	8447

Figures 3 and 4 show the comparison of the obtained range of activation energy data for experimental and calculated on cluster-associate pattern viscosity with the degree of cluster association for the metals under investigation,  $E_a = f(\bar{a})$ .



$E_a$  is the activation energy, J/mole;  $\bar{a}$  is the average degree of cluster association.

Points are experimental data, line is approximation of experimental data by equation  $E_a = A + B\bar{a}$

Figure 3. Dependence of activation energy for experimental data on the degree of clusters association for 28 metals

As can be seen from the figures, the activation energy data obtained by processing the calculated values from the generalized pattern are described better by the approximate dependence.

The approximate equation for experimental data on viscous flow activation energy is expressed as:

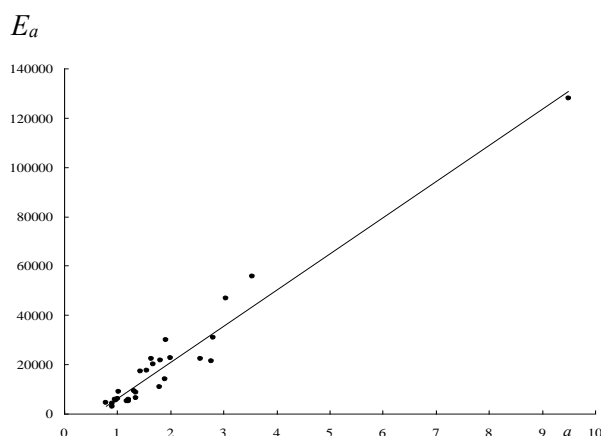
$$E_a(\text{inf}) = B\bar{a} + A = 9957 \bar{a} - 2731. \quad (5)$$

For calculated on cluster-associate model (1):

$$E_a'(\text{calc}) = B'\bar{a} + A' = 14695 \bar{a} - 8525. \quad (6)$$

The approximation dependability value for the information data on viscous flow activation energy depending on the degree of cluster association gives 0.9277, for the calculated from the model (1) — 0.9754.

Virtually, the coefficient  $B$  in equation (5) and  $B'$  in equation (6) make up the value of the activation energy corresponding to one cluster and are expressed as J/(mole·cluster). For experimental data, this coefficient is equal on average to ~10 kJ/(mole·cluster), and for calculated values is equal to ~15 kJ/(mole·cluster).



$E_a$  is the activation energy, J/mole;  $\bar{a}$  is the average degree of cluster association. Points are experimental data, line is approximation of data calculated according to the model (1) by equation  $E_a' = B' \bar{a} + A'$

Figure 4. Dependence of activation energy calculated on model (1) on the degree of clusters association for 28 metals

Shown above calculations confirm the functional nature of the cluster-associate pattern, taking into account the degree of clusters association from crystal mobile particles, which are the basis of a single model, and allow to consider the obtained approval as another proof of objectivity of chaotized particles concept.

### Conclusions

1. The interconnection of clusters association degree in cluster-associate pattern of metals viscosity with their ionization potentials for all periods of D.I. Mendeleev element system reveals their regular relation similar to the previously proposed [2] three separated patterns. This confirms the functional nature of the new pattern, which retains clusters from crystal mobile particles as a physical basis, with additional consideration of their association.

2. Analysis of activation energy values obtained from the modified Fraenkel equation on the basis of experimental (information) and calculated on cluster-associate pattern data for 28 metals showed their adequate straight-line dependence, moreover the description of their interconnection with the degree of clusters association on the basis of the calculated from the proposed pattern activation energy values is more accurate.

3. The obtained data based on the new cluster-associate pattern can be considered as another confirmation of the concept fruitfulness of chaotized particles.

### References

- 1 Kazhikenova A.Sh. Efficiency of applying cluster-associated model of viscosity of liquid metals / A.Sh. Kazhikenova, D.B. Alibiyeu, E.S. Ibrayeva // Bulletin of the Karaganda University. Chemistry Series. — 2017. — No. 4(88). — P. 58–64.
- 2 Турдукожаева А.М. Применение распределения Больцмана и информационной энтропии Шеннона к анализу твердого, жидкого и газообразного состояний вещества (на примере металлов): автореф. дис. ... д-ра техн. наук: 05.16.08 — «Теория металлургических процессов» / А.М. Турдукожаева. — Караганда, 2008. — 32 с.
- 3 Малышев В.П. Плавкость и пластичность металлов / В.П. Малышев, Б.Т. Абдрахманов, А.М. Нурмагамбетова. — М.: Научный мир, 2004. — 148 с.
- 4 Киттель Ч. Квантовая теория твердых тел / Ч. Киттель. — М.: Наука, 1967. — 491 с.

А.Ш. Қажикенова, Д.Б. Алибиев, А.Б. Сейтимбетова, Ж.М. Тентекбаева

## Кластерлік-ассоциативті модель бойынша металдардың иондың потенциалының ассоцирленген кластерінің дәрежесінің өзара байланысы

Мақалада сұйық металдардың кинематикалық тұтқырлығының кластерлік-ассоциаттық моделі қарастырылған. Бұл модель хаотизирленген бөлшектер тұжырымдамасының негізінде алынды. Ұсынылған үлгіге сәйкес авторлар сұйық металдағы кластерлердің ассоциациялану дәрежесінің орташа мәндерін есептеді. Есептеу үшін Д.И. Менделеевтің элементтері кестесінің екінші — алтыншы кезеңдерінің 28

металдары зерттелген. Авторлардың жұмысында металдарды иондаудың бірінші әлеуетін кластерлердің ассоциациялану дәрежесінің алынған мәндерімен салыстыру келтірілген. Бұл салыстыру бірінші иондау әлеуетінің өзгеруімен тығыз байланыста кластерлер қауымдастығы дәрежесінің заңды өзгеруін көрсетті. Френкель теңдеуімен біріктірілгенде активтендіру энергиясын есептеу үшін аппроксимирлеуші теңдеуі алынды. Тұтқырлықтың температуралық тәуелділігінің кластерлік-ассоциаттық моделі үшін алынған теңдеу жиырма сегіз металл үшін балкыманың тұтқыр ағысын активтендіру энергиясын есептеу кезінде пайдаланылған. Активтендіру энергиясы бойынша алынған нәтижелерді авторлар эксперименталды мәліметтермен салыстырды. Бұл салыстыру ұсынылған модель бойынша алынған белсендіру энергиясы бойынша деректер аппроксимациялық тәуелділіктен жақсы сипатталатынын көрсетті. Алынған нәтижелерді көрнекі растау үшін жұмыста кестелер мен суреттер келтірілген. Осылайша, Д.И. Менделеев элементтері жүйесінің барлық кезеңдері бойынша металдарды иондаудың бірінші әлеуетін кластерлер ассоциациясының дәрежесімен салыстыру кезінде олардың заңды байланысы анықталды. Бұл байланыс кластерлік-қауымдасқан модельдің функционалдык сипаты туралы бекітуге мүмкіндік береді.

*Кілт сөздер:* тұтқырлық, ретсізделген бөлшектер, ассоциирленген кластердің дәрежесі, кластерлі-ассоциативті модел, сұйық металдар, активтендіру энергиясы, кристалл қозғалысты бөлшектер, иондау әлеуеті, Френкельдің модификацияланған теңдеуі.

А.Ш. Кажикенова, Д.Б. Алибиев, А.Б. Сейтимбетова, Ж.М. Тентекбаева

### **Взаимосвязь степени ассоциированности кластеров с потенциалами ионизации металлов по кластерно-ассоциатной модели**

В статье рассмотрена кластерно-ассоциатная модель кинематической вязкости жидких металлов. Модель была получена на основе концепции хаотизированных частиц. Авторами, согласно предложенной модели, были рассчитаны средние значения степени ассоциированности кластеров, содержащихся в жидком металле. Для расчета были исследованы 28 металлов второго – шестого периодов таблицы элементов Д.И. Менделеева. Кроме того, приведено сопоставление первого потенциала ионизации металлов с полученными значениями степени ассоциированности кластеров. Данное сопоставление показало закономерное изменение степени ассоциации кластеров в тесной связи с изменением первого потенциала ионизации. В комбинации с уравнением Френкеля получено аппроксимирующее уравнение для расчета энергии активации. Уравнение для кластерно-ассоциатной модели температурной зависимости вязкости использовано при расчете энергии активации вязкого течения расплава для двадцати восьми металлов. Полученные результаты по энергии активации авторы сравнили с экспериментальными данными. Результаты сопоставления показали, что данные по энергии активации, полученные по предлагаемой модели, описываются лучше аппроксимирующей зависимостью. В работе для большей наглядности полученных результатов приведены таблицы и рисунки. Таким образом, при сопоставлении первого потенциала ионизации металлов по всем периодам системы элементов Д.И. Менделеева со степенью ассоциации кластеров выявлена их закономерная связь, которая позволяет утверждать о функциональном характере кластерно-ассоциатной модели.

*Ключевые слова:* вязкость, хаотизированные частицы, степень ассоциированности кластеров, кластерно-ассоциатная модель, жидкие металлы, энергия активации, кристаллоподвижные частицы, потенциал ионизации, модифицированное уравнение Френкеля.

### **References**

- 1 Kazhikenova, A.Sh., Alibiyev, D.B., & Ibrayeva, E.S. (2017). Efficiency of applying cluster-associated model of viscosity of liquid metals. *Bulletin of the Karaganda University, Chemistry series*, 4(88), 58–64.
- 2 Turdukozhaeva, A.M. (2008). *Primenenie raspredelenia Boltsmana i informatsionnoi entropii Shennona k analizu tverdoho, zhidkoho i hazoobraznoho sostoianii veshchestva (na primere metallov)* [Application of the Boltzmann distribution and Shannon information entropy to the analysis of solid, liquid and gaseous states of matter (on the example of the metals)]. *Extended abstract of Doctor's thesis*. Karaganda [in Russian].
- 3 Malyshev, V.P., Abdrahmanov, B.T., & Nurmagambetova, A.M. (2004). *Plavkost i plastichnost metallov [Melting and ductility of metals]*. Moscow: Nauchnyi mir [in Russian].
- 4 Kittel, Ch. (1967). *Kvantovaya teoriya tverdykh tel [Quantum theory of solids]*. Moscow: Nauka [in Russian].

A.A. Seitmagzimov, G.M. Seitmagzimova, Zh.K. Dzhanmuldaeva

*M. Auezov South Kazakhstan State University, Shymkent, Kazakhstan  
(E-mail: galinaseit@mail.ru)*

## **Hydrothermal grown iron oxide films on the surface of titanium and conductive glasses and their current characteristics in water photolysis**

The relevance of photolysis on semiconductor electrodes since the pioneer work of Fujishima and Honda on metallic titanium does not lose sharpness due to new possibilities for developing new materials, such as conductive glasses, for which photolysis cells with semi-transparent semiconductor layer can be created. We have compared properties of such glasses with a metal for hydrothermal conditions of iron oxide synthesis. Iron oxide films have also been obtained by introducing a number of cations to modify semiconductor systems ( $\text{Fe}_2\text{O}_3$ ). It turned out that the nature of the substrate significantly affects the properties of the formed conductive film, which ultimately forms the level of anodic photocurrents in the layer of iron oxide semiconductor. We have investigated current characteristics of such films; it was shown that charging processes occur better on metallic titanium than on conductive glasses. We consider that the metal substrate significantly reduces regeneration processes both in the semiconductor layer and at the interface. Thus, formed  $\text{Ti}/\text{Fe}_2\text{O}_3$  electrolyte heterojunction is more efficient than the conducting glass/ $\text{Fe}_2\text{O}_3$  electrolyte system. However, this does not mean that glass is less promising for photolysis systems. It is necessary to achieve more acceptable conditions for the synthesis of semiconductor material.

*Keywords:* iron oxide, conductivity, spectrum, current-voltage characteristic, anode photocurrent, band gap, semiconductor, doping.

### *Introduction*

Semiconductor transition metal oxides are known for their properties as anode materials for the model processes of water photoelectrolysis [1]. Among this variety of anode materials ( $\text{TiO}_2$ ,  $\text{ZnO}$ ,  $\text{Fe}_2\text{O}_3$ ,  $\text{WO}_3$ , etc.), iron oxide has always attracted itself as an optimal material from point of view of its optical characteristics — the band gap width equals 2.1 eV, herewith the photo corrosion for this material is minimal. On the other hand, this material has intrinsic essential disadvantages, namely increased recombination [2, 3] and it's very limited thickness of an active layer, just a few nanometers [4]. From this point of view, the production of  $\text{Fe}_2\text{O}_3$  films in hydrothermal conditions is always attractive, because this method is an universal one and it allows to vary the properties of films in very wide range, both in thickness and in composition.

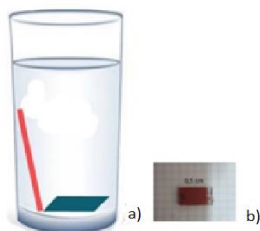
It was shown earlier that under the studied conditions of hydrothermal synthesis [5] at certain concentration ranges of iron chloride (III) it is possible to dope titanium dioxide films with iron ions. It gives a significant improvement of current characteristics of photoelectrodes. It was of interest to study the formation of iron oxide films under the same conditions on pure films of metallic titanium and on a conducting glass. For that we raised concentration of the electrolyte  $\text{FeCl}_3 \cdot 5\text{H}_2\text{O}$  solution, which allowed to grow films of pure iron oxide on the surface of titanium and conductive glass in hydrothermal conditions.

### *Experimental*

The investigations were conducted on metallic titanium plates of size  $1.5 \times 1.5$  cm (VT6 titanium grade) of composition Ti-6.25 Al-4.1 with small admixture of aluminum and vanadium (Government Standard 19807–91) with a current collector of the same titanium, as well as on conductive glass Fluorine Tin Oxide (FTO) with conductivity less than 15 ohms/cm<sup>2</sup> of firm «LATECH».

Previously we applied 2.0–2.5 g/l  $\text{FeCl}_3 \cdot 5\text{H}_2\text{O}$  solution for modification of titanium dioxide films on the metallic titanium with hydrochloric acid solution acidifying. We raised the concentration of iron chloride to 5–10 g/l, which allowed us to form under the same conditions (190 °C, 5 hours) iron oxide films in an autoclave.

Hydrothermal synthesis of films was carried out in a laboratory autoclave under pressure of 0.5 MPa with plates position shown in Figure 1. After the hydrothermal synthesis, the films were washed with distilled water, dried and then annealed in air at 500 °C for 1 hour. In parallel, plates of conductive glasses were processed in the same fluoroplastic glass. Then the plates after washing with water were also annealed at 500 °C for an hour.



*a* — titanium plate (vertical position) and glass plate (horizontal position);  
*b* — the size of the glass electrode with iron oxide layer

Figure 1. Scheme of samples arrangement in the autoclave

X-ray analysis of films was performed at the stationary installation of DRONE-3 with Cu-K $\alpha$  radiation directly from the metallic plates of anodized titanium.

The anodic photocurrent of titanium-oxide electrodes was conducted by a three-electrode scheme; a platinum wire served as the counter electrode, the comparison electrode was silver- chloride one. For iron oxide film illumination a xenon lamp without light filters was used. Illumination of the samples was measured with a light meter and accounted for xenon lamp as  $(160-180) \cdot 10^3$  Lux and for UV lamp — as  $12 \cdot 10^3$  Lux. The level of illumination on the sun in the latitude of Shymkent (South Kazakhstan) in June, measured at midday, was  $130 \cdot 10^3$  Lux. Current-voltage characteristic was double-checked for different synthesis conditions, the accuracy was confirmed by 3–4 parallel sample measurements, and the photocurrent dependence was constructed from their averaged values. Relative standard deviation from the average value is 0.5 %.

Micrographs and semi-quantitative analysis of the electrode surface were performed using scanning electron microscope JSM-6490LV (JEOL, Japan). Optical spectra of glasses were recorded on a Cary-50 spectrophotometer in a transmission mode.

### Results and Discussion

Simultaneous hydrothermal treatment of titanium and glasses in the autoclave allowed to form a layer of iron oxide film on the surface of the plates when changing iron trichloride solution concentration. This can be clearly seen from the cross-section of the glass plate (Fig. 2).

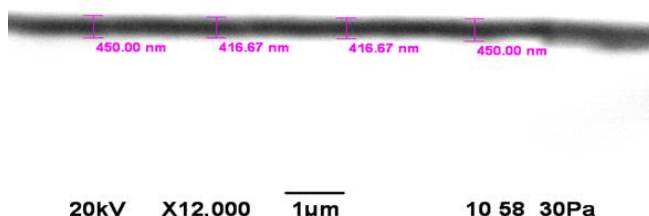


Figure 2. Micrograph of iron oxide film of on the glass plate (inverted image)

It is possible to determine the thickness of iron oxide layer in the limit of 416–450 nm, with the transmission spectrum (Fig. 3) identified as a layer of iron oxide. For example, it is in good agreement with the spectra of iron oxide in [5] in the limit of 350–800 nm. We can see the absorption limit which is in line with approximately 400 nm.

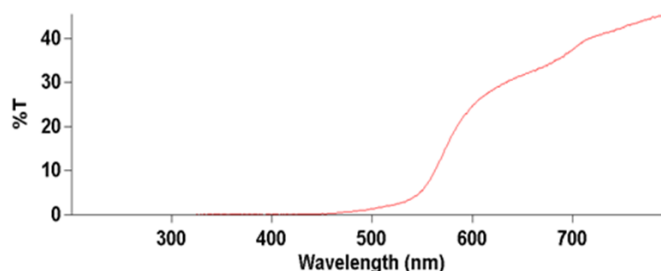


Figure 3. Transmission spectra of glass after glass treatment with iron trichloride in an autoclave

The presence of iron oxide film on titanium is also recorded on metal plate X-ray diffraction pattern (Fig. 4). However, due to the hematite signal weakness, the main peak of metallic titanium outweighs the iron peak.

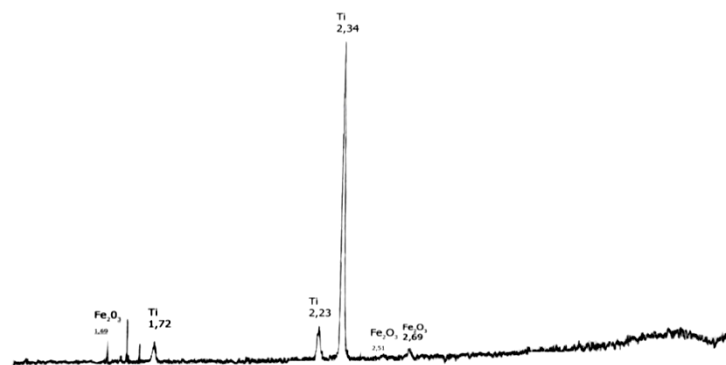


Figure 4. X-ray diffraction pattern of titanium plate with iron oxide layer

Figure 5 shows the current-voltage characteristic of the dark current for the electrode on titanium. It can be seen that there is no dark current within the potentials up to 800 mV.

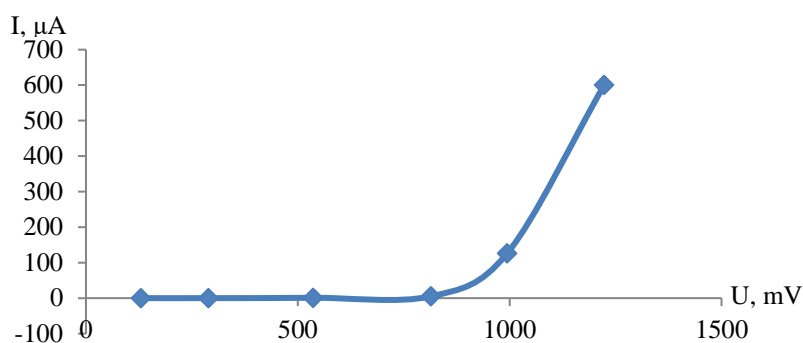


Figure 5. Current-voltage characteristic of a titanium electrode without lighting

An interesting current characteristic for titanium after titanium annealing in the air at 500 °C is given in Figure 6 (blue line). Annealing of titanium in the air leads to the formation of titanium dioxide film, and its current characteristics are insignificant — 15–20 μA (blue line), but increased current characteristics for iron oxide after hydrothermal synthesis and subsequent annealing of such a sample at 500 °C for 1 hour (red line) are obvious.

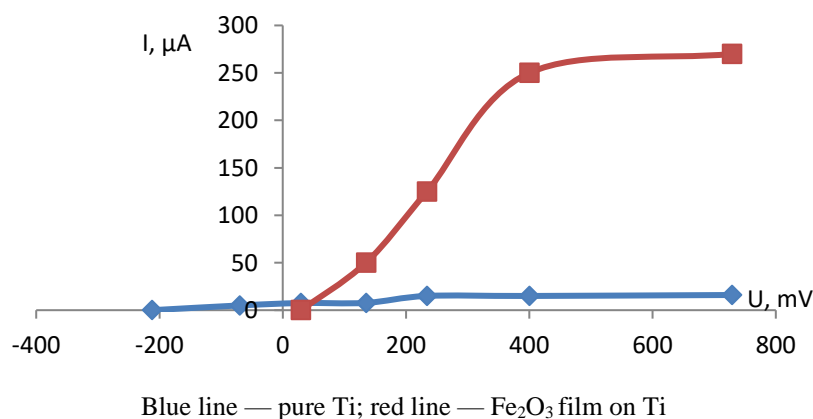
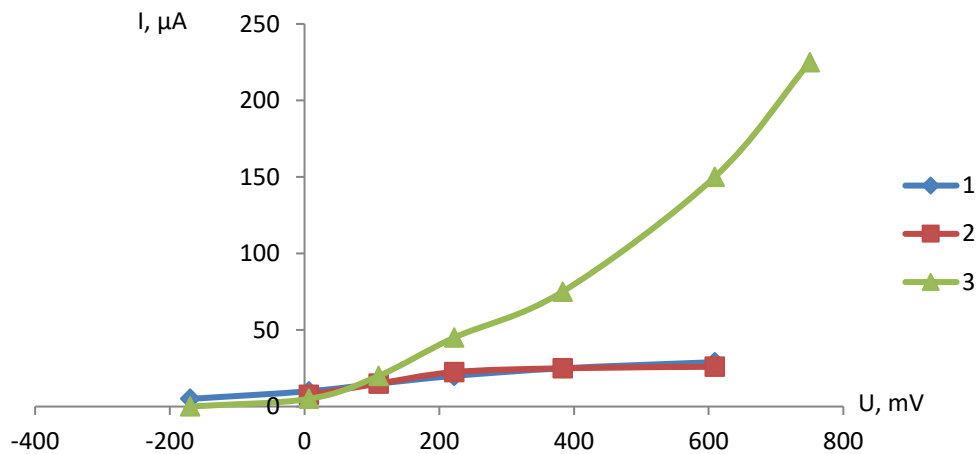


Figure 6. Current-voltage characteristic of pure titanium after annealing titanium dioxide film (blue line) and iron oxide film on titanium after annealing at 500 °C (red line)

Current characteristics for hematite on glass are almost identical (Fig. 7). Since the synthesis conditions for pairs of Ti/Fe<sub>2</sub>O<sub>3</sub> and glass/Fe<sub>2</sub>O<sub>3</sub> were identical (Fig. 1), we associate such a difference of current characteristics with the formation of the hematite boundary with the substrate, where in the case of glass the current characteristics are minimal, and when the titanium — hematite boundary is formed, the current characteristics are much higher. Perhaps it is precisely the recombination processes at the substrate, because hematite interface is significantly reduced in the case of Ti/Fe<sub>2</sub>O<sub>3</sub> pair as compared with the glass/Fe<sub>2</sub>O<sub>3</sub> pair.



1 — glass electrode, T = 500 °C, τ = 1 h; 2 — glass electrode, T = 500 °C, τ = 1 h; 3 — Ti electrode

Figure 7. Anodic photo current of iron oxide films on glass and titanium

Figure 7 clearly shows the growth of current characteristics up to 250 μA. Photo current on glass electrodes is insignificant and does not exceed 30 μA (blue line — photo current during annealing at 500 °C for 1 hour and red line — photo current during annealing glass at 700 °C for 10 minutes). It can be seen at Figure 7 that the glass annealing does not lead to significant change of current characteristics of hematite on the glass. At the same time, a sharp (more than 5 times) increase of photo current on titanium electrodes is observed (green line). We assume that such a significant increase of photo current is associated with the formation of the Ti/Fe<sub>2</sub>O<sub>3</sub> heterojunction. We suppose that the conductivity incompleteness at the boundary is significantly reduced compared to the same transition at the glass/Fe<sub>2</sub>O<sub>3</sub> boundary, so the conductivity of the «titanium» electrode is significantly higher than that of the «glass» electrode.

We have attempted to introduce other ions (for example, Ni, Co, Ag, Cu as well as a number of other cations) into the process of synthesis of iron oxide films and thereby to change film conductivity. To do this, 20 to 100 g/l of the corresponding cation was introduced into the initial electrolyte containing 2–2.5 g/l FeCl<sub>3</sub>·5H<sub>2</sub>O. The Figure 8 shows the spectrogram of the film, to which we tried to introduce a solution Ni(NO<sub>3</sub>)<sub>2</sub>·6H<sub>2</sub>O. Then this solution was also autoclaved like for the initial iron oxide electrolyte and the preparation was carried out similarly.

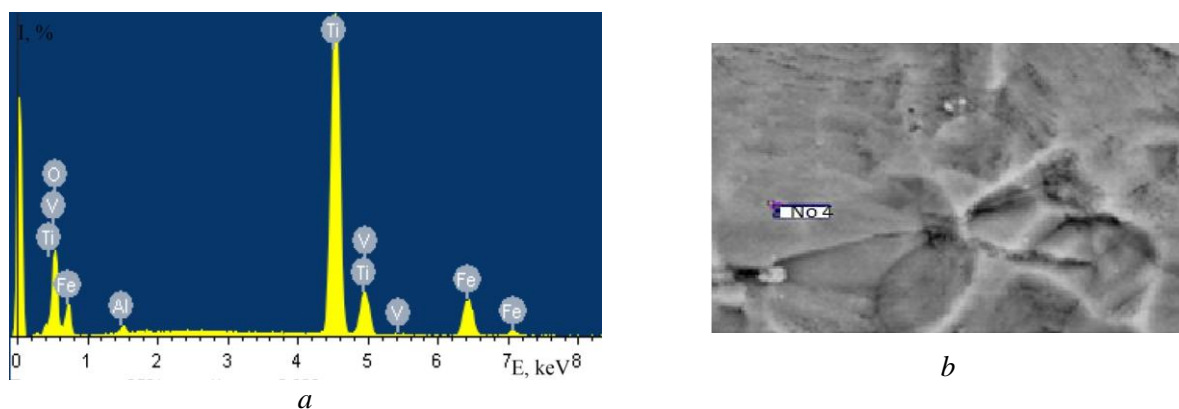


Figure 8. Spectrogram (a) and micrograph (b) of the iron oxide film with another cation introduction

We couldn't find any traces of the cation injected in the titanium film; only Fe and Ti elements and traces of Al and V elements are found on the spectrogram (Figure 8). Thus, hydrothermal conditions do not allow to introduce the accompanying cations into the synthesized film and the iron oxide film is formed on the surface in pure form. Thus, we did not find any improvement or degradation of the iron oxide layer on the current characteristics of the synthesized films (Fig. 8).

Current-voltage characteristic is peculiar as well in this case (Fig. 9). The current values fluctuate (red line) at approximately the same values as for the original iron oxide (blue line). Such insignificant fluctuations fit into the general paradigm of current-voltage characteristic dependence. Thus, we did not detect the improvement or degradation of the iron oxide layer in synthesized films with a cation.

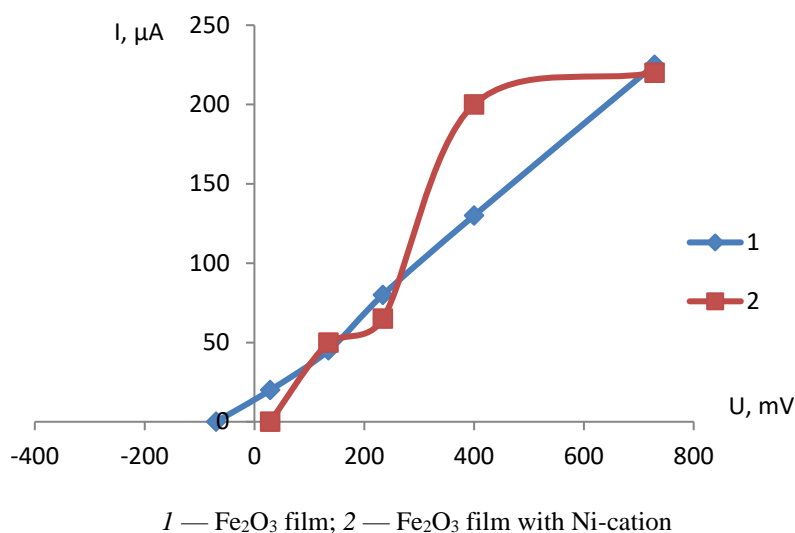


Figure 9. Current-voltage characteristics of iron oxide films (blue line) and films obtained in the presence of much nickel cations in a solution (red line)

We suppose that under hydrothermal conditions, an iron oxide film was formed on titanium, the electro-physical properties of which are very dependent on the properties of the substrate, i.e. titanium (Fig. 10).

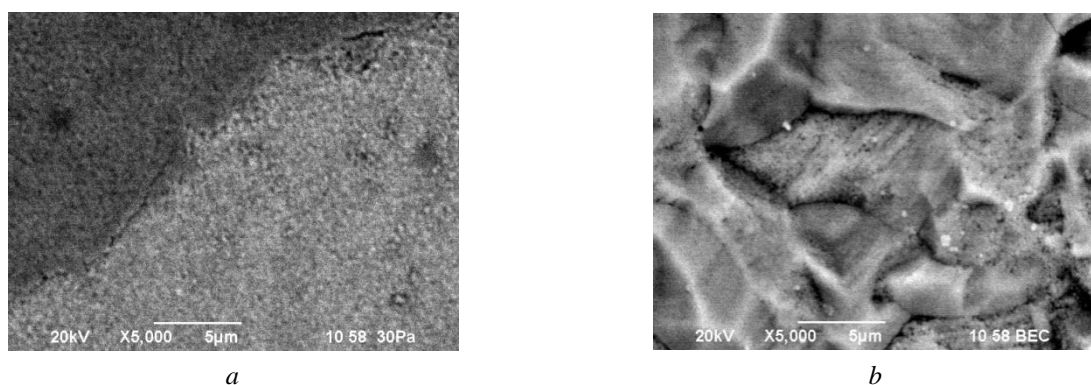


Figure 10. Micrographs of iron films on glass (*a*) and titanium (*b*)

In this case, we assume that the Ti/ $\text{Fe}_2\text{O}_3$  heterojunction, as well as the Ti/ $\text{Fe}_2\text{O}_3$ -NaOH electrolyte system itself, is a system that significantly reduces regeneration processes in the semiconductor layer and this sharply raises current characteristics of photoelectrodes. From these positions, perhaps, similar processes are described by authors of the publication [7], who obtained current characteristics three times the best of ours, i.e.  $1.1 \text{ mA/cm}^2$ .

### Conclusion

Iron oxide films were formed and obtained under hydrothermal conditions on metallic titanium and conductive glasses. It was shown that the current characteristics of the metallic substrate are more than an order

of magnitude better than for glass. It is obvious that under identical synthesis conditions (hydrothermal growth, conducting basis) the formation of heterojunction largely depends on the substrate nature. A significant difference in current characteristics for different substrates is associated with the formation of a semiconductor layer, where the regeneration processes are very reduced for metallic titanium than for conductive glass.

### References

- 1 Плесков Ю.В. Фотоэлектрохимическое преобразование солнечной энергии / Ю.В. Плесков. — М.: Химия, 1990. — 176 с.
- 2 Dare-Edwards M.P. Electrochemistry and Photoelectrochemistry of Iron (III) oxide / M.P. Dare-Edwards, J.B. Goodenough, A. Hamnett, P.R. Trevellick // Journal of the Chemical Society, Faraday Trans. — 1983. — Vol. 1, No. 79. — P. 2027–2041.
- 3 Kay A. New Benchmark for Water Photooxidation by Nanostructured A-Fe<sub>2</sub>O<sub>3</sub> Films / A. Kay, I. Cesar, M. Grätzel // Journal of the American Chemical Society. — 2006. — No. 128. — P. 15714–15721.
- 4 Kennedy J.H. Photoactivity of Polycrystalline Alpha-Fe<sub>2</sub>O<sub>3</sub> Electrodes Doped with Group IVa Elements / J.H. Kennedy, M. Anderman, R. Shinar // Journal of the Electrochemical Society. — 1981. — No. 11. — P. 2371–2373.
- 5 Seitmagzimov A.A. Modification of Titanium Oxide Films by Ferric Ions in Hydrothermal Conditions and their Photo-Electrochemical Properties / A.A. Seitmagzimov, G.M. Seitmagzimova // Asian Journal of Chemistry. — 2015. — Vol. 27, No. 4. — P. 1521–1524.
- 6 Xu Zong. A scalable colloidal approach to prepare hematite films for efficient solar water splitting / Zong Xu, Thaweesak Supphasin, Xu Hongyi, Xing Zheng, Zou Jin, Lua Gaoqing (Max), Wang Lianzhou // Physical Chemistry Chemical Physics. — 2013. — Vol. 15, No. 29. — P. 12314–12321. DOI: 10.1039/c3cp52153b.
- 7 Jin Hyun Kim. Hetero-type dual photoanodes for unbiased solar water splitting with extended light harvesting / Jin Hyun Kim, Ji-Wook Jang, Yim Hyun Jo, Fatwa F., Young Hye Lee, Roel van de Krol, Jae Sung Lee // Nature Communications. — 2016. — No. 7. — P. 13380. DOI: 10.1038/ncomms13380.

А.А. Сейтмагзимов, Г.М. Сейтмагзимова, Ж.К. Джанмулдаева

### Титан және өткізуші шынылар бетіндегі гидротермалды өсірілген темір оксидінің қабықшалары және олардың су фотолизіндегі тоқтық сипаттамалары

Фуджишима мен Хонданың алғашқы жұмыстарынан бастап жартылай өткізгіш электродтардағы фотолиздің өзектілігі жаңа материалдарды игерудің мүмкіндіктеріне байланысты өткірлігін жоғалтпайды, атап айтқанда өткізгіш шынылар олар үшін жартылай өткізгіштің жартылай мөлдір қабаты бар фотолизді ұяшықтар жасалуы мүмкін. Темір оксиді синтезінің гидротермалдық жағдайлары үшін осы шынылардың металмен салыстырғандағы қасиеттері салыстырылған. Сондай-ақ жартылай өткізгіш жүйелерді модификациялау үшін (Fe<sub>2</sub>O<sub>3</sub>) бірнеше катиондар енгізіп, темір оксидінің қабықшалары алынды. Төсеніштің табиғаты қалыптасатын өткізгіш қабықшаның қасиеттеріне елеулі әсер ететіні анықталды, бұл соңында темір оксидті жартылай өткізгіштің қабатында анодты фототоктар деңгейін қалыптастырды. Авторлар қабықшалардың ток сипаттамаларын зерттеген, олардың нәтижелері металл титанда өткізуші шынылармен салыстырғанда зарядтау процестері жақсы жүретінін көрсетті. Біз металл төсеніш жартылай өткізгіштің қабатындағы және фазалар шекарасында регенерациялық процестерді айтарлықтай төмендетеді деп есептейміз. Осылайша, қалыптасатын Ti/Fe<sub>2</sub>O<sub>3</sub> әртекті өткізу «өткізуші шыны/Fe<sub>2</sub>O<sub>3</sub>–электролит» жүйесіне қарағанда тиімдірек. Дегенмен, шынылардың фотолиздік жүйелер үшін болашағы жоқ деп айтуға болмайды. Жартылай өткізгіш материалдарды синтездеудің қолайлы жағдайларына қол жеткізу қажет.

*Кілт сөздер:* темір оксиді, өткізгіштік, спектр, вольтамперлік сипаттама, анодты фототок, тыйым салынған аймақтың ені, жартылай өткізгіш, допирлеу.

А.А. Сейтмагзимов, Г.М. Сейтмагзимова, Ж.К. Джанмулдаева

### Гидротермально выращенные пленки оксида железа на поверхности титана и проводящих стеклов и их токовые характеристики при фотолизе воды

Актуальность фотолиза на полупроводниковых электродах со времен пионерской работы Фуджишима и Хонды на металлическом титане не теряет остроты ввиду новых возможностей освоения новых материалов, таких как проводящие стекла, для которых могут быть созданы фотолизные ячейки с

полупрозрачным слоем полупроводника. Нами сопоставлены свойства таких стекол по сравнению с металлом для гидротермальных условий синтеза оксида железа. Также получены пленки оксида железа при введении ряда катионов для модификации полупроводниковых систем ( $\text{Fe}_2\text{O}_3$ ). Как оказалось, природа подложки существенным образом влияет на свойства формируемой проводящей пленки, что, в конечном итоге, формирует уровень анодных фототоков в слое железоксидного полупроводника. Авторами исследованы токовые характеристики таких пленок и показано, что на металлическом титане лучше происходят зарядные процессы, чем на проводящих стеклах. Мы считаем, что металлическая подложка существенно снижает регенерационные процессы как в слое полупроводника, так и на границе фаз. Таким образом, формируемый гетеропереход  $\text{Ti}/\text{Fe}_2\text{O}_3$ –электролит более эффективен, чем система «проводящее стекло/ $\text{Fe}_2\text{O}_3$ –электролит». Однако это не свидетельствует о том, что стекла менее перспективны для фотолизных систем. Необходимо добиваться более приемлемых условий синтеза полупроводникового материала.

*Ключевые слова:* оксид железа, проводимость, спектр, вольтамперная характеристика, анодный фототок, ширина запрещенной зоны, полупроводник, допирование.

## References

- 1 Pleskov, Yu.V. (1990). *Fotoelektrokhimicheskoe preobrazovanie solnechnoi enerhii [Photoelectrochemical conversion of solar power]*. Moscow: Khimiia [in Russian].
- 2 Dare-Edwards, M.P., Goodenough, J.B., Hamnett, A., & Trelvellick, P.R. (1983). Electrochemistry and Photoelectrochemistry of Iron (III) oxide. *Journal of the Chemical Society, Faraday Trans, 1*, 79, 2027–2041.
- 3 Kay, A., Cesar, I., & Grätzel, M. (2006). New Benchmark for Water Photooxidation by Nanostructured A- $\text{Fe}_2\text{O}_3$  Films. *Journal of the American Chemical Society*, 128, 15714–15721.
- 4 Kennedy, J.H., Anderman, M., & Shinar, R. (1981). Photoactivity of Polycrystalline Alpha- $\text{Fe}_2\text{O}_3$  Electrodes Doped with Group IVa Elements. *Journal of the Electrochemical Society*, 11, 2371–2373.
- 5 Seitmagzimov, A.A., & Seitmagzimova, G.M. (2015). Modification of Titanium Oxide Films by Ferric Ions in Hydrothermal Conditions and their Photo-Electrochemical Properties. *Asian Journal of Chemistry*, 27, 4, 1521–1524.
- 6 Xu Zong, Supphasin Thaweesak, Hongyi Xu, Zheng Xing, Jin Zou, & Gaoqing (Max), et.al. (2013). A scalable colloidal approach to prepare hematite films for efficient solar water splitting. *Physical Chemistry Chemical Physics*, 15, 29, 12314–12321. DOI: 10.1039/c3cp52153b.
- 7 Jin Hyun Kim, Ji-Wook Jang, Yim Hyun Jo, Fatwa F., Young Hye Lee, & Roel van de Krol, et.al. (2016). Hetero-type dual photoanodes for unbiased solar water splitting with extended light harvesting. *Nature Communications*, 7. DOI: 10.1038/ncomms13380.

M.M. Usmanova<sup>1</sup>, V.V. Dolgov<sup>1</sup>, N.R. Ashurov<sup>1</sup>, S.Sh. Rashidova<sup>1</sup>, T. Dadahodzhayev<sup>2</sup>

<sup>1</sup>*Institute of polymer chemistry and physics Uzbekistan Academy of Sciences, Tashkent, Uzbekistan;*

<sup>2</sup>*Innovation Center of JSC «Uzkimyosanoat» and JSC «Maksam-Chirchik», Tashkent, Uzbekistan  
(E-mail: polymer@academy.uz)*

### **Obtaining of nanocatalyzers for low-temperature conversion of oxide carbon (CuO/ZnO/Al<sub>2</sub>O<sub>3</sub>) with reduced copper content**

The main goal of the work was to reduce the content of copper (in terms of copper (II) oxide) in the composition of the conversion catalyst, and to preserve high catalytic and physico-mechanical characteristics. As an alternative to the known technology for producing oxide catalysts from precursors of metal hydroxocarbonates, there have been selected a manner in which the precursor is copper/zinc hydroxocarbonate. It has been shown that of the many salts obtained from precursors — metal hydroxocarbonates, copper/zinc double hydroxocarbonate with an aurichalcite structure is most effective. The decomposition of these compounds results in the formation of nanosized metal copper clusters, which have a high specific surface area and high activity in the redox reaction of carbon monoxide conversion with water vapor to produce hydrogen. The coprecipitation conditions and the structure of copper/zinc hydroxocarbonate determine the subsequent activity of the oxide catalyst. A technology for producing nanocatalysts for low-temperature conversion of carbon monoxide with a low (up to 20 % — from 54 to 34 wt.%) copper content was proposed and the conditions for obtaining a precursor and catalyst were optimized.

*Keywords:* Aurichalcite, catalysts, conversion, copper content, low temperature, metal hydroxocarbonates.

#### *Introduction*

In recent years, the need for catalysts used in the production of hydrogen and hydrogen-containing gases by the method of hydrocarbon conversion has increased.

Existing methods for the preparation of copper-containing catalysts are based on the use of deposition processes and ammonia-carbonate technology. These preparation methods of copper-containing low-temperature catalysts are characterized by a complex, multi-stage and expensive main production scheme, which necessitates the improvement of existing technologies of catalysts' producing for the cost of low-temperature catalysts.

In the course of this work, a significant amount of sources on this issue was analyzed [1–3]. It has been established that the main condition for solving this problem is the formation of a certain structure of the corresponding metal hydroxides obtained by decomposition of ammonia-carbonate complexes of copper and zinc, followed by separation of the precipitate and heat treatment of the mass pressing.

As shown in [3], increased catalyst activity was achieved by chemical interaction of the catalyst components at an early stage of preparation, as well as by decomposition of ammonia-carbonate complexes. The completeness of the interaction was achieved by the processes in the kinetic mode (i.e., with intensive mixing of 150–500 rpm) at the solid — liquid interface.

Under these conditions, the aurichalcite phase (CuZn)<sub>5</sub>(CO<sub>3</sub>)<sub>2</sub>(OH)<sub>6</sub> was detected in the obtained precursor. According to the differential thermal and x-ray phase analysis, the decomposition of the obtained precursor

is accompanied by the formation of highly dispersed oxides of copper and zinc (6–7 nm and 8–10 nm, respectively).

It is shown that of the many salts obtained from precursors — metal hydroxocarbonates, copper/zinc double hydroxocarbonate with an aurichalcite structure, which has a high specific surface area and activity, is the most effective.

Based on this, the main attention is paid to the conditions for the formation of copper/zinc hydroxocarbonate with the structure of aurichalcite as a precursor of the oxide solid catalyst solution, as well as the conditions for the formation of the oxide catalyst itself.

In this regard, the main goal of the work is to improve the existing technologies by optimizing the conditions for their production and cheapening low-temperature catalysts by reducing the copper component in the catalyst, by creating a nanostructured morphology of a solid solution of copper/zinc oxides while maintaining its high catalytic and physicochemical characteristics.

### *Experimental*

The copper/zinc hydroxocarbonate with an aurichalcite structure was prepared by precipitation from copper (II) nitrates and zinc, and sodium bicarbonate. It is shown that of copper/zinc hydroxocarbonate with the aurichalcite structure is formed both at a Cu:Zn ratio of 70:30 mol.% And at a ratio of 30:70 mol.%.

The wet weight of copper / zinc hydroxocarbonate after filtering the suspension and thoroughly washing from the concomitant salt of sodium nitrate was 271.00 g (of which 68.34 % moisture). The mass of dried (at 100 °C, for 2.5 days, and then at 120–125 °C, for 1 day) of copper/zinc hydroxocarbonate was 85.81 g (sample III.3).

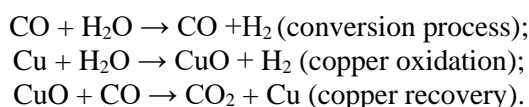
Three compositions of copper/zinc hydroxocarbonate were obtained, which differ in color. The pronounced light blue color is expressed for the sample — II.2; bluish-green for the sample — I.1 and dark blue — for the sample of copper/zinc hydroxocarbonate No. III.3, and during the drying process at a temperature of 100 °C it darkens, which indicates that a certain proportion of malachite is formed, decaying at temperatures of 80–100 °C. It was also noted that the sample of copper/zinc hydroxocarbonate — III.3 is characterized by a rather large size of well crystallized particles of a flat shape, in comparison with the two previous samples of copper/zinc hydroxocarbonate. The color of samples I.1 and II.2 after drying in the temperature range of 100–110 °C is stable.

### *Results and Discussion*

This study examined the industrial conditions for the preparation of the catalyst used in the process of low-temperature conversion of carbon monoxide with water vapor: CuO — 54 %, Cr<sub>2</sub>O<sub>3</sub> — 24 %, ZnO — 11 %, Al<sub>2</sub>O<sub>3</sub> — 19.5 % by weight.

The main role of the catalyst is the conversion of CO to CO<sub>2</sub> in the presence of water vapor at 270 °C with the formation of hydrogen for the synthesis of ammonia.

We present the probable redox reactions of CO conversion on a copper-zinc-chromium catalyst:



It has been shown that under industrial conditions occurs a formation of a catalyst with a zinc-malachite structure, which has low thermal stability.

In this regard, the main solution to the problem is to search for conditions for the formation of a specific structure of catalyst precursors — copper/zinc hydroxocarbonate; obtained by co-precipitation of nitrates of the corresponding metals in a precipitating medium, the preparation of which is shown in Figure 1.

The mixture contains various amorphous compounds, the structure of which depends on the dosage rate, the concentration of the base or precipitant. Depending on the change in conditions, precursors of various structures are formed. The reaction of the formation of hydrozincite (E) or aurichalcite (D) realizes by substitution from Na<sub>2</sub>Zn<sub>3</sub>(CO<sub>3</sub>)<sub>4</sub>.

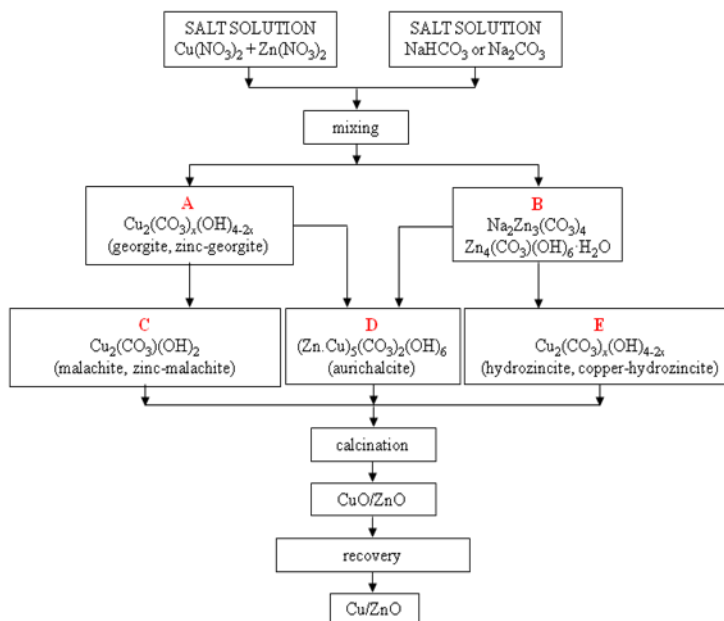


Figure 1. Formation of precursors and their structure

The catalytic activity of oxide catalysts was studied with varying the content of components in it (Tables 1 and 2). It has been shown that both the alumina content and the mass ratio of copper (II) oxide to zinc oxide (obtained under various conditions for the synthesis of copper/zinc hydroxocarbonate), as well as the total fraction of the latter in the composition of the catalyst, determine its properties (Table 1).

Table 1

**Activity, specific surface area and chemical composition of four-component oxide catalysts for low temperature conversion CO/H<sub>2</sub>O**

Catalyst	$A_{mean}$ , %	$S_{unit}$ , m <sup>2</sup> /g	w[CuO], mass. %	w[ZnO], mass. %	w[Cr <sub>2</sub> O <sub>3</sub> ], mass. %	w[Al <sub>2</sub> O <sub>3</sub> ], mass. %
Normative (Technical specifications of Rep. of Uzb. 6.3–57–95)	80 (no less)	–	54.0	11.0	14.0	19.5
CuO/ZnO/Al <sub>2</sub> O <sub>3</sub>	84.00	43.16	42.7	44.5	–	8.8
	91.00	68.50	41.3	39.2	–	17.8
	86.31	105.38	35.0	35.4	–	27.4
	76.54	123.93	30.6	29.7	–	38.0

As can be seen from the Table 1, the alumina content, as well as the mass ratio of copper (II) oxide to zinc oxide (obtained under various conditions for the synthesis of copper/zinc hydroxocarbonate), as well as the total fraction of the latter in the composition of the catalyst, determine its properties.

Table 2

**The activity, specific surface area and chemical composition of three-component oxide catalysts for low temperature conversion CO/H<sub>2</sub>O**

Catalyst	w[CuO], mass. %	w[ZnO], mass. %	w[Al <sub>2</sub> O <sub>3</sub> ], mass. %	$S_{unit}$ , m <sup>2</sup> /g	$P_{unit} \times 10^{-2}$ , cm <sup>3</sup> /g	$A_{mean}$ , %
CuO/ZnO/Al <sub>2</sub> O <sub>3</sub>	36.80	58.60	2.80	147.89	6.40	92.22
	34.20	56.10	8.80	145.15	6.30	81.30
	31.70	49.90	17.10	160.38	6.90	76.00

As shown in the Table 2, copper/zinc hydroxocarbonate with an aurichalcite structure is formed both at a Cu:Zn ratio of 70:30 mol.% and at a ratio of 30:70 mol.%. It is shown that copper/zinc hydroxocarbonate

with the aurichalcite structure was obtained by precipitation from copper (II) nitrates and zinc, and sodium bicarbonate.

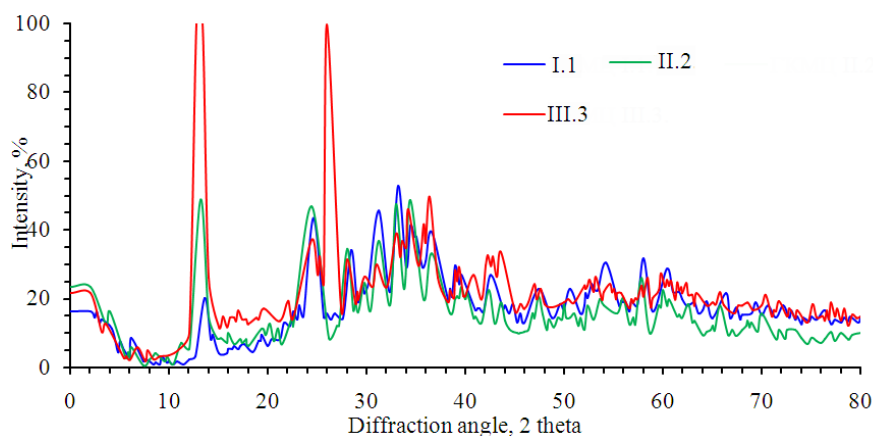


Figure 2. X-ray diffraction patterns of hydroxocarbonate samples copper/zinc obtained in three syntheses

The diffraction patterns of three samples of copper/zinc hydroxocarbonate, similar to the structure of aurichalcite are depicted in the Figure 2. According to the presented curves, three samples of copper/zinc hydroxocarbonate-HC Cu/Zn are characterized by the intensity of reflexes. The position of reflexes in all three samples remains almost constant.

In the spectrum of sample No. III.3, an intense reflection is observed in the range of  $27^\circ$ , the prevalence of the individual phase of copper (II) oxide in which, apparently, affects the structure and properties of the catalyst as a whole.

It has been revealed that the content of composing catalysts, the main part occupied a solution based on a zinc oxide lattice with copper (II) oxide clusters embedded in it during calcination of copper/zinc hydroxocarbonate with an aurichalcite structure.

All three catalysts obtained by varying the ratio Cu:Zn from copper/zinc hydroxocarbonate with the structure of aurichalcite have different properties, because a continuous series of solid solutions of copper/zinc hydroxocarbonate with the structure of aurichalcite is formed.

It has been noted that for an oxide low-temperature catalyst, the ratio Cu:Zn = 30:70 mol% is optimal. Violation of stoichiometry in the composition of copper/zinc hydroxocarbonate inevitably affects the structure and properties of the oxide catalyst. The coprecipitation conditions and the structure of copper/zinc hydroxocarbonate determine the subsequent activity of the oxide catalyst.

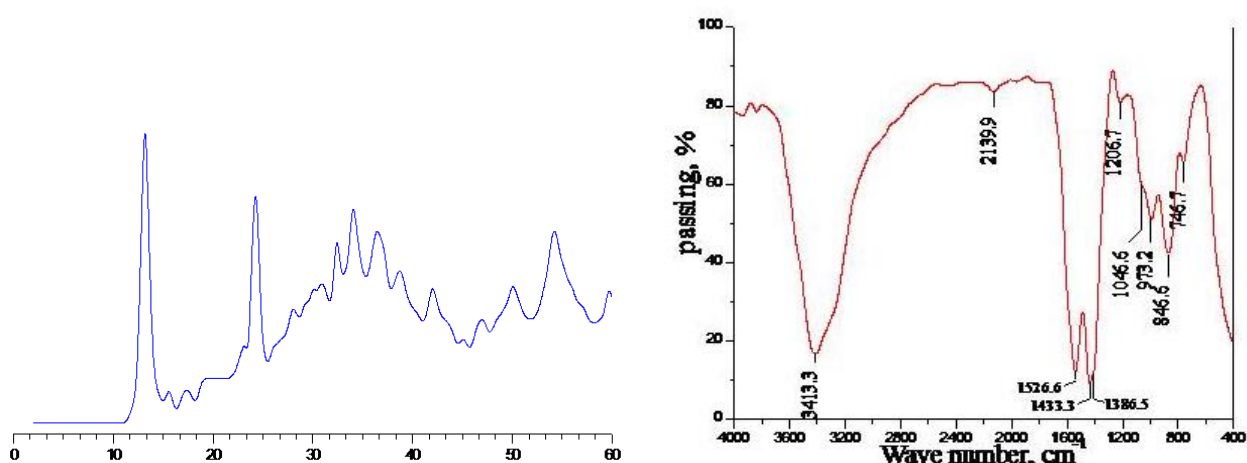


Figure 3. X-ray diffraction pattern and IR-spectrum of copper/zinc hydroxocarbonate {aurichalcite  $(\text{Cu}_{5-5x}\text{Zn}_{5x})(\text{CO}_3)_2(\text{OH})_6$ }

During the calcination of copper/zinc hydroxocarbonate with the aurichalcite structure  $(\text{Zn}_x\text{Cu}_{1-x})_5(\text{CO}_3)_2(\text{OH})_6$  (Fig. 3), a solid solution of copper/zinc oxides is formed with a maximum distortion

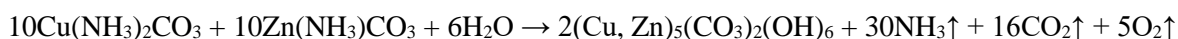
of the crystal lattice of copper (II) oxide. After preliminary activation of the catalyst (hydrogen reduction), there were formed the clusters of metallic copper with a high active surface area.

The aurichalcite spectra are characterized by: strong absorption vibrations at 1415 and 1340  $\text{cm}^{-1}$  of nitrate groups in gerhardtite; georgite is characterized by weak absorption vibrations below 1350  $\text{cm}^{-1}$ , except for carbonate groups at 838  $\text{cm}^{-1}$ ; hydroxyl groups at 3407, 3317  $\text{cm}^{-1}$  for malachite. Also, a slight difference is observed in the spectra of hydrozincite and aurichalcite, which makes impossible to distinguish which was monophase.

DSC can also be used as a method of identifying a mixture of phases and allows to determine the degree of homogeneity of zinc/copper. It is important that hydrozincite and aurichalcite have different destruction maxima of 241 °C and 325 °C, respectively, which makes it quite easy to identify hydrozincite present in the aurichalcite sample or vice versa. Thus, the optimal conditions for obtaining a catalyst with aurichalcite structure are established.

*The formation of catalyst precursors — hydroxocarbonate salt of copper and zinc with the structure of aurichalcite*

Under the action of mechanochemical activation of metals in a gaseous environment, copper and zinc ammonia are formed, which subsequently form a double hydroxocarbonate salt of copper and zinc with the structure of aurichalcite in the next stage of steam treatment:



The decomposition of such a precursor allows one to obtain copper and zinc oxides, the crystal lattices of which are distorted as much as possible, while after hydrogen reduction of such a solid solution, nanosized metal copper clusters are formed that have a high specific surface and high activity in the redox reaction of carbon monoxide conversion with water steam to produce hydrogen.

This technology is of significant interest as catalysts in the production of hydrogen and hydrogen-containing gases by the conversion of hydrocarbons, in the production of ammonia, methyl alcohol, etc.

### Conclusions

It was shown that of the many salts obtained from the precursors — metal hydroxocarbonates, copper/zinc double hydroxocarbonate with the aurichalcite structure is the most effective as a catalyst for the low-temperature conversion of carbon monoxide with water vapor.

The technology of producing nanocatalysts of low-temperature conversion of carbon monoxide with the aurichalcite structure was proposed, and the conditions for producing a precursor and catalyst with a reduced copper content of up to 20 % (from 54 to 34 wt.%) were optimized.

The conditions for obtaining a solid solution of copper/zinc oxides with an aurichalcite structure with a maximum distortion of the crystal lattice of copper oxide and the formation of nanoscale clusters of metallic copper with a high specific surface and activity in the redox reaction of carbon monoxide conversion with water vapor were determined.

### References

- 1 Shen G.C. Preparation of precursors for the Cu/ZnO methanol synthesis catalysts by coprecipitation methods: Effects of the preparation conditions upon the structures of the precursors / G.C. Shen, S. Fujita, N. Takezawa // *Journal of Catalysis*. — 1992. — Vol. 138, No. 2. — P. 754–758.
- 2 Овсиенко О.Л. Исследование влияния условий приготовления на физико-химические и каталитические свойства медь-цинк-алюминиевого катализатора синтеза метанола: автореф. дис. ... канд. хим. наук: 02.00.15 / О.Л. Овсиенко. — М., 1994. — 19 с.
- 3 Семенова Т.А. Формирование медноцинкового соединения из аммиачно-карбонатных растворов при термической обработке / Т.А. Семенова, И.П. Зрелова, З.В. Комова, А.Я. Волынкина // *Вопросы кинетики и катализа: межвуз. сб.* — Иваново: Иванов. хим.-технол. ин-т, 1986. — С. 33–36.
- 4 Ильин А.П. Научные основы приготовления катализаторов. Творческое наследие и дальнейшее развитие работ профессора И.П. Кириллова / А.П. Ильин. — Иваново: ИГХТУ, 2008. — 156 с.

М.М. Усманова, В.В. Долгов, Н.Р. Ашууров, С.Ш. Рашидова, Т. Дадаходжаев  
**Мыс құрамы төмендеген (CuO/ZnO/Al<sub>2</sub>O<sub>3</sub>) көміртегі оксидінің төмен температуралы конверсиясында нанокатализаторларды алу**

Жұмыстың негізгі мақсаты конверсиялық катализатор құрамындағы мыс құрамын төмендету ((II) мыс оксидіне қайта есептегенде) және жоғары каталитикалық және физика-механикалық сипаттамаларды сақтау болды. Металдардың гидроксокарбонаттарынан оксидті катализаторларды алудың белгілі технологиясына балама ретінде мыс/мырыш гидроксокарбонаты болып табылатын әдіс таңдалды. Түзілуден алынған көптеген тұздардың — метал гидроксокарбонаттары, аурихальцит құрылымы бар мыс/мырыш қос гидроксокарбонаты ең тиімді болып табылады, олардың ыдырауынан кейін металл мен мыстың наноөлшемді кластерлері пайда болады, үстіңгі беті бар және көміртегі оксидінің су буында сутекке айналу конверсиясының тотығу — қалпына келтіру реакциясында белсенділікке ие. Мыс/мырыш гидроксокарбонатының тұндыру жағдайлары мен құрылымы, оксидті катализатордың келесі белсенділігін анықтайды. Төмен температуралы конверсиясының нанокатализаторын алу технологиясы ұсынылды (20 %-ға дейін 54-тен, 34-ші массаға дейін) және прекурсор мен катализаторды алу шарттары оңтайландырылған.

*Кілт сөздер:* төмен температуралы, катализаторлар, металдардың гидроксокарбонаттары, көміртегі оксиді конверсиясы, аурихальцит, мыс құрамы.

М.М. Усманова, В.В. Долгов, Н.Р. Ашууров, С.Ш. Рашидова, Т. Дадаходжаев  
**Получение нанокатализаторов низкотемпературной конверсии оксида углерода (CuO/ZnO/Al<sub>2</sub>O<sub>3</sub>) с пониженным содержанием меди**

Основной целью работы ставилось снижение содержания меди (в пересчете на оксид меди (II)) в составе катализатора конверсии и сохранение высоких каталитических и физико-механические характеристик. В качестве альтернативы известной технологии получения оксидных катализаторов из предшественников гидроксокарбонатов металлов был выбран способ, в котором предшественник представлял собой гидроксокарбонат меди/цинка. Показано, что из многих солей, полученных из предшественников — гидроксокарбонатов металлов, двойной гидроксокарбонат меди/цинка со структурой аурихальцита является наиболее эффективным, после разложения которого образуются наноразмерные кластеры металла и меди, которые имеют высокую удельную поверхность и активность в окислительно-восстановительной реакции конверсии оксида углерода водяным паром с образованием водорода. Показано, что условия соосаждения и структура гидроксокарбоната меди/цинка определяют последующую активность оксидного катализатора. Предложена технология получения нанокатализаторов низкотемпературной конверсии оксида углерода с пониженным (до 20 % — с 54 до 34 масс.%) содержанием меди и оптимизированы условия получения прекурсора и катализатора.

*Ключевые слова:* низкотемпературный, катализатор, гидроксокарбонаты металлов, конверсия оксида углерода, аурихальцит, содержание меди.

## References

- 1 Shen, G.C., Fujita, S., & Takezawa, N. (1992). Preparation of precursors for the Cu/ZnO methanol synthesis catalysts by coprecipitation methods: Effects of the preparation conditions upon the structures of the precursors. *Journal of Catalysis*, 138, 2, 754–758.
- 2 Ovsienko, O.L. (1994). Issledovanie vlianiia uslovii prihotovleniia na fiziko-khimicheskie i kataliticheskie svoistva med-tsink-aliuminievoho katalizatora sinteza metanola [Study of the influence of cooking conditions on the physicochemical and catalytic properties of copper-zinc-aluminum methanol synthesis catalyst]. *Extended abstract of candidate's thesis*. Moscow [in Russian].
- 3 Semenova, T.A., Zrelova, I.P., Komova, Z.V., & Volynkina, A.Ya. (1986). Formirovanie mednotsinkovoho soedineniia iz ammiachno-karbonatnykh rastvorov pri termicheskoi obrabotke [The formation of a copper-zinc compound from ammonia-carbonate solutions during heat treatment]. *Voprosy kinetiki i kataliza — Questions of kinetics and catalysis*. Ivanovo: Ivanovo chemical-technological institute, 33–36 [in Russian].
- 4 Ilyin, A.P. (2008). *Nauchnye osnovy prihotovleniia katalizatorov. Tvorcheskoe nasledie i dalneishee razvitie rabot professora I.P. Kirillova [Scientific basis for the preparation of catalysts. Creative heritage and further development of the works of Professor I.P. Kirillov]*. Ivanovo: IGHU [in Russian].

G.L. Katkeeva, G. Burkitseterkyzy, Yu.P. Morozov, E.M. Zhunussov

*Zh. Abishev Chemical-Metallurgical Institute, Karaganda, Kazakhstan  
(E-mail: gulmarzhan.94@mail.ru)***Thermodynamic analysis of oxidized copper minerals interaction with modified reagent**

Practicality of preliminary sulphidization of oxidized copper minerals for the purpose of oxidized ore concentration is shown in the paper. For the first time the thermodynamic analysis was carried out for interaction of modified sulphidizing reagent with major components of oxidized copper ore — malachite, azurite and chrysocolla. Ammonium polysulfide formed in the solution of sodium polysulfide and ammonium sulfate was used as modified sulphidizing reagent. Temperature dependence of standard Gibbs energy for the reaction of ammonium polysulfide with oxidized copper minerals was determined. It was noted that standard Gibbs energy for malachite and azurite interaction with modified reagent has negative values in the temperature range of 298,15–373 K, thus showing high probability of interaction, which grows together with temperature. Interaction with chrysocolla is less active than with malachite and azurite but is still possible at mentioned temperature, with interaction probability again proportional to temperature. Thus, the possibility of oxidized copper minerals sulphidization with modified sulphidizing reagent is determined in the research.

*Keywords:* oxidized minerals, chrysocolla, malachite, azurite, modified sulphidizing reagent, sulphidization, thermodynamic analysis, Gibbs energy.

*Introduction*

Cheap flotation enrichment methods, conventional for sulfide ore, are less effective for oxidized ore due to natural hydrophilicity of oxidized copper minerals surface [1–3].

One of feasible solutions is chemical modification of minerals via sulphidization resulting in transformation of oxidized minerals into sulfidized ones, which can improve the flotation enrichment efficiency [4–9].

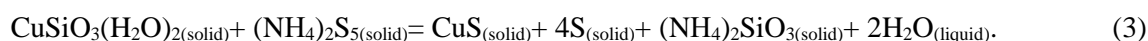
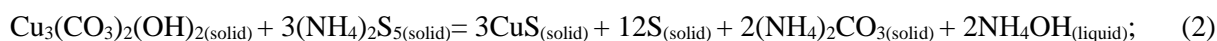
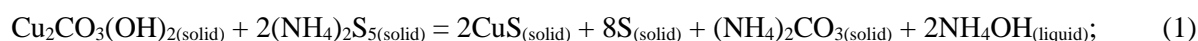
The thermodynamic analysis of possible reactions with determination temperature dependence of standard Gibbs energy has been carried out in order to assess the possibility of sulphidization with modified reagent.

Ammonium polysulfide formed in the solution of sodium polysulfide and ammonium sulfate was used as modified sulphidizing reagent.

The objective of work was to find the temperature dependence of ammonium polysulfide interaction with major components of oxidized copper ore, such as malachite, azurite and chrysocolla.

*Experimental*

Three types of interaction of modified reagent with copper compounds — malachite, azurite and chrysocolla have been studied:



Probability of reactions was estimated by alteration of standard Gibbs energy.

Calculation of temperature dependence of standard Gibbs energy is based on Hess law [10] and was made using the formula

$$\Delta_r G^0_T = \sum \Delta_r G^0_T(\text{products}) + \sum \Delta_r G^0_T(\text{init.}), \quad (4)$$

where  $\Delta_r G^0_T$  — standard Gibbs energy at temperature (T),  $\sum \Delta_r G^0_T(\text{products})$  — sum of standard Gibbs energy of reactions products formation at temperature (T),  $\sum \Delta_r G^0_T(\text{init.})$  — sum of standard Gibbs energy of initial components formation at temperature (T).

Temperature dependence of reaction velocity constant was calculated using the next formula:

$$\lg K_{P(T)} = -\Delta_f G^0_T / (2.303RT), \quad (5)$$

where R is the universal gas constant.

Temperature dependence of standard Gibbs energy of reactions products formation was determined by approximated method of Temkin-Schwartzman [11, 12], taking  $\Delta C_p^0 = \text{const}$ , by the formula

$$\Delta_f G^0_T = \Delta_f H^0_{298.15} - T\Delta_f S^0_{298.15} - TM\Delta_f C_p^0_{298.15}, \quad (6)$$

where  $\Delta_f H^0_{298.15}$  is the standard enthalpy of compound formation at 298.15 K;  $\Delta_f S^0_{298.15}$  is the standard entropy of compound formation at 298.15 K;  $\Delta_f C_p^0_{298.15}$  is the standard heat of compound formation at 298.15 K; M is the coefficient, equal to

$$M = 298,15/T - 1 + \ln(T/298,15). \quad (7)$$

Standard entropy was determined by formula

$$\Delta_f S^0_{298,15} = S^0_{298,15} - \sum S^0_{298,15}(\text{elementary substance}), \quad (8)$$

where  $S^0_{298,15}$  is the standard entropy of compound at 298.15 K;  $\sum S^0_{298,15}(\text{elementary substance})$  is the sum of standard entropies of substances forming the compound at 298,15 K.

Standard heat capacity of compound formation was determined by the formula:

$$\Delta_f C_p^0_{298,15} = C_p^0_{298,15} - \sum C_p^0_{298,15}(\text{elementary substance}), \quad (9)$$

where  $C_p^0_{298,15}$  is the standard heat capacity of compound at 298,15 K;  $\sum C_p^0_{298,15}(\text{elementary substance})$  is the sum of standard heat capacities of substances forming the compound, at 298,15K.

In case of insufficiency of the available literature data, the necessary values have been determined by proximate methods.

Standard heat capacity was estimated by the Kumok method [13] based on heat capacity increments system:

$$C_p^i_{298,15}(A_m B_n) = mC_p^i_{298,15}(A^{n+}) + nC_p^i_{298,15}(B^{m-}), \quad (10)$$

where  $C_p^i_{298,15}(A^{n+})$  is the increment of cation heat capacity;  $C_p^i_{298,15}(B^{m-})$  is the increment of anion heat capacity.

### Results and Discussion

The standard enthalpy values of compound formation at 298.15 K are given in the Table 1. Values for  $H_2O_{(\text{liquid})}$ ,  $NH_4OH_{(\text{liquid})}$ ,  $(NH_4)_2CO_{3(\text{solid})}$ ,  $CuS_{(\text{solid})}$ ,  $Cu_2CO_3[OH]_{2(\text{solid})}$ ,  $Cu_3[CO_3]_2[OH]_{2(\text{solid})}$  compounds are from [6–8].  $S_{(\text{solid})}$  equals to  $S_{8(\text{g})}$  with enthalpy data by [14]. Standard enthalpy for  $(NH_4)_2S_{5(\text{solid})}$ ,  $(NH_4)_2CO_{3(\text{solid})}$  and  $(NH_4)_2SiO_{3(\text{solid})}$  was calculated by Kassenov method from ionic increments [12]. Lacking data on increment of  $S_5^{2-}$ ,  $SiO_3^{2-}$  ions were found by evaluation method using standard enthalpy of sodium pentasulfide and silicates of First Group metals [16]. Data for  $CuSiO_3 \cdot nH_2O_{(\text{solid})}$  are from [18].

Table 1

#### Standard enthalpy of compound formation

Substance	$-\Delta_f H^0_{298,15}, \text{kJ} \cdot \text{mol}^{-1}$
$H_2O_{(\text{liquid})}$	285.829
$NH_4OH_{(\text{liquid})}$	361.271
$S_{(\text{solid})}$	12.735
$(NH_4)_2S_{5(\text{solid})}$	94.9
$(NH_4)_2CO_{3(\text{solid})}$	821.1
$CuS_{(\text{solid})}$	53.136
$(NH_4)_2SiO_{3(\text{solid})}$	1251.6
$Cu_2CO_3[OH]_{2(\text{solid})}$	1051.020
$Cu_3[CO_3]_2[OH]_{2(\text{solid})}$	1631.341
$CuSiO_3 \cdot nH_2O_{(\text{solid})}$	1747.3

There are standard entropy values of compound formation at 298.15 K in the Table 2.

Data for  $H_2O_{(\text{liquid})}$ ,  $NH_4OH_{(\text{liquid})}$ ,  $S_{(\text{solid})}$ ,  $CuS_{(\text{solid})}$ ,  $Cu_2CO_3[OH]_{2(\text{solid})}$ ,  $Cu_3[CO_3]_2[OH]_{2(\text{solid})}$ ,  $CuSiO_3 \cdot nH_2O_{(\text{solid})}$  were calculated by formula (8) based on [14–17]. For chrysocolla accepted  $n = 2$ . Standard

entropy at 298.15 K for  $(\text{NH}_4)_2\text{S}_{5(\text{solid})}$ ,  $(\text{NH}_4)_2\text{CO}_{3(\text{solid})}$ ,  $(\text{NH}_4)_2\text{SiO}_{3(\text{solid})}$  was determined using entropy data found by Kumok method [13].

Table 2

### Standard entropy of compound formation

Substance	$\Delta_f S^0_{298,15}, \text{J} \cdot \text{mol}^{-1} \cdot \text{K}^{-1}$
$\text{H}_2\text{O}_{(\text{liquid})}$	-162.955
$\text{NH}_4\text{OH}_{(\text{liquid})}$	-359.004
$\text{S}_{(\text{solid})}$	23.567
$(\text{NH}_4)_2\text{S}_{5(\text{solid})}$	-579.1
$(\text{NH}_4)_2\text{CO}_{3(\text{solid})}$	-841.3
$\text{CuS}_{(\text{solid})}$	1.453
$(\text{NH}_4)_2\text{SiO}_{3(\text{solid})}$	-857.5
$\text{Cu}_2\text{CO}_3[\text{OH}]_{2(\text{solid})}$	-503.504
$\text{Cu}_3[\text{CO}_3]_2[\text{OH}]_{2(\text{solid})}$	-671.479
$\text{CuSiO}_3 \cdot n\text{H}_2\text{O}_{(\text{solid})}$	-629.305

Standard heat capacity of compounds formation at 298,15 K is shown in the Table 3.

For  $\text{H}_2\text{O}_{(\text{liquid})}$ ,  $\text{NH}_4\text{OH}_{(\text{liquid})}$ ,  $\text{S}_{(\text{solid})}$ ,  $\text{CuS}_{(\text{solid})}$ ,  $\text{Cu}_2\text{CO}_3[\text{OH}]_{2(\text{solid})}$  compounds the data were taken from [14–17]. Values for  $(\text{NH}_4)_2\text{S}_{5(\text{solid})}$ ,  $(\text{NH}_4)_2\text{CO}_{3(\text{solid})}$ ,  $(\text{NH}_4)_2\text{SiO}_{3(\text{solid})}$  compounds were found using Kumok method [13], those for  $\text{CuSiO}_3 \cdot n\text{H}_2\text{O}_{(\text{solid})}$  are from [19].

Table 3

### Standard heat capacity of compounds formation

Substance	$\Delta_f C_p^0_{298,15}, \text{J} \cdot \text{mol}^{-1} \cdot \text{K}^{-1}$
$\text{H}_2\text{O}_{(\text{liquid})}$	31.793
$\text{NH}_4\text{OH}_{(\text{liquid})}$	53.576
$\text{S}_{(\text{solid})}$	-2.594
$(\text{NH}_4)_2\text{S}_{5(\text{solid})}$	-17.633
$(\text{NH}_4)_2\text{CO}_{3(\text{solid})}$	-14.3
$\text{CuS}_{(\text{solid})}$	0.712
$(\text{NH}_4)_2\text{SiO}_{3(\text{solid})}$	-18.8
$\text{Cu}_2\text{CO}_3[\text{OH}]_{2(\text{solid})}$	-5.309
$\text{Cu}_3[\text{CO}_3]_2[\text{OH}]_{2(\text{solid})}$	4.203
$\text{CuSiO}_3 \cdot n\text{H}_2\text{O}_{(\text{solid})}$	45.288

By means of the equation 6 the temperature dependence of standard Gibbs energy for every interacting compound have been calculated. The results are given in the Table 4.

Table 4

### Temperature dependence of standard Gibbs energy of compounds formation

Substance	T, K					
	298.15	313	328	343	358	373
	$\Delta_f G^0_T, \text{kJ} \cdot \text{mol}^{-1}$					
$\text{H}_2\text{O}_{(\text{liquid})}$	-237.244	-234.836	-232.426	-230.038	-227.67	-225.323
$\text{NH}_4\text{OH}_{(\text{liquid})}$	-254.234	-248.922	-243.595	-238.305	-233.05	-227.828
$\text{S}_{(\text{solid})}$	5.708	5.359	5.009	4.660	4.313	3.967
$(\text{NH}_4)_2\text{S}_{5(\text{solid})}$	77.759	86.365	95.070	103.788	112.517	121.258
$(\text{NH}_4)_2\text{CO}_{3(\text{solid})}$	-570.266	-557.768	-545.133	-532.488	-519.834	-507.171
$\text{CuS}_{(\text{solid})}$	-53.569	-53.591	-53.614	-53.637	-53.66	-53.684
$(\text{NH}_4)_2\text{SiO}_{3(\text{solid})}$	-995.936	-983.196	-970.313	-957.417	-944.509	-931.589
$\text{Cu}_2\text{CO}_3[\text{OH}]_{2(\text{solid})}$	-900.9	-893.423	-885.869	-878.301	-870.736	-863.167
$\text{Cu}_3[\text{CO}_3]_2[\text{OH}]_{2(\text{solid})}$	-1431.139	-1421.166	-1411.09	-1401.01	-1390.928	-1380.843
$\text{CuSiO}_3 \cdot 2\text{H}_2\text{O}_{(\text{solid})}$	-1559.673	-1550.344	-1540.953	-1531.594	-1522.264	-1512.963

Using respective data from Table 4 in the equation (4) the temperature dependence of standard Gibbs energy for the reactions (1–3) was determined. Formula (5) was used to calculate temperature dependence of equilibrium constant for the reaction (Table 5).

Table 5

Temperature dependence of standard Gibbs energy and equilibrium constant

Reaction	T, K	298.15	313	328	343	358	373
10	$-\Delta_r G_T^0, \text{kJ} \cdot \text{mol}^{-1}$	394.826	399.229	403.75	408.367	413.048	417.808
	Equation	$\Delta_r G_T^0 = -0.307T - 303.1$					
	$\lg K_p$	69.25	66.70	64.37	62.26	60.34	58.58
11	$-\Delta_r G_T^0, \text{kJ} \cdot \text{mol}^{-1}$	543.349	547.774	552.31	556.931	561.615	566.377
	Equation	$\Delta_r G_T^0 = -0.307T - 451.5$					
	$\lg K_p$	95.30	91.52	88.06	84.91	82.04	79.41
12	$-\Delta_r G_T^0, \text{kJ} \cdot \text{mol}^{-1}$	19.247	21.044	22.86	24.684	26.51	28.346
	Equation	$\Delta_r G_T^0 = -0.121T + 16.99$					
	$\lg K_p$	3.38	3.52	3.64	3.76	3.87	3.97

Based on Table 5 data, the temperature dependence diagrams were built for interaction of malachite, azurite and chrysocolla with modified reagent (Fig. 1).

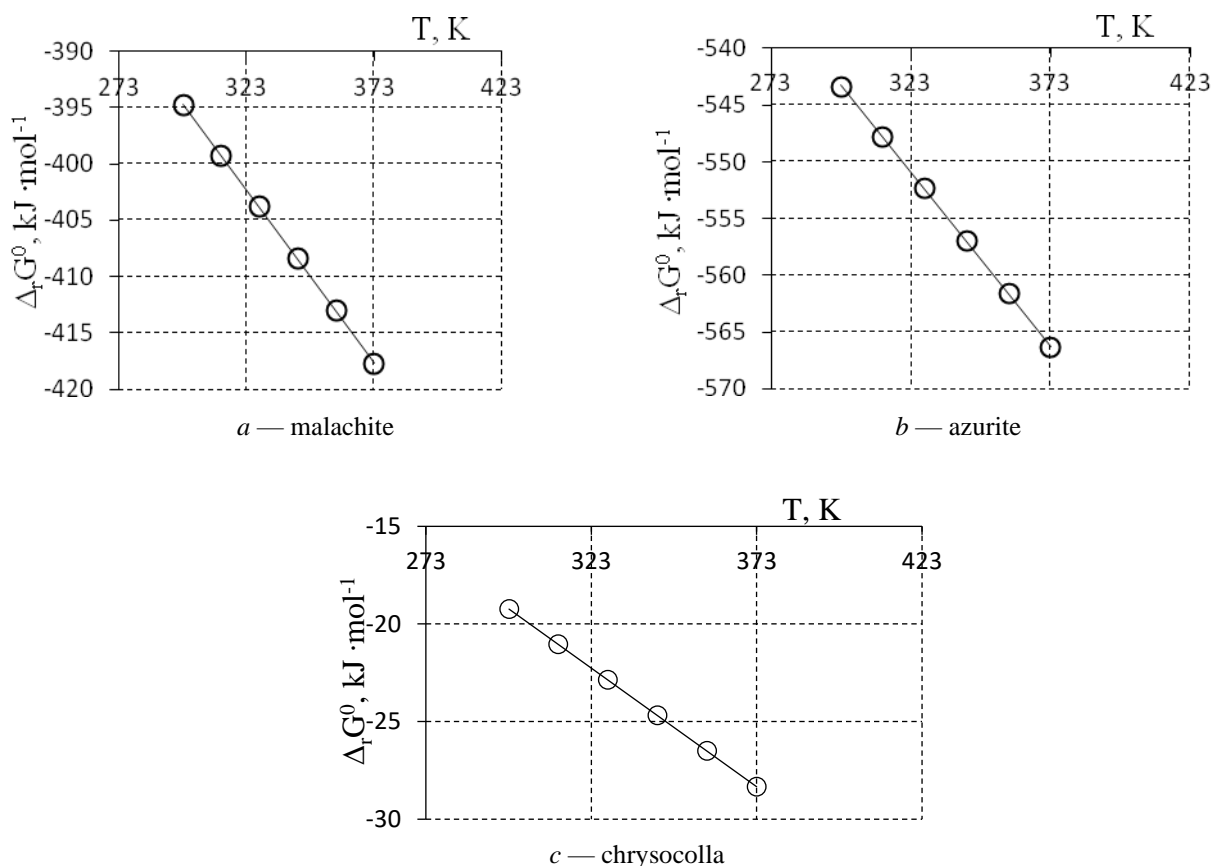


Figure 1. Temperature dependence of standard Gibbs energy for interaction of copper minerals with modified reagent

As follows from Figure 1, standard Gibbs energy for malachite and azurite is negative in the whole temperature range, indicating high probability of interaction, growing with temperature. Interaction with chrysocolla is less active than with malachite and azurite but is still possible at mentioned temperature, with interaction probability again proportional to temperature growth.

Interaction of a modified reagent with chrysocolla in interval of 298.15–373 K is lower than for malachite and azurite. But also it can proceed in this temperature interval. Raise of temperature also is able to increase the probability of interaction.

### Conclusions

Based on the results of thermodynamic analysis the modified reagent is recommended as oxidized copper minerals sulphidizer for flotation enrichment of oxidized copper ore. In particular, the possibility of sulphidizing the ore containing malachite, azurite and chrysocolla as major components, is demonstrated in the study.

*Financial support of scientific research was carried out under the project AP 05130454 «Development of an effective technology for the processing of oxidized copper ores using a modified reagent» of the Ministry of education and sciences of the Republic of Kazakhstan.*

### References

- 1 Митрофанов С.И. Исследование руд на обогатимость / С.И. Митрофанов. — М.: Metallurgizdat, 1954. — 23 с.
- 2 Feng Q.C. Effect of reagent Regime on Flotation Performance of Refractory Oxidized Copper Ores Containing a High Content of Slime / Q.C. Feng, S.M. Wen, W.J. Zhao, C.Y. Chen, H.F. Zhao, Y.J. Wang // *Advanced Materials Research*. — 2013. — P. 2351–2355.
- 3 Elgillani D.A. Classroom notes on Surface Chemistry and Flotation / D.A. Elgillani. — Dept. of Mining Engineering, Faculty of Engineering, Cairo University, 2008.
- 4 Corina K.C. The recovery of oxide copper minerals from a complex copper ore by sulfidization / K.C. Corina, M.O. Kalichinia, C.T. Connora, S. Simukanga // *Minerals Engineering*. — 2017. — P. 15–17.
- 5 Бектурганов Н.С. Применение сульфидизации при переработке окисленных медных руд Удоканского месторождения / Н.С. Бектурганов, Г.Л. Каткеева, И.М. Оскембеков, М.А. Акубаева // *Цветные металлы*. — 2016. — № 9. — С. 22–27.
- 6 Каткеева Г.Л. Изучение влияния электрохимической обработки на сульфидизацию и флотацию окисленных медных минералов и руд / Г.Л. Каткеева, Н.С. Бектурганов, З.Б. Сагиндыкова и др. // *Обогащение руд*. — 2004. — № 6 — С. 20–22.
- 7 Бектурганов Н.С. Физико-химические особенности процесса гидротермального сульфидирования окисленных и смешанных видов сырья цветной металлургии / Н.С. Бектурганов, А.К. Базаев, С.П. Сим и др. // *Сб. науч. тр. АН СССР*. — 1989. — С. 51–59.
- 8 Патент № 30898 РК, МПК С22В 15/00. Способ обогащения окисленных медных руд / И.М. Оскембеков, Н.С. Бектурганов, Г.Л. Каткеева, Ж.С. Оскембекова, Ж.А. Шайке. — Оpubл. 15.02.2016. — Бюл. — № 2.
- 9 Патент № 32695 РК, МПК В03В 7/00. Способ обогащения окисленной медной руды / И.М. Оскембеков, Н.С. Бектурганов, Г.Л. Каткеева, Ж.С. Оскембекова, М.А. Акубаева, Д.Р. Гизатуллина, Ж.А. Шайке, Е.М. Жунусов, А.М. Жунусов. — Оpubл. 05.03. 2018. — Бюл. — № 9.
- 10 Герасимов Я.И. Курс физической химии. — Т. I. / Я.И. Герасимов. — М.: Госхимиздат, 1963. — 624 с.
- 11 Рябин В.А. Термодинамические свойства веществ / В.А. Рябин, М.А. Остроумов, Т.Ф. Свит. — Л.: Химия, 1977. — 392 с.
- 12 Касенов Б.К. Термодинамические методы в химии и металлургии / Б.К. Касенов, А.С. Пашинкин, М.К. Алдабергенов. — Алматы: Рауан, 1994. — 256 с.
- 13 Кумок В.Н. Проблема согласования методов оценки термодинамических характеристик. Прямые и обратные задачи химической термодинамики / В.Н. Кумок. — Новосибирск: Наука, 1987. — С. 108–123.
- 14 Термические константы веществ: справоч. — Вып. I / под ред. В.П. Глушко. — М.: Наука, 1965. — 146 с.
- 15 Термические константы веществ: справоч. — Вып. VI / под ред. В.П. Глушко. — М.: Наука, 1972. — 370 с.
- 16 Термические константы веществ: справоч. — Вып. III / под ред. В.П. Глушко. — М.: Наука, 1968. — 222 с.
- 17 Термические константы веществ: справоч. — Вып. II / под ред. В.П. Глушко. — М.: Наука, 1966. — 96 с.
- 18 Термические константы веществ: справоч. — Вып. IV / под ред. В.П. Глушко. — М.: Наука, 1970. — 510 с.
- 19 Сайт журнала «Свойства минералов». [Электронный ресурс]. — Режим доступа: <http://www.74rif.ru/mineral-gl.html>.

Г.Л. Каткеева, Г. Бүркітсетерқызы, Ю.П. Морозов, Е.М. Жунусов

### Тотыққан мыс минералдарының модификацияланған реагентпен әрекеттесуінің термодинамикалық талдауы

Тотыққан мыс кендерін байыту кезінде тотыққан мыс минералдарын алдын ала сульфидтеу керектігі көрсетілген. Алғаш рет тотыққан мыс кендерінің негізін құраушы — малахит, азурит және хризоколланың модификацияланған сульфидтеуші реагентпен әрекеттесуінің термодинамикалық талдауы жүргізілді. Модификацияланған сульфидтеуші реагент ретінде натрий полисульфиді мен аммоний сульфатының ерітіндісінде пайда болған аммоний полисульфиді қолданылды. Аммоний полисульфидінің тотыққан мыс минералдарымен реакциясының стандартты Гиббс энергиясының температуралық тәуелділігі айқындалды. Малахит пен азурит үшін 298,15–373 К аралығында модификацияланған реагентпен реакциясы кезінде стандартты Гиббс энергиясы теріс әсер көрсететіндігі анықталды. Сондықтан модификацияланған реагенттің малахит және азуритпен әрекеттесу ықтималдығы жоғары. Температураның

жоғарылауы өзара әсер ету ықтималдығын арттырады. Модификацияланған реагенттің хризоколламен әрекеттесуі малахит пен азуритке қарағанда әлсіз көрсетілген. Алайда осы температура интервалында ағып кетуі мүмкін. Температураның жоғарылауы сонымен қатар өзара әсер ету ықтималдылығын арттырады. Осыған байланысты, тотыққан мыс минералдарының модификацияланған сульфидтеуші реагенті — аммоний полисульфидімен сульфидтенуінің мүмкіндігі көрсетілген.

*Кілт сөздері:* тотыққан минералдар, хризокола, малахит, азурит, сульфидтеуші модификацияланған реагент, сульфидтеу, термодинамикалық талдау, Гиббс энергиясы.

Г.Л. Каткеева, Г. Буркитсетеркызы, Ю.П. Морозов, Е.М. Жунусов

## Термодинамический анализ взаимодействия окисленных минералов меди с модифицированным реагентом

Показана необходимость предварительной сульфидизации окисленных минералов меди при обогащении окисленной медной руды. Впервые проведен термодинамический анализ взаимодействия модифицированного сульфидирующего реагента с основными составляющими окисленной медной руды — малахитом, азуритом и хризоколлой. В качестве модифицированного сульфидирующего реагента применен полисульфид аммония, образованный в растворе полисульфида натрия и сульфата аммония. Определена температурная зависимость стандартной энергии Гиббса реакции полисульфида аммония с окисленными медными минералами. Показано, что изменение стандартной энергии Гиббса реакции для малахита и азурита с модифицированным реагентом в интервале 298,15–373 К принимает отрицательные значения. Следовательно, высока вероятность взаимодействия модифицированного реагента с малахитом и азуритом. Повышение температуры способствует увеличению вероятности взаимодействия. Связь модифицированного реагента с хризоколлой выражена слабее, чем малахита и азурита. Однако она может протекать в данном температурном интервале. Повышение температуры также способствует увеличению вероятности взаимодействия. Таким образом, установлена принципиальная возможность сульфидизации окисленных медных минералов модифицированным сульфидирующим реагентом — полисульфидом аммония.

*Ключевые слова:* окисленные минералы, хризоколла, малахит, азурит, модифицированный сульфидирующий реагент, сульфидизация, термодинамический анализ, энергия Гиббса.

### References

- 1 Mitrofanov, S.I. (1954). *Issledovanie rud na obohatimost [Ore research on enrichment]*. Moscow: Metallurhizdat [in Russian].
- 2 Feng, Q.C., Wen, S.M., Zhao, W.J., Chen, C.Y., Zhao, H.F. & Wang, Y.J. (2013). Effect of reagent Regime on Flotation Performance of Refractory Oxidized Copper Ores Containing a High Content of Slime. *Advanced Materials Research*, 2351–2355.
- 3 Elgillani, D.A. (2008). *Classroom notes on Surface Chemistry and Flotation*. Department of Mining Engineering, Faculty of Engineering, Cairo University.
- 4 Corina, K.C., Kalichinia, M.O., Connora, C.T. & Simukanga, S. (2017). The recovery of oxide copper minerals from a complex copper ore by sulfidization. *Minerals Engineering*, 15–17.
- 5 Bekturganov, N.S., Katkeeva, G.L., Oskembekov, I.M. & Akubaeva, M.A. (2016). Primenenie sulfidizatsii pri pererabotke oksilennykh mednykh rud Udokanskogo mestorozhdeniia [The use of sulfidization in the processing of oxidized copper ores of the Udokan deposit]. *Tsvetnye metally — Non-ferrous metals*, 9, 22–27 [in Russian].
- 6 Katkeeva, G.L., Bekturganov, N.S. & Sagindykova, Z.B. et al. (2004). Izuchenie vliianiia elektrokhimicheskoi obrabotki na sulfidizatsiiu i flotatsiiu oksilennykh mednykh mineralov i rud [Study of the effect of electrochemical treatment on the sulfidization and flotation of oxidized copper minerals and ores]. *Obohashchenie rud — Ores enrichment*, 6, 20–22 [in Russian].
- 7 Bekturganov, N.S., Bazaev, A.K. & Sim, S.P. et al. (1989). Fiziko-khimicheskie osobennosti protsessa hidrotermalnoho sulfidirovaniia oksilennykh i smeshannykh vidov syria tsvetnoi metallurhii [Physico-chemical characteristics of the process of hydrothermal sulfidation of oxidized and mixed raw materials of non-ferrous metallurgy]. *Sbornik nauchnykh trudov AN SSSR — Collection of scientific papers of the USSR Academy of Sciences*, 51–59 [in Russian].
- 8 Oskembekov, I.M., Bekturganov, N.S., Katkeeva, G.L., Oskembekova, Zh.S. & Shayke, Zh.A. (2016). Sposob obohashcheniia oksilennykh mednykh rud [A method of enrichment of oxidized copper ores]. *Patent No. 30898 RK, MPK S22V 15/00*. Publ. BI, 2 [in Russian].
- 9 Oskembekov, I.M., Bekturganov, N.S., Katkeeva, G.L., Oskembekova, Zh.S., Akubaeva, M.A., & Gizatullina, D.R., et al. (2018). Sposob obohashcheniia oksilennoi mednoi rudy [A method of enrichment of oxidized copper ore]. *Patent No. 32695 RK, MPK V03V 7/00*. Publ. BI, 9 [in Russian].
- 10 Gerasimov, Ya.I. (1963). *Kurs fizicheskoi khimii [Physical Chemistry Course]*. (Vol. 1). Moscow: Hoskhimizdat [in Russian].
- 11 Ryabin, V.A., Ostroumov, M.A. & Svit, T.F. (1977). *Termodinamicheskie svoystva veshchestv [Thermodynamic properties of substances]*. Leningrad: Khimiia [in Russian].
- 12 Kasenov, B.K., Pashinkin, A.S. & Aldabergenov, M.K. (1994). *Termodinamicheskie metody v khimii i metallurhii [Thermodynamic methods in chemistry and metallurgy]*. Almaty: Rauan [in Russian].

- 13 Kumok, V.N. (1987). *Problema sohlasovaniia metodov otsenki termodinamicheskikh kharakteristik. Priamye i obratnye zadachi khimicheskoi termodinamiki [The problem of harmonization of methods for assessing thermodynamic characteristics. Direct and inverse problems of chemical thermodynamics]*. Novosibirsk: Nauka [in Russian].
- 14 Glushko, V.P. (Eds.) (1965). *Termicheskie konstanty veshchestv: spravochnik [Thermal constants of substances. Directory]*. (Iss. I). Moscow: Nauka, 146 [in Russian].
- 15 Glushko, V.P. (Eds.) (1972). *Termicheskie konstanty veshchestv: spravochnik [Thermal constants of substances. Directory]*. (Iss. VI). Moscow: Nauka, 370 [in Russian].
- 16 Glushko, V.P. (Eds.) (1968). *Termicheskie konstanty veshchestv: spravochnik [Thermal constants of substances. Directory]*. (Iss. III). Moscow: Nauka, 222 [in Russian].
- 17 Glushko, V.P. (Eds.) (1966). *Termicheskie konstanty veshchestv: spravochnik [Thermal constants of substances. Directory]*. (Iss. II). Moscow: Nauka, 96 [in Russian].
- 18 Glushko, V.P. (Eds.) (1970). *Termicheskie konstanty veshchestv: spravochnik [Thermal constants of substances. Directory]*. (Iss. IV). Moscow: Nauka, 510 [in Russian].
- 19 Sait zhurnalu «Svoistva mineralov» [Site of journal «Mineral Properties»]. [www.74rif.ru](http://www.74rif.ru). Retrieved from <http://www.74rif.ru/mineral-gl.html> [in Russian].

E.S. Mustafin<sup>1</sup>, Kh.B. Omarov<sup>1</sup>, A.S. Borsynbaev<sup>1</sup>, D. Havlicek<sup>2</sup>, A.M. Pudov<sup>1</sup>,  
D.A. Kaykenov<sup>1</sup>, A.A. Muratbekova<sup>1</sup>, D.T. Sadyrbekov<sup>1</sup>, A.A. Ainabaev<sup>1</sup>

<sup>1</sup>*Ye.A. Buketov Karaganda State University, Kazakhstan;*

<sup>2</sup>*Charles University, Prague, Czech Republic*

*(E-mail: askhat.9@mail.ru)*

## **Possibility of enrichment of ore processing waste from Karagaily and Zheskazgan mining plants by dry separation method**

This study aims at review of the effects of dry separation method on the ore flotation efficiency and thoroughly discusses the possibility of waste enrichment by sieving through fine-mesh sieves with sizes ( $d > 0.4$ ;  $0.16 < d < 0.4$ ;  $0.08 < d < 0.16$ ;  $d < 0.08$  mm). A granulometric analysis of four samples waste production, was carried out and the copper content in each fraction was determined. According to the results of the study, the following was established: 1) the largest proportion has a grain size fraction over the range 0.16–0.08 mm in the «current tails» of the Karagaily ore-processing plant, in this fraction turned out to be the highest copper content; 2) a larger amount of copper is contained in coarse fraction of «stored tails» and «current tails» of Zheskazgan ore-processing plant 1–2, therefore, it is possible to sift out a finely dispersed fraction; 3) the largest fraction by grain size is over the range of 0.16–0.08 mm in «aged tails» of Zheskazgan PP 3, but the largest weight percentage of copper is over the range  $0.08 < d < 0.16$ . As a result of the studies, it was found that «current tails» and «stored tails» are applicable for the ore enrichment by dry separation method. The «Current tails» of the KPP are not suitable for enrichment by dry separation.

*Keywords:* concentration plant, tailings samples, analysis, fraction, grain sizes, screening, copper content, dry separation.

### *Introduction*

The problem of handling solid waste is the most urgent component of ensuring national security for our country, since the volumes of accumulated waste are considered as one of the factors of the progressive environmental crisis. The sphere of secondary use of resources in Kazakhstan is at the stage of active formation. The purpose of this research was to study the possibility of using dry separation method for enrichment of ore processing waste from mining plants.

Today, special attention is paid to the problem of utilization of mining waste, as the use of technogenic mineral resources is not only one of the reserves of mineral raw materials for the mining industry, but also an important part of the state policy of resource saving and environmental protection.

Around the world, the process of mining and processing metal ores forms a large amount of waste of various aggregation state. At present, they contain billions of tons of ore that has undergone certain processing. Further accumulation of mining complex waste causes a serious problems of the environmental situation on the planet. The urgent issue is the creation of new environmentally friendly technologies for mining, focused on their maximum use [1].

Recent years, there is an increase in waste accumulation, therefore the environmental factor significantly impacts to the economy. According to the estimates of specialists from German metallurgical companies, the items of taxes and environmental costs of production have begun to gain the most weight recently. Therefore, progressive technologies for the production of metals from recycled materials are increasingly being introduced abroad. The sources of such raw materials are solid waste storage facilities of mining and metallurgical industries, the so-called technogenic deposits [2].

### *Experimental*

The difficulty in separating of contaminants is caused mainly due to the moisture of the mass: with its increase, the stickiness of the impurities grows. In addition to moisture, the degree of stickiness is influenced by the grain and mineralogical compositions: the greatest stickiness is observed in clay and loamy soils, and less — in sandy loam, sand and stone dust formed during crushing. With the dry enrichment method, it is advisable to use cyclones for screening small fractions, since the use of vibrosieve with small mesh sizes is impossible due to the constant contamination of the holes [3, 4].

Therefore, for the enrichment of granules with a diameter of less than 1 mm by dry separation method, vibration systems are used. They are supplied with the platform and a separation plate with air blowing, which are inclined at certain angle to the horizontal. In this case it is possible to separate the mineral in accordance with their size under the influence of the vibration friction force.

The dry separation and enrichment unit includes a second vibration platform, which is installed on the second one-navigation separation. The angle of inclination and the direction of vibration force is approximately 20~60°. At least one gutter is installed on the indicated vibration platform, which is placed under the material inlet, a grating part is installed inside the gutter, the angle of the grating part and the vibration of the second platform is 2~20°. The sealed chamber is closed by the grating part, on the side wall of the gutter there is a gas inlet, at least one outlet for deposition and one more for the upper drain, a first, second, third, fourth partitions are installed around the side wall of the gutter. The above mentioned output for deposition is installed in the direction of low end of the sieve piece.

A useful effect is achieved by means of the vibration platform and a strainer, which are inclined to the vibration force. Enrichment and separation can be carried out in accordance with the mineral density. Moreover, due to the outlet for the upper discharge, the lighter material can be separated by the pouring method, which allows to achieve a good separation effect [5].

Four samples of the following grades have been taken for the experiment: 1) «current tails» of the Karagaily processing plant (KPP); 2) «stored tails» of the Zhezkazgan processing plant (ZHPP) No. 1, 2; 3) «current tails» of ZHPP; 4) «stored tails» of ZHPP No. 3 (grain sizes in samples are 0.01–0.5 mm). These samples have been subjected to study in terms of the possibility of enrichment with sieve methods.

Dispersion of the samples was determined by sieve analysis. It has been taken 250 grams of powder from the processing plants. This samples were passed through sieves with sizes 0.4, 0.16, and 0.08. Before sifting large lumps of the sample were grinded in the mortar. Each fraction was weighed and the copper content was determined on the atomic absorption spectrometer «Varian AA-140».

### Results and Discussion

The aim of our research work was to determine the feasibility of enriching these wastes by sieving through fine mesh sieves with sizes ( $d > 0.4$ ;  $0.16 < d < 0.4$ ;  $0.08 < d < 0.16$ ;  $d < 0.08$  mm). In order to achieve this purpose has been conducted a particle size analysis of mentioned above samples.

Assuming the dividing out of the number of grains by size to be the normal distribution, using the approximation and the Gauss function, it was determined the position of the distribution maximum and other statistical characteristics such as, the mathematical expectation and variance (Fig. 1).

For KPP «current tails», the distribution is described by a Gaussian curve with the following parameters: expectation is 0.11 mm, variance = 0.05, which confirms the normal distribution, i.e. uniform distribution in all fractions.

Based on the results of the mineralogical analysis, the granulometric analysis of the «Karagaily current tails» sample has been carried out. According to the results copper was in the form of chalcopyrite, due to its hardness that is contained in large fractions. Granulometric analysis of the remaining samples was also performed.

The results of this work are presented in the tables and depicted in the graphs below. As a result of conducted experiments the next data have been obtained. According to this values the sieves sizes, namely diameter impacts to the composition and copper content of considered samples. A maximum amount of mass fraction and copper content corresponds to the sieves with diameter between 0.08 and 0.16 mm.

Table 1

Results of particle size analysis of the sample «Current tails» (KPP)

Sieve diameter, mm	Mass fraction		Average copper content, %
	g	%	
$d > 0.4$	0	0	0
$0.16 < d < 0.4$	71.18	28.47	0.02
$0.08 < d < 0.16$	145.12	58.05	0.18
$d < 0.08$	33.7	13.48	0.01
For all fractions	250.0	100	0,11

The average copper content for all fractions was calculated by the formula

$$A = \sum_i p_i x_i = 0.0 \cdot 0 + 0.2847 \cdot 0.02 + 0.5805 \cdot 0.18 + 0.1348 \cdot 0.01 = 0.11$$

As a result of the analysis (Table 1) it has been determined that the largest fraction of the grain size is in the range of 0.16–0.08 mm, therefore, there is the highest copper content in this fraction.

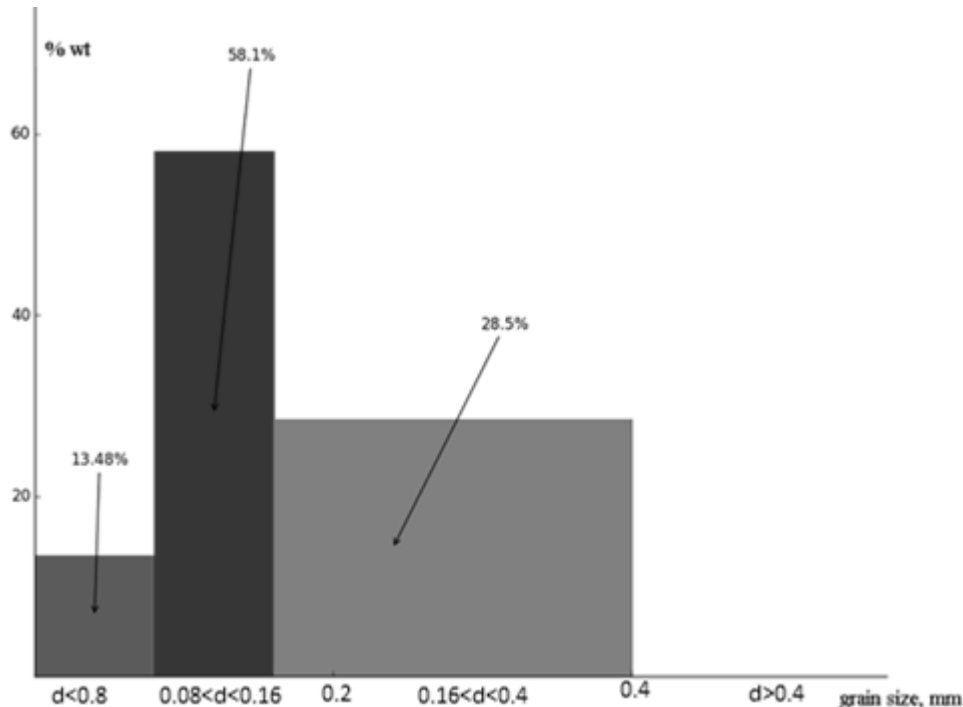


Figure 1. Distribution of the sample «current tails» of KPP by grain sizes

Based on the analysis, it was shown that division into fractions for enrichment is not feasible for the «current tailings» of KPP, since after sieving the percentage of waste will be much higher than in other samples. This fact makes the dry separation method ineffective for the mentioned above sample.

According to the results of the analysis of the «stored tailings» sample of ZHPP 1, 2 (Table 2) more copper is contained in the larger fractions of the sample therefore, it is possible to sift out the finely dispersed fraction and enrich the copper content of the tailings (Fig. 2).

Table 2

#### Results of the granulometric analysis of the sample «Stored tails» of ZHPP 1,2

Sieve diameter, mm	Mass fraction,		Average copper content, %
	g	%	
d > 0.4	0	0	0
0.16 < d < 0.4	97.14	38.86	0.11
0.08 < d < 0.16	124.54	49.82	0.08
d < 0.08	28.32	11.32	0.01
For all fractions	250.0	100	0.08

According to the analysis results of the sample «current tailings» of ZHPP 1, 2 (Table 3) it is clear that, as well as the previous one, more copper is contained in the larger fractions of the sample, and in the diapason of  $0.16 < d < 0.4$  the largest amount (0.09 %), therefore, it is possible to sift out the finely dispersed fraction and enrich the copper content (Fig. 3).

As a result of the analysis of the «stored tails» of ZHPP 3, it was determined that the largest fraction of the grain size is in the range of 0.4–0.16 mm, but the largest percentage of the mass fraction of copper is in the fraction of  $0.08 < d < 0.16$ . In this case, it is advisable to sift out the coarse fraction  $d > 0.4$  (Fig. 4).

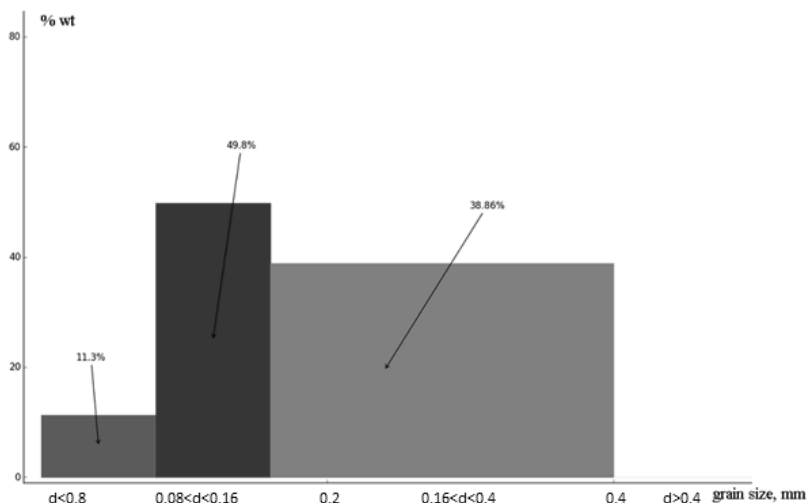


Figure 2. Distribution of the «stored tails» sample of ZHPP 1, 2 by grain size

Table 3

**Results of the granulometric analysis of the sample «Current tails» of ZHPP 1, 2**

Sieve diameter, mm	Mass fraction,		Average copper content, %
	g	%	
d > 0.4	0	0	0
0.16 < d < 0.4	128.01	51.20	0.09
0.08 < d < 0.16	91.71	36.68	0.08
d < 0.08	30.28	12.12	0.01
For all fractions	250.0	100	0.07

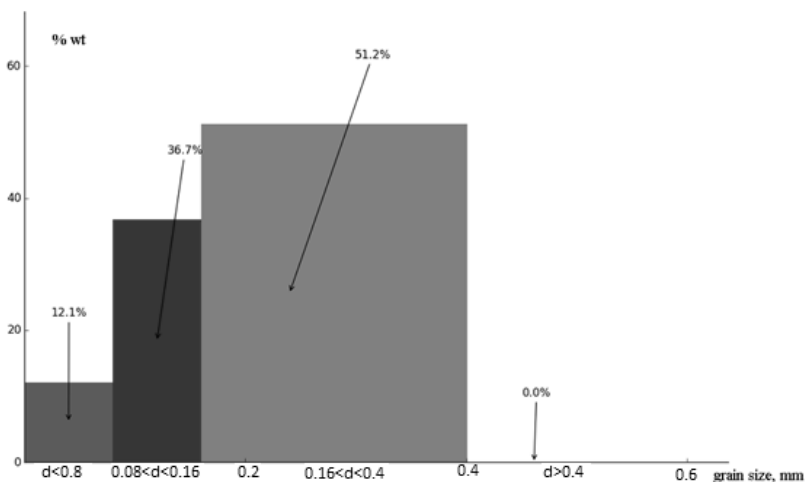


Figure 3. Distribution of current tailings sample by grain size 1, 2

Table 4

**Results of the particle size analysis of the sample «Stored tails» ZHPP 3**

Sieves diameter, mm	Mass fraction,		Average copper content, %
	g	%	
d > 0.4	11.88	4.75	0.02
0.16 < d < 0.4	120.08	48.03	0.06
0.08 < d < 0.16	59.67	23.87	0.09
d < 0.08	58.37	23.35	0.01
For all fractions	250.0	100	0.06

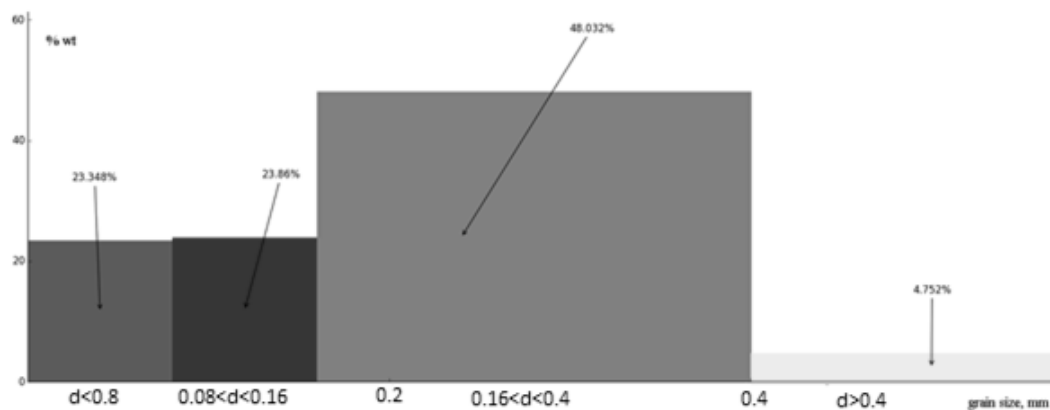


Figure 4. Distribution of the «stored tails» sample of the ZHPP 3 by grain size

The results obtained in this study indicate that the both «Current tails» and «Stored tails» of Zhezkazgan ore plant processing 1, 2, and «Stored tails» of third sample KPP are suitable for the dry separation enrichment method. However the current tails of Karagaily plant have a Gaussian normal distribution of all fractions and the copper content is appropriate, so these samples are not suitable for enrichment by dry separation. The application of the dry separation method for this sample forms a large amount of waste, therefore, for this fraction, dry separation is ineffective.

The dry separation method allows to use the units with double vibrating platforms and sieve components located one above the other. The material for enrichment must be dried to a moisture content of 5 %.

The difficulty of separation of contaminants is mainly due to the humidity: the wetter is the sample, the stickier impurities are. The degree of stickiness, in addition to moisture, is influenced by grain and mineralogical compositions. The greatest stickiness is observed in clay and loamy soils, smaller one in sandy, sand and stone dust formed during crushing.

Therefore, to enrich granules with a diameter of less than 1 mm by the method of dry separation, vibration systems are used with the help of a platform and separation plate with a blow-by air, which are inclined at an angle to the horizon, then under the influence of vibration friction force it is possible to separate the mineral according to the size.

### Conclusions

As a result of the research, it is established that the «current tails» of the ZHPP 1, 2 are suitable for enrichment by means of dry separation method; «stored tails» of the ZHPP 1, 2 and «stored tails» of the KPP 3 are applicable too.

Thus, dry separation plants with double vibration platforms and sieves located one above the other can be used to enrich the concentration plants tails by the dry separation method. The material for enrichment must be entirely dried to a humidity of 1.5–5.0 %.

The dry separation process is required to enrich maximum ore and obtain copper from sample materials, which is advantageous for the copper separation in subsequent processes.

The validation of the dry separation method allowed to demonstrate that the presence of copper in the ore tailings can be determined by means of simple methods of analysis. The pretreatment of the ore tailings is established under technical considerations, environmental pollution, capital costs and operational risks.

The advantages of dry separation method are the low capital and energy costs, in addition to the great flexibility to be environmental friendly. When used in the removal of soil contaminants, it reduces disposal costs and allows the recovery of precious metals.

### References

- 1 Абрамов А.А. Технология переработки обогащения руд цветных металлов: учеб. пос. / А.А. Абрамов. — М.: Изд-во МГУ, 2005. — 330 с.
- 2 Алгебраистова Н.К. Технология обогащения руд цветных металлов: учеб. пос. / Н.К. Алгебраистова. — Красноярск: Изд-во СФУ, 2009. — 270 с.

3 Чернегов Ю.А. Научно-технический прогресс и эффективность минерально-сырьевого комплекса / Ю.А. Чернегов // Горн. журн. — 2009. — № 1. — С. 43.

4 Руководство по обогащению отсева дробления разнопрочных каменных материалов. — [Электронный ресурс]. — Режим доступа: [http://kitab.tnda.az/upload-files/document/files/54/\\_\\_\\_\\_6.pdf](http://kitab.tnda.az/upload-files/document/files/54/____6.pdf)

5 Патент 2577343 Россия. Способ сухой сепарации и обогащения и система для сухой сепарации и обогащения / ВАН Чжунву // Опубл. 03.20.2016.

Е.С. Мустафин, Х.Б. Омаров, А.С. Борсынбаев, Д.Хавличек, А.М. Пудов,  
Д.А. Кайкенов, А.А. Муратбекова, Д.Т. Садырбеков, А.А. Айнабаев

### **Қарағайлы және Жезқазған кен-байыту фабрикаларының қалдықтарын құрғақ бөлу әдісімен байыту мүмкіндігі**

Мақала құрғақ бөлу әдісінің кенді байыту тиімділігіне әсерін талдауға бағытталған. Сонымен қатар, өлшемдері ұсақ електерді ( $d > 0,4$ ;  $0,16 < d < 0,4$ ;  $0,08 < d < 0,16$ ,  $d < 0,08$  мм) елеуіштер арқылы өткізіп, қалдықтарды байыту мүмкіндігі қарастырылған. Төрт қалдық үлгілерінің гранулометриялық сараптама-сы жүргізіліп, олардың әрбір фракцияларындағы мыстың құрамдық мөлшері анықталған. Зерттеу нәтижелері бойынша: 1. Қарағайлы байыту фабрикасының «ағымдық қалдықтарының»  $0,16-0,08$  мм аралығындағы фракцияларында бөлшектердің өлшемі ең жоғары болатыны және осы фракцияларда мыстың ең жоғары мөлшері табылған; 2. Жезқазған байыту фабрикасының  $1-2$  үлгілерінің «ағымдық» және «жинақталған» қалдықтарында да мыстың мөлшері жоғары болады; 3. Бөлшектер мөлшерінің өлшемі бойынша ең үлкен фракция Жезқазған байыту комбинатының  $3$ -үлгісіндегі  $0,16-0,08$  мм аралығындағы «жинақталған» қалдықтарда кездеседі. Зерттеулер нәтижесінде «ағымдық» және «жинақталған» қалдықтарды құрғақ бөлу әдісі арқылы байытуға болатыны анықталды. Қарағайлы байыту комбинатының «ағымдық» қалдықтары құрғақ бөлу әдісімен байытуға жарамайды.

*Кілт сөздер:* байыту фабрикасы, қалдық үлгілері, сараптама, фракция, түйіршік өлшемдері, елеу, мыстың құрамы, құрғақ бөлу.

Е.С. Мустафин, Х.Б. Омаров, А.С. Борсынбаев, Д.Хавличек, А.М. Пудов,  
Д.А. Кайкенов, А.А. Муратбекова, Д.Т. Садырбеков, А.А. Айнабаев

### **Возможность обогащения отходов Карагайлинской и Жезказганской горно-обогатительных фабрик методом сухого разделения**

Статья направлена на анализ влияния метода сухого разделения на эффективность обогащения руды. Кроме того, обсуждены возможности обогащения отходов путем просеивания через мелкие сита с размерами ( $d > 0,4$ ;  $0,16 < d < 0,4$ ;  $0,08 < d < 0,16$ ,  $d < 0,08$  мм). Был проведен гранулометрический анализ четырех образцов и определено содержание меди в каждой фракции. По результатам исследования было установлено: 1) наибольший размер зерна имеют фракции в диапазоне  $0,16-0,08$  мм в «текущих хвостах» Карагайлинского обогатительного комбината, в этой же фракции оказалось самое высокое содержание меди; 2) большое количество меди также обнаружено в крупной фракции «лежалых хвостов» и «текущих хвостов» Жезказганского обогатительного комбината  $1-2$ , поэтому здесь можно отфильтровать мелкодисперсную фракцию; 3) самая большая фракция по размеру зерна находится в диапазоне  $0,16-0,08$  мм в «лежалых хвостах» Жезказганского обогатительного комбината  $3$ , но наибольший весовой процент меди находится в диапазоне  $0,08 < d < 0,16$ . В результате исследований было установлено, что «текущие хвосты» и «лежалые хвосты» применимы для обогащения руды методом сухого разделения. «Текущие хвосты» Карагайлинского обогатительного комбината не подходят для обогащения путем сухого разделения.

*Ключевые слова:* обогатительная фабрика, образцы хвостов, анализ, фракция, размеры зерна, просеивание, содержание меди, сухая сепарация.

#### References

- 1 Abramov, A.A. (2005). *Tekhnolohiia pererabotki obohashcheniia rud tsvetnykh metallov [Technology for processing and concentration of non-ferrous metal ores]*. Moscow: MSU Publ. [in Russian].
- 2 Algebraistova, N.K. (2009). *Tekhnolohiia obohashcheniia rud tsvetnykh metallov [Non-ferrous metal concentration technology]*. Krasnoyarsk: SFU Publ. [in Russian].

3 Chernegov, Yu.A. (2009). Nauchno-tehnicheskii progress i effektivnost mineralno-syrevoho kompleksa [Technical progress and the effectiveness of the mineral resource complex]. *Hornyi zhurnal — Mountain journal*, 1, 43 [in Russian].

4 Rukovodstvo po obohashcheniiu otseva drobleniia raznoprochnykh kamennykh materialov [Guidelines for the enrichment of screening crushing different-strength stone materials] (n.d). *kitab.tnda.az* Retrieved from [http://kitab.tnda.az/upload-files/document/files/54/\\_\\_\\_\\_\\_6.pdf](http://kitab.tnda.az/upload-files/document/files/54/_____6.pdf) [in Russian].

5 Chzhunvu, V. (2016). Sposob sukhoi separatsii i obohashcheniia i sistema dlia sukhoi separatsii i obohashcheniia [The method of dry separation and enrichment and a system for dry separation and enrichment]. *Patent 2577343*. Russia. Publ. 03.20.2016 [in Russian].

---

## АВТОРЛАР ТУРАЛЫ МӘЛІМЕТТЕР СВЕДЕНИЯ ОБ АВТОРАХ INFORMATION ABOUT AUTHORS

- Ainabayev, A.A.** — Candidate of chemical sciences, Senior research fellow of laboratory «Physicochemical methods of investigations», Ye.A. Buketov Karaganda State University, Kazakhstan.
- Aldabergenova, M.A.** — 2<sup>nd</sup> year master student, Chemical technologies and ecology department, Shakarim State University of Semey, Kazakhstan.
- Alibiyeu, D.B.** — Candidate of physical and mathematical sciences, Associate professor of applied mathematics and informatics department, Ye.A. Buketov Karaganda State University, Kazakhstan.
- Ashurov, N.** — Doctor of technical sciences, Professor, Head of the laboratory, Institute of polymer chemistry and physics of Academy of Sciences of Uzbekistan, Tashkent, Uzbekistan.
- Badamshina, E.R.** — PhD, Chief Researcher, Department of Polymers and Composite Materials, Institute of Problems of Chemical Physics of Russian Academy of Sciences, Chernogolovka, Russia.
- Bakibaev, A.A.** — Doctor of chemical sciences, Engineer, Institute for Problems of Chemical and Energetic Technologies SB RAS, Biysk, Russia.
- Bakibaev, A.A.** — Doctor of chemical sciences, Leading researcher, National Research Tomsk State University, Russia.
- Borsynbayev, A.S.** — Second year postdoctoral student, Ye.A. Buketov Karaganda State University, Kazakhstan.
- Burkeev, M.Zh.** — Doctor of chemical sciences, Professor, Director of the Research institute of chemical problems, Ye.A. Buketov Karaganda State University, Kazakhstan.
- Burkitseterkyzy, G.** — Engineer, Zh. Abishev Chemical and Metallurgical Institute, Karaganda, Kazakhstan.
- Chernyayev, D.A.** — PhD student, Junior Researcher, Department of Polymers and Composite Materials, Institute of Problems of Chemical Physics of Russian Academy of Sciences, Chernogolovka, Russia.
- Dadahodzhaev, T.** — Doctor of chemical sciences, Professor, Head of the laboratory of Innovation Center of JSC «Uzkimyosanoat» and JSC «Maksam-Chirchik», Tashkent, Uzbekistan.
- Dolgov, V.** — PhD of chemicals sciences, Research worker, Institute of polymer chemistry and physics of Academy of Sciences of Uzbekistan, Tashkent, Uzbekistan.
- Dzhalmukhanova, A.S.** — PhD, Researcher, Department of Polymers and Composite Materials, Institute of Problems of Chemical Physics of Russian Academy of Sciences, Chernogolovka, Russia.
- Dzhanmuldaeva, Zh.K.** — Candidate of technical sciences, Professor, Department «Chemical Technology of Inorganic Substances», M. Auevov South-Kazakhstan State University, Shymkent, Kazakhstan.
- Fazylov, S.D.** — Doctor of chemical sciences, Professor, Ye.A. Buketov Karaganda State University; Institute of organic synthesis and coal chemistry of the Republic of Kazakhstan, Karaganda, Kazakhstan.
- Figurine, I.V.** — Candidate of chemical sciences, Senior researcher, Karaganda Medical University, Kazakhstan.
- Havlicek, D.** — Doc. RnDr., Associate professor, Department of Inorganic Chemistry, Faculty of science, Charles University, Prague, Czech Republic.
- Il'yasov, S.G.** — Doctor of chemical sciences, Head of Laboratory, Institute for Problems of Chemical and Energetic Technologies SB RAS, Biysk, Russia.
- Jumadilov, T.K.** — Doctor of chemical sciences, Professor, Chief Researcher, A.B. Bekturov Institute of chemical sciences, Almaty, Kazakhstan.

- 
- Kaikenov, D.A.** — PhD, Senior research fellow of laboratory «Physicochemical methods of investigations», Ye.A. Buketov Karaganda State University, Kazakhstan.
- Karipova, G.Zh.** — Master of education, Researcher of the Laboratory of synthesis of biologically active substances, Institute of Organic Synthesis and Coal Chemistry of the Republic of Kazakhstan, Karaganda, Kazakhstan.
- Karpov, S.V.** — PhD, Senior Researcher, Department of Polymers and Composite Materials, Institute of Problems of Chemical Physics of Russian Academy of Sciences, Chernogolovka, Russia.
- Kassymova, Zh.S.** — Candidate of biological sciences, Associate professor, Shakarim State University of Semey, Kazakhstan.
- Kasyanova, A.S.** — Assistant chemist, National Research Tomsk State University, Russia.
- Katkeeva, G.L.** — Candidate of engineering sciences, Associate Professor, Zh. Abishev Chemical and Metallurgical Institute, Karaganda, Kazakhstan.
- Kazhikenova, A.Sh.** — Candidate of Technical Sciences, Associate professor of mathematics and informatics teaching technique department, Ye.A. Buketov Karaganda State University, Kazakhstan.
- Khalitova, A.I.** — Candidate of chemical sciences, Senior researcher, Ye.A. Buketov Karaganda State University, Kazakhstan.
- Khamitova, T.O.** — Doctor PhD, Leading researcher, Ye.A. Buketov Karaganda State University, Kazakhstan.
- Klimova, T.E.** — Doctor PhD, Full Professor, Senior researcher, National Autonomous University of Mexico, Mexico.
- Komratova, V.V.** — Researcher, Department of Polymers and Composite Materials, Institute of Problems of Chemical Physics of Russian Academy of Sciences, Chernogolovka, Russia.
- Kudaibergen, G.K.** — Doctor PhD, Senior researcher, Ye.A. Buketov Karaganda State University, Kazakhstan.
- Lodygina, V.P.** — Senior Researcher, Department of Polymers and Composite Materials, Institute of Problems of Chemical Physics of Russian Academy of Sciences, Chernogolovka, Russia.
- Malkov, G.V.** — PhD, Head of Department of Polymers and Composite Materials, Institute of Problems of Chemical Physics of Russian Academy of Sciences, Chernogolovka, Russia.
- Malkov, V.S.** — Candidate of chemical sciences, Head of laboratory, National Research Tomsk State University, Russia.
- Malkov, V.S.** — Candidate of chemical sciences, Head of laboratory, National Research Tomsk State University, Russia.
- Medeshova, A.T.** — Candidate of pharmaceutical sciences, Senior researcher, Karaganda Medical University, Kazakhstan.
- Morozov, Yu.P.** — Doctor of technical sciences, Full Professor, Ural State Mining University, Yekaterinburg, Russia.
- Mukasheva, A.Zh.** — Master of science, Researcher of the Laboratory of synthesis of biologically active substances, Institute of Organic Synthesis and Coal Chemistry of the Republic of Kazakhstan, Karaganda, Kazakhstan.
- Muratbekova, A.A.** — Candidate of chemical sciences, Ye.A. Buketov Karaganda State University, Kazakhstan.
- Mussabayeva, B.Kh.** — Candidate of chemical sciences, Associate professor, Shakarim State University of Semey, Kazakhstan.
- Mustafin, Ye.S.** — Doctor of chemical sciences, Professor, Director of Research Center «Applied Chemistry», Ye.A. Buketov Karaganda State University, Kazakhstan.
- Myrzakhmetova, N.O.** — Candidate of chemical sciences, Associate professor, Kazakh National Women's Teacher Training University, Almaty, Kazakhstan.

- 
- Nurkenov, O.A.** — Doctor of chemical sciences, Professor, Head of the laboratory synthesis of biologically active substances, Institute of organic synthesis and coal chemistry of the Republic of Kazakhstan, Karaganda, Kazakhstan.
- Omarov, Kh.B.** — Doctor of technical sciences, Professor, Senior staff scientist of Research Center «Applied Chemistry», Ye.A. Buketov Karaganda State University, Kazakhstan.
- Pudov, A.M.** — Candidate of biological sciences, Senior research fellow of Research Center «Applied Chemistry», Ye.A. Buketov Karaganda State University, Kazakhstan.
- Rashidova, S.** — Doctor of chemical sciences, Professor, Academician, Director, Institute of polymer chemistry and physics of Academy of Sciences of Uzbekistan, Tashkent, Uzbekistan.
- Ryabykh, A.V.** — Fifth year student, Department of Physical and Inorganic Chemistry, Altai State University, Barnaul, Russia.
- Sadyrbekov, D.T.** — Candidate of chemical sciences, Senior researcher of laboratory «Physicochemical methods of investigations», Ye.A. Buketov Karaganda State University, Kazakhstan.
- Saparbekova, I.S.** — Candidate of chemical sciences, Kazakh National Women's Teacher Training University, Almaty, Kazakhstan.
- Sarsenbekova, A.Zh.** — Doctor PhD, Senior researcher, Ye.A. Buketov Karaganda State University, Kazakhstan.
- Satpaeva, Zh.B.** — PhD student, Ye.A. Buketov Karaganda State University, Kazakhstan.
- Seilkhanov, T.M.** — Candidate of chemical sciences, Full professor, Head of the laboratory of engineering profile NMR, Sh. Ualikhanov Kokshetau State University, Kazakhstan.
- Seitimbetova, A.B.** — Teacher of mathematics and informatics teaching technique department, Ye.A. Buketov Karaganda State University, Kazakhstan.
- Seitmagzimov, A.A.** — Candidate of chemical sciences, Senior researcher, Regional Testing Laboratory of Engineering Profile, M. Auezov South-Kazakhstan State University, Shymkent, Kazakhstan.
- Seitmagzimova, G.M.** — Candidate of technical sciences, Professor, Department «Chemical Technology of Inorganic Substances», M. Auezov South-Kazakhstan State University, Shymkent, Kazakhstan.
- Selikhova, N.Yu.** — Candidate of chemical sciences, Senior researcher, National Research Tomsk State University, Russia.
- Shipunov, B.P.** — PhD in Chemistry, Associate Professor, Department of Physical and Inorganic Chemistry, Altai State University, Barnaul, Russia.
- Shulgau, Z.T.** — National Center for Biotechnology, Nur-Sultan, Kazakhstan.
- Sotchenko, R.K.** — Candidate of chemical sciences, Senior researcher, Karaganda Medical University, Kazakhstan.
- Takibayeva, A.T.** — Candidate of chemical sciences, Assistant Professor of the Department of Chemistry and Chemical Technology, Karaganda State Technical University, Kazakhstan.
- Tatarenko, O.V.** — Junior researcher, National Research Tomsk State University, Tomsk, Russia.
- Tentekbayeva, Zh.M.** — Senior teacher of foreign languages department, MEd, Karaganda State Technical University, Kazakhstan.
- Tomabayeva, A.G.** — 1<sup>st</sup> year master, Karaganda State Technical University, Kazakhstan.
- Totkhuskyzy, B.** — Master of science, Doctoral student, Kazakh National Women's Teacher Training University, Almaty, Kazakhstan.
- Tuguldurova, V.P.** — Engineer, Institute for Problems of Chemical and Energetic Technologies SB RAS, Biysk, Russia.
- Usmanova, M.** — PhD of chemical sciences, Scientific Secretary, Institute of polymer chemistry and physics of Uzbekistan Academy of Sciences, Tashkent, Uzbekistan.
- Yskak, L.K.** — Master of science, Doctoral student, Kazakh National Women's Teacher Training University, Almaty, Kazakhstan.
- Zhumanazarova, G.M.** — PhD student, Ye.A. Buketov Karaganda State University, Kazakhstan.
- Zhunusov, E.M.** — Master student, Karaganda State Technical University, Kazakhstan.
- Zorin, A.O.** — Junior researcher, National Research Tomsk State University, Tomsk, Russia.